



Report of the 2016 STARS4ALL/LoNNe Intercomparison Campaign

Report Authors: Salvador J Ribas^{1,2}, Martin Aubé³, Salvador Bará⁴, Constantinos Bouroussis^{5,6}, Ramon Canal-Domingo¹, Brian Espey⁷, Andreas Hänel⁸, Andreas Jechow^{9,10}, Zoltán Kolláth^{11,12}, Guillem Martí², Pol Massana², Wim Schmidt¹³, Henk Spoelstra¹⁴, Günther Wuchterl¹⁵, Jaime Zamorano¹⁶, Christopher CM Kyba^{9,10}

Institutions:

¹ Parc Astronòmic Montsec, Àger, Spain

² Dept. Astronomia i Meteorologia, Universitat de Barcelona, Barcelona, Spain

³ Département de Physique, Cégep de Sherbrooke, Sherbrooke, Canada

⁴ Área de Óptica, Departamento de Física Aplicada, Universidade de Santiago de Compostela, Santiago de Compostela, Galicia, Spain

⁵ Lighting Laboratory, National Technical University of Athens, Athens, Greece

⁶ LiGHTiNG 3 - Lighting Three Technology, Athens, Greece

⁷ School of Physics, Trinity College Dublin, Dublin, Ireland

⁸ Museum am Schölerberg, Klaus-Strick-Weg 10, 49082, Osnabrück

⁹ Deutsches GeoForschungsZentrum (GFZ), Potsdam, Germany

¹⁰ Leibniz Institute of Freshwater Ecology and Inland Fisheries, Berlin, Germany

¹¹ Konkoly Observatory, Budapest, Hungary

¹² University of West Hungary Savaria Campus, Szombathely, Hungary

¹³ Sotto le Stelle, The Netherlands

¹⁴ Lumineux Consult, Westervoort, The Netherlands

¹⁵ Thüringer Landessternwarte, Sternwarte 5, 07778 Tautenburg, Germany

¹⁶ Dept. de Astrofísica y CC. de la Atmósfera, Universidad Complutense de Madrid, Madrid, Spain

Campaign Participants

Local organizers: Salvador J. Ribas, Ramon Canal-Domingo

LoNNe IC coordinator: Salvador J. Ribas

Participants: Martin Aubé, Salvador Bará, Constantinos A. Bouroussis, Ramon Canal-Domingo, Brian Espey, Andreas Hänel, Andreas Jechow, Zoltán Kolláth, Christopher Kyba, Guillem Martí, Pol Massana, Salvador J. Ribas, Wim Schmidt, Henk Spoelstra, Günther Wuchterl, Jaime Zamorano

1) Introduction

The 2016 LoNNe (Loss of the Night Network) intercomparison campaign is the fourth of four campaigns planned during EU COST Action ES1204. The first campaign took place in 2013 in Lastovo, Croatia, the second in Madrid, Spain (Bará et al 2015), the third in Torriella and Florence, Italy (Kyba et al 2015a). The 2016 campaign took place at the Parc Astronòmic Montsec (PAM). The campaign was supported by the European Collective Awareness Platform for Social and Sustainable Innovation (CAPPSI) STARS4ALL, in which the activity is planned to become a continuous light pollution initiative (LPI). The financing of this campaign, which is listed as a milestone in the MoU of the COST Action ES1204, was unexpectedly waived by the EU-COST Office due to administrative complications and re-organization of the grant-periods. The campaign continued the strategy of taking measurements at multiple sites, this year with a main fixed site and then excursions to other sites. The goals of the campaigns included:

- Understanding the difference between extinction measurements made by DSLR photometry and classical astronomical (telescope) photometry, and also understanding the relation between extinction and sky brightness at these two sites.
- Examining the difference in radiance measured with the mosaic technique of the US National Parks Service camera compared to all-sky fisheye imagery
- Examining the relationships between all-sky and zenith radiance reported by different instruments
- Quantifying the sky brightness at the sites, including full zenith spectral radiance at selected locations
- Measuring the systematic uncertainty on handheld SQM observations due to unit-to-unit differences

This report provides a brief synopsis of the campaign and its preliminary outcomes. **Section 2** describes the measurement locations, the detailed activities of the participants, the instruments used, and the environmental conditions. **Section 3** describes a meeting with local authorities that took place during the campaign. **Section 4** provides some preliminary results, outlines the ongoing analyses, and presents research questions for the next campaign to address. **Section 5** provides recommendations for future intercomparison campaigns.

The Municipality of Balaguer coordinated with us regarding the time that architectural lamps were turned off, and the village of Àger allowed us to turn all street lighting off at a time of our choice.

2) Campaign details

Measurement locations

- 1.- Parc Astronòmic Montsec-COU: (42.0248N, 0.7368E, 813 m elevation)
- 2.- Observatori Astronòmic del Montsec OAdM (42.0514N, 0.7293E, 1573 m elevation)
- 3.- Outskirts of Balaguer: (41.791100N, 0.797494E, 273m elevation)
- 4.- Port d'Àger: (41.979070N, 0.750630E, 908m elevation)
- 5.- Village of Àger: (42.002437N, 0.760763E, 607m elevation)
- 6.- Near Cal Maciarol (Hotel): (42.01939N, 0.7436E, 750 m elevation)
- 7.- Coll d'Ares: (42.04167N, 0.75833E, 1600m elevation)

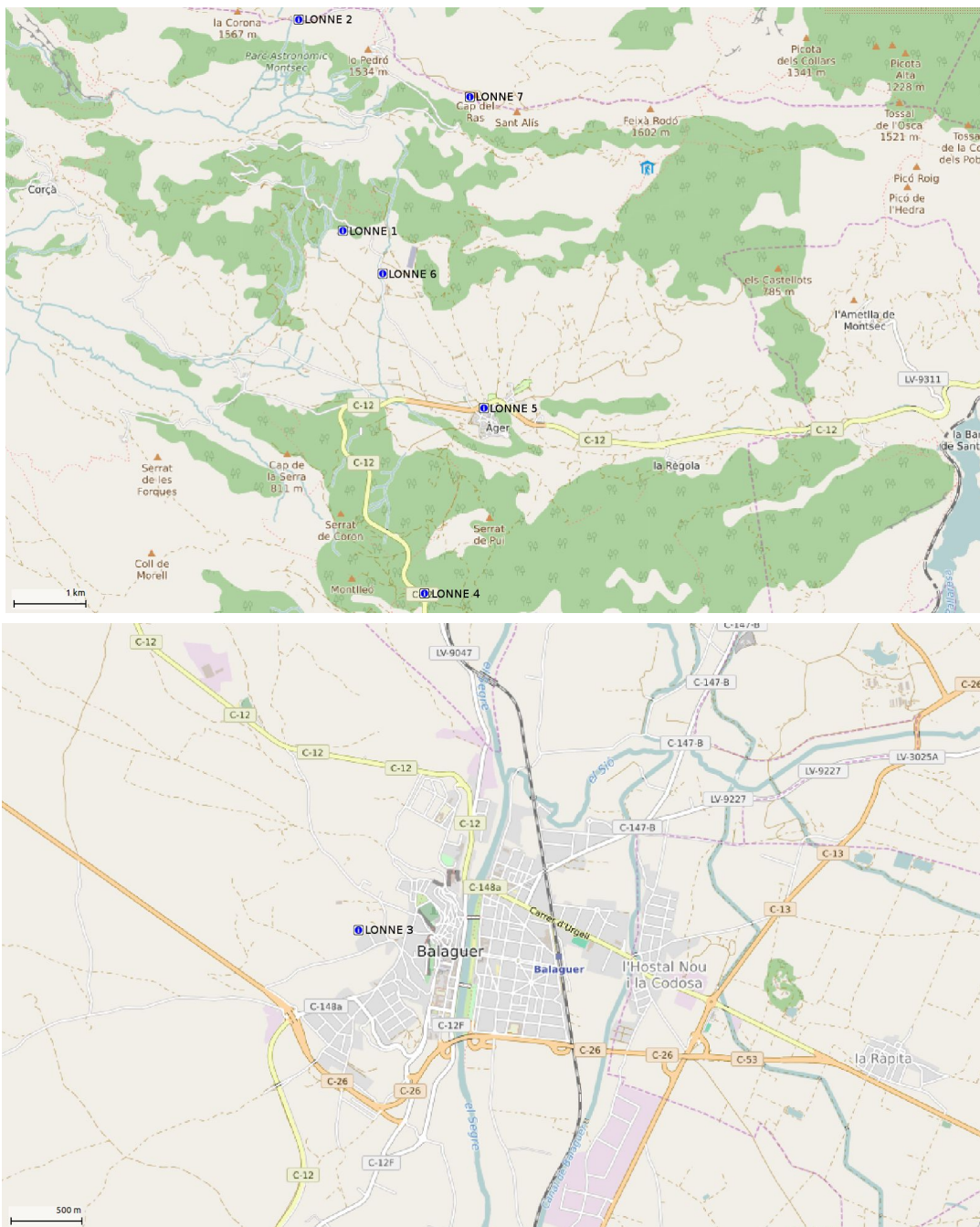


Figure 1: Location of the measurement sites. Each site is labelled with the number of observing sites list. Map source © OpenStreetMap.

Measurement Instruments

- ASTMON all-sky cameras (two Lite devices of different epochs)
- AVT-GE CCD camera with SIGMA 4.5mm fisheye lens
- AVT-GC CCD camera with Fujinon panomorph lens
- Luminance Meter Minolta LS 100
- 2x Handheld portable spectrometers (for checking lamps): Bluewave STD-vis-25 (for checking lamps (Bará and Aubé))
- 2x SAND spectrometers (SAND-4B, SAND-4C)
- Canon 20D camera with 200mm lens V Johnson filter & B filter (not used), mounted on astrotec
- Canon 60D camera with 4.5mm Sigma fisheye lens
- Canon 40D camera with 4.5mm Sigma fisheye lens
- 2x Canon 6D with 8mm Sigma fisheye lens
- Canon 5D Mark II with 8mm Sigma fisheye lens (Zamorano)
- Canon 5D Mark II with 8mm Sigma fisheye lens (Ribas)
- Sony A7S with several lenses, mainly 14mm Samyang lens
- DigiLum
- Canon 1200D with Sigma 4.5mm fisheye (Bará)
- Canon 550D with Sigma 4.5 mm and 30 mm (Haenel)
- Canon 700D (modified without filter) with Sigma 4.5 mm and 30 mm (Haenel)
- Luminance Meter Gossen Mavo-Spot 2 USB (Haenel)
- TESS-V1 (stars2)
- TESS-V1 (stars3)
- NSB mapper
- Loss of the Night app
- Sky Quality Meters (SQM) (see detailed list below)
- IYA - Lightmeters
 - 2x Lightmeter mark 2.3L (Wucherl)
 - 1x Lightmeter mark 2.3L (IGB)
 - 1x Lightmeter mark 2.3 (Wuchterl)
 - 1x Lightmeter mark 2.3 (Espey)
 - 3x Lightmeter mark 2.3 (IGB)
- Additional cameras for non-scientific work

List of SQMs used

SQM:

527 - Haenel
2008 - Schmidt - considerable scratches on window
3111 - Espey – a few scratches on window
8768 - Aubé - a bit scratched

SQM-L:

2536 - Haenel
3158 - Haenel (GaN, metal shade on front window))
3204 - Espey - some minor scratches
3298 - Zamorano - a bit scratched on window

3960 - Haenel (VdS)
4432 - Ribas
6508 - Hölker - a bit scratched on window
6386 - Kyba – considerably scratched window
7963 - Jechow
7964 - Kyba
7980 - Hölker/Jechow
7983 - Hölker/Jechow
8139 - Espey
8144 - Bará
8197 - Espey
9320 - Schmidt

SQM-LE:

0729 - Schmidt (non-standard housing)
0980 - Spoelstra (standard housing - sample rate 10 seconds, attached to DigiLum)
0849 - Kyba FU Berlin (standard housing)
1687 - Kyba FU Berlin (“SQM-E” standard housing)
1759 - Kolláth (standard housing from FU)
1786 - Kai Pong Tong (standard housing)
2437 - Ribas (standard housing - 45 s sample rate)
2444 - Kai Pong Tong (standard housing)
2606 - Aubé (no housing)
3180 - Catalan Network - Ribas (standard housing)
3181 - Catalan Network - Ribas (standard housing)
3186 - Catalan Network - Ribas (standard housing)

SQM-LU (or connected LU-DL):

0857 - Kyba (standard housing)
1055 - Kyba (standard housing)
1118 - Kyba (standard housing)
2113 - Spoelstra (not connect to raspberry pi on first day, standard housing DL)
2117 - Spoelstra (standard housing DL)

SQM-LU-DL:

2089 - Schmidt (standard housing)
2124 - Schmidt (standard housing)
2129 - Bará (standard housing, newer Unihedron glass)
2548 - Kyba (standard housing)
2549 - Kyba (standard housing)
2552 - Hoelker (standard housing)
2555 - Hoelker/Jechow (standard housing)
1988(ex2556) - Hoelker/Jechow (standard housing)
2634 - Espey (standard housing)
2749 - Ribas (standard housing)
2762 - Bará (standard housing, newer Unihedron glass)
2766 - Bará (standard housing, newer Unihedron glass)

SQM-LU-DL-V:

2998 - Kyba/Ribas/Unihedron (no housing)

3003 - Bará (just for after campaign measurements)

3281 - Espey (standard housing when used in permanent station mode)

SQM-LR:

0932 - Espey (no housing, with special filters: ND, and broadband Custom Scientific filters for V, R, and luminance)

Additional SQMs

Potentially used later for roadrunner measurements:

1040 - Ribas (Roadrunner setup)

1871 - Univ. Barcelona (Roadrunner setup)

1049 - Haenel SQM-LU without housing on roof with Baader green filter during dawn 04-05-2016, otherwise SQMDroid

2486 - Haenel SQM-LU (Roadrunner, own housing) measurements on roof night 04/05-05-2016

1738 - Zamorano (Roadrunner setup)

The US National Parks Service sent their all-sky mosaic camera system (Duriscoe et al. 2007) to participate in the campaign by courier. Unfortunately, customs agents refused to allow the shipment into Spain despite a written declaration that the system was to be shipped back to the USA immediately following the conclusion of the campaign.

Detailed information about the instruments and their use in skyglow measurement is available in the following references:

- ASTMON (Aceituno et al. 2011)
- Canon all-sky (Kolláth 2010)
- Loss of the Night app (<http://tinyurl.com/zvs6v5c>)
- Lightmeters (Müller et al. 2011)
- Sky Quality Meters (Cinzano 2005; den Outer et al. 2011; Kyba et al. 2015b)

Timeline of the campaign

In the following, all times quoted are UTC. The observation period was chosen to be around the time of New Moon (which occurred on 6th May at 19:30), so moonlight would not interfere with dark sky measurements.

Day of May 2

Participants arrived at the Parc Astronòmic Montsec - Centre d'Observació de l'Univers (PAM-COU), setup of instruments starting in the afternoon and lasting until sunset. Participants left for dinner shortly after sunset.

Night of May 2-3

Weather and environment:

Some clouds were present at sunset, a bit at zenith and more at the horizon. After sunset we went to dinner at the hotel. The weather was remarkably clear during the night, with no clouds overhead for the entire night.

Description of activities:

Stand-alone instruments were run through twilight and during the night. The sample rates for connected SQM-LE and LU were 2 seconds, and for SQM-LU-DL running on batteries it was 1 minute. Four of the Lightmeters had been run connected to a USB hub, which unfortunately did not provide adequate power for them to stay connected through the whole night.

At about 11:30 pm we left to head to the PAM in order to pick up instruments. We then drove to the Observatory (OAdM) to do measurements, arriving shortly after midnight.

Kyba and Spoelstra performed measurements from 0:49 to 1:54 with 13 handheld SQM and SQM-L. The procedure was as recommended by LoNNe IC 2014 report (Bará et al 2015), and is described in the results section. Additional handheld measurements were made before the systematic check started (some recorded by participants). Espey noted that pointing the SQM at Jupiter resulted in brighter observations (about 0.2-0.3 mpsas).

Kolláth and Jechow did DLSR all-sky imaging at the Observatory. After leaving the Observatory, both returned to PAM to do additional all-sky images and time-lapse images. In addition to all-sky images, Jechow took horizontal fisheye images.

Zamorano operated TESS-V1 on the roof. TESS-V1 via wifi (stars2) did not connect to the broker due to a software malfunction, TESS-V1 (stars3) connected to PC computer by USB port and took data until midnight. NSB mapper to all-sky map did not work at observatory level due to a malfunction of the electronics.

Aubé ran the SAND spectrometers on the PAM roof. He tried to sample the twilight, but integration times were not ideal (only one spectrum correct). For the rest of the night the integration time of the SAND-4B was set to 2 hours, the 4C to 90 minutes. They worked simultaneously and ran all night long.

Schmidt did extinction measurements for 6 places on the sky from the Observatory, all observations in the western part of the sky. He repeated this for 7 places later from the PAM.



Figure 2: Preparation of measurement site on the roof of Parc Astronomic Montsec.

Instruments operated:

SQMs:

Stationary SQMs:

LE: 0729, 0980, 0849, 1687, 1759, 1786, 2437, 2444, 3180, 3181, 3186

LU: 0857, 1055, 1118, 2117

LU-DL: 2089, 2124, 2548, 2549, 2552, 2555, 1988 (ex2556), 2634, 2749

Handheld SQMs:

13 handheld SQMs had 3x4 (observation x direction) measurements at Observatory

Lightmeters: all installed on PAM roof

3 Lightmeter mark 2.3L

5 Lightmeter mark 2.3

DigiLum (pointing at zenith) on PAM roof (Spoelstra)

Cameras:

Different Canon EOS and Sony A7S operated by Z. Kolláth and A. Jechow at PAM-COU and OAdM.

Apps: None

Day of May 3

Participants had free time (informal work and discussions) until lunch around 2:30PM. Following lunch, we met to record the events from the last evening and prepare the plan for the coming evening.

Bouroussis arrived and installed luminance meters and cameras. Wuchterl went up to Observatory to get a Lightmeter working that was not recording data. Bará arrived and installed new SQM-LU-DL (2129, 2762, 2766).

Night of May 3-4

Weather and environment:

Day was clear with some cirrus. There was significant cirrus around sunset, but the clouds disappeared by about nautical twilight. There were no clouds at all by astronomical twilight and this lasted through the entire night, including during the morning twilight. At the end of the night, the humidity level increased up to 78% (PAM-COU Weather Station).

The town of Balaguer switched off the first set of monumental lighting at 11:30PM, between 11:30 to 11:42 light was switched off on those monument lamps that could be manually switched. The hotel switched off lights at 11:55 pm. The town of Àger switched off lights starting at 2:40 am and the last section was switched off by 2:52. Switch-on of Àger lights started 4:22 am and was finished at 4:33 am. At 4:00 am there was also a switch off of room 3 at PAM.

Description of activities:

We ordered dinner in advance for 8pm so that we would be ready for twilight. Automatic instruments were left measuring in advance of twilight. Shortly after astronomical twilight, people went onto the roof to align the ASTMON cameras and to set up the luminance meter and AVT cameras. Two cars left for roadrunner measurements with stops every 20 km or so. The cars arrived in Balaguer in time for the illumination switch off

Schmidt did extinction measurements at 11 and midnight (local time) from PAM, and then went up to the Observatory OAdM to do one session from about 2-2:30 am. Then he returned to PAM to do two more extinction measurements, finishing around 5:00 am. He also did about eight zenith measurements, about every 45 minutes (along with darks, etc.). All observations were following a standard method (inspired by Falchi methods see for example Falchi 2011).

Kyba made naked eye limiting magnitude observations with the Loss of the Night app during evening twilight from 21:21 until 22:17, and again during the morning twilight from 5:11 until 6:34. During the evening twilight the phone had problems obtaining the GPS position. After a phone restart and turning on airplane mode the phone did a better job of getting the position. Some observations during the evening twilight were therefore taken in "Demo mode" with no GPS location.

Kyba & Spoelstra drove to the site at the outskirts of Balaguer at about 11PM to do three sets of four observations with 15 handheld SQMs, following the same procedure as the night before. Measurements lasted from 23:29 until 0:12.

Spoelstra's Digilum was run all night on the walkway in front of the PAM, and was covered for dark current measurements hourly by Kolláth.



Figure 3: New position of Digilum for the next nights

Espey and Ribas did extinction measurements with the 50cm telescope at PAM from about 12:00 to 2:00. 8 stars plus zenith measurements. Espey also ran SQM-DL #2634 and SQM-LR #932 in twilight to examine the linearity of the SQM units, particularly as filtered observations in dark locations can lead to fainter readings than the units were designed to cope with. A number of spot checks with a SQM-DL-V unit (which contains a new design lens) were also made.

Wuchterl ran 3 lightmeters at 10 Hz, the other 4 at 1 Hz, all at PAM. The lightmeters were in a slightly different position compared to the first night: they were relocated to put them at a similar height as the SQMs.

Jechow performed DSLR measurements at a number of locations. He traveled to the site on the outskirts of Balaguer to observe the switch-offs by taking timelapse images. Then he traveled with Massana and Martí doing SQM roadrunner observations doing a transect from Balaguer to Àger, ending at the Port of Àger. There he did a timelapse of the switch-off of Àger. There were a number of stops in between, GPS was recording data on the camera. Then they went into the town of Àger and took a timelapse image of the switch-on from within the town.

Bará and Zamorano complemented the work of Jechow's team. While Jechow was in Balaguer they drove from the hotel to Balaguer measuring with roadrunner and taking some all-sky photographs. They returned together to Àger following the same route with a 5 minute difference in the positions of the cars. They have complimentary all-sky images taken from about 15 kilometers from Balaguer. The two teams were unfortunately never at the same sites at the same time.

In addition to the extinction measurements with Espey, Ribas and Canal-Domingo set up two ASTMON cameras on the roof at PAM. The ASTMON cameras comprised the older one from the park, and the newer one belonging to Andreas Hänel. The alignment was done after

astronomical twilight, and began to run in scientific mode from 11:45 pm until 4:00 am. They went on the roof at 11:30 pm to start, and at 4:00 am to disconnect. The only light they might have produced would have been from a computer screen.

Aubé synchronized his two spectrometers at the same site on the PAM roof and programmed them to have the same sequence of exposures. He took two spectra during twilight, and spent the rest of the night using 90 minute integration time with each instrument, with nearly identical starting times. Aubé was on the roof several times, but did not use light (except for sometimes opening his laptop).

Kolláth ran 5 different cameras from 9:00 pm until 5:00 am (not all for the entire night). The cameras included his 60D, the IGB 6D, Ribas's 5D, and Costas's 40D. He was located in front of the entrance of PAM, and should not have made any light. Only two cameras were working with Magic Lantern, so it was quite a lot of work to operate so many cameras.

Bouroussis installed his instruments at 6pm, starting with the luminance meter. He took measurements with the luminance meter at zenith (1 degree FOV) until 10:20 pm. He started logging with the all sky cameras at 9:30, and operated them until 1:30 am.

Zamorano operated TESS-V1 (stars3) connected to PC computer by USB port and took data all night long.

On his way to Montsec, Hänel stayed overnight in the French Parc Naturel Régional de Millevaches en Limousin, which seems to be one of the darkest places in central Europe (Lorenz atlas 2006: <http://djlorenz.github.io/astronomy/lp2006/>, Falchi et al. 2016). The clouds cleared in the late afternoon and the night was very clear. Individual measurements were taken at 3 places with SQM-L #2536 with darker values than have ever been measured before with this instrument. At the same places, all sky photos have been taken. This confirms the extraordinary darkness of the site. Roadrunner measurements with SQM-LU #2486 were taken roughly north - south through the parc along street D36, confirming the dark sky.

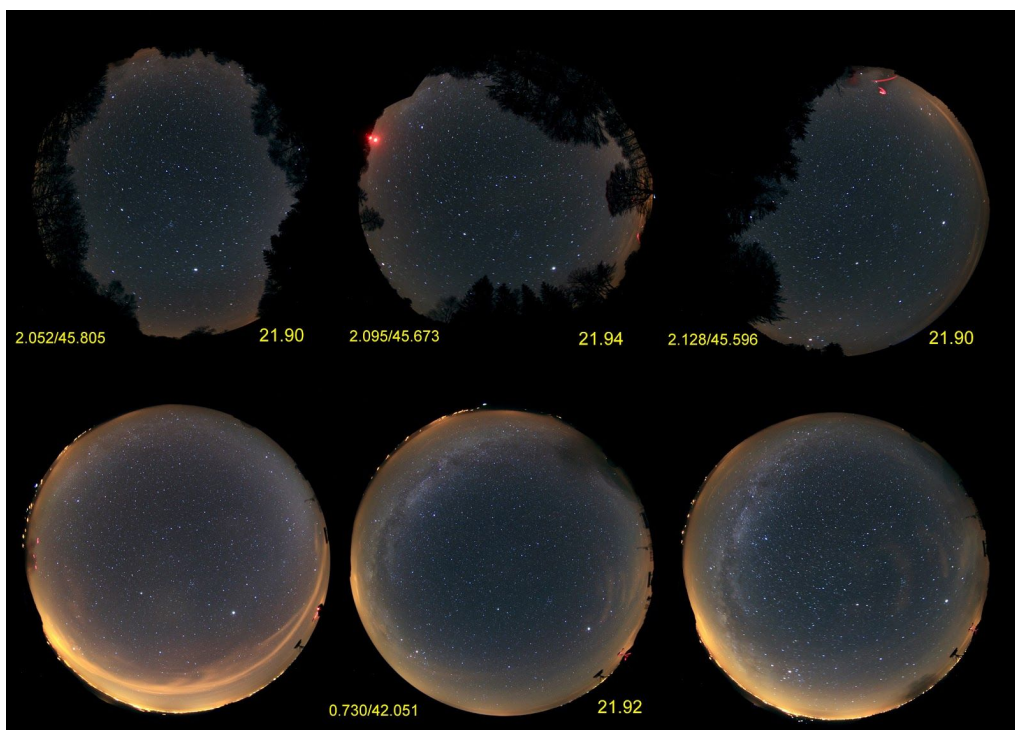


Figure 4: Top: all-sky pictures (Canon D550, 2.8/4.5mm, ISO 800, 3 min) from PNR de Millevache en Limousin (3 places with long/lat and SQM brightness), Bottom: same next night from Parc Astronòmic Montsec-COU.

Instruments operated:

SQMs: all automatically running SQMs were left running on PAM roof, handheld SQMs were used in Balaguer. Vector SQM 3281 was installed as SQM-LU-DL for this evening. New devices from Bará were installed.

Roadrunner: There was two teams taking measurements. Team 1 with Jechow, Massana and Martí were using two SQM in RoadRunner setup (1040 & 1871). Team 2 with Zamorano and Bará were using on SQM in Road Runner (1738). Both teams did measurements between Balaguer and Àger and also taking all sky images at different positions.

DigiLum (pointing at zenith): installed on the walkway in front of the PAM (see Figure 3), and was covered for dark current measurements hourly by Kolláth.

ASTMON: Both were installed on PAM roof

Lightmeters: 9 on roof

Luminance meter

Cameras:

AVT CCD cameras installed on a sub-roof to avoid light from laptop influencing other instruments: Bouroussis

DSLRs: Kolláth, Jechow x1, Bará, Ribas, Zamorano

Wim Schmidt: Observatory first and then 4-5 measurements from the parking area of PAM-COU

Apps: VdN app used during twilight from camping area next to Hotel

Spectrometer: Both spectrometers run from the roof

Day of May 4

At noon, an event was held with representatives from the area, including major of Àger, president of County Council, vice-mayor of municipality of Balaguer. Ribas introduced each participant to the authorities, and the authorities had an opportunity to ask questions of the participants. More details can be found in Section 3.

In the afternoon, team members rested, analyzed data, or prepared for the next night. Andreas Hänel arrived in the early evening, and his SQMs were connected on the roof of PAM.

Night of May 4-5

Weather and environment:

The sky was perfectly clear during the day, with a forecast for cirrus increasing overnight. At sunset there were cirrus clouds far in the South and West, but the rest of the sky was clear blue, and this was also the condition at nautical twilight. At the beginning of the night there was considerable cirrus, but after about 1 am the situation became quite stable and quite dark. According to ceilometer data, there were high clouds during almost all night, only disappearing after 5am. The humidity level remained below 65% throughout the night.

Switch off in Balaguer was in two steps again: first the automatic switch off at 11:30, followed by the manual switch off around 11:44. The dome of the planetarium was opened for ten minutes around 11:00 pm, green laser pointers were used from the telescopes from 11-12. The public left around midnight, and some used lamps that affected the DigiLum and the cameras.

Description of activities:

Kyba, Jechow, Zamorano and Bará went to Balaguer, Jechow to the same site as the day before but with a 5D Mark II and Sigma 8mm in order to watch the switch off. Bará and Zamorano observed the switch off from 41.8275N, 0.7581E with a canon 5D Mark II and a Canon 120D. Bará and Zamorano also recorded the brightness with an SQM (#1738). In Balaguer there was some significant cirrus, especially away from zenith.

Wuchterl reconfigured the lightmeters during the late afternoon, 3 continued on the PAM roof, 4 were moved to the Observatory and installed at the Montsec B lightmeter location. In the end only two ran from that site, for the whole night. Mohar (external to the IC) joined Wuchterl and tried to use his nanoluxmeter, but experienced difficulties with the measurements, perhaps associated with the electronics of other instruments at the site.

Bouroussis measured from PAM using the luminance meter (measuring at zenith) and his all-sky cameras and the canon 40D taking images until about 3:30 am.

Spoelstra operated the DigiLum pointing to zenith on the walkway in front of the PAM, with dark current measurements every hour.

Hänel measured with SQM-LU #2486 installed with a green filter and with the luminance meter Mavo-Spot during dawn. At the Observatory he took all-sky images with a 550D and 4.5mm fisheye and panorama images (to compare to similar photos taken 5 years ago); he also took all-sky images at PAM and took test measurements with SQM-Droid.

Kolláth did parallel fisheye observations from Observatori and PAM (Spoelstra assisted from PAM), starting at about 4:00 he was at PAM and together with Jechow made parallel measurements with nearly all of the all-sky cameras. He tried to detect the switch-off of Balaguer from the Observatory, but was not able to detect it.

At the PAM, Espey made SQM linearity checks at twilight with the two SQMs and neutral density filter, and also took SQM-V observations around about 2-3 am.

Schmidt did two extinction series from the Observatory, until about 2 am.

Ribas ran the two ASTMOM on the PAM roof starting at 11:20 pm and lasting until 3:30 am. The ASTMOM from Andreas stopped from 0:45 am until 2 am due to a problem. Ribas also did SQM-V observations at 1:15 am. Jechow did a second SQM-V measurement shortly before 4am. Classical photometric observations were not made because it was unclear that the weather conditions would be sufficient.

Aubé ran the two SAND spectrometers with identical parameters as yesterday, but using an integration time of 2 hours. Only evening twilight observations were taken.

One NSB map was obtained with the NSB mapper operated by Zamorano at the PAM-COU parking.

Instruments operated:

SQMs: all automatically running SQMs were left running on PAM roof. New devices from Hänel were installed.

DigiLum (pointing at zenith): installed on the walkway in front of the PAM.

ASTMON: Both were installed on PAM roof.

Lightmeters: Two lightmeters running in Observatory OAdM and others in PAM-COU

Luminance Meter

Cameras:

AVT CCD cameras installed on a sub-roof to avoid light from laptop influencing other instruments: Bouroussis

DSLRs: Kolláth, Jechow x1, Bará, Ribas, Zamorano, Kyba

Wim Schmidt: Observatory extinction measurements

Apps: None

Spectrometer: Both spectrometers run from the roof

Day of May 5

Participants had free time in the morning and afternoon and some went to the Observatory to see the telescope during the daytime. Ribas arranged for a switch-off of the streetlights in Àger after 1:30 am. The automatic switch off in Balaguer happened at 11:30, but the manual switch-off of ornamental lighting did not occur as the lights were already off.

Night of May 5-6

Weather and environment:

The sky became progressively cloudier throughout the day, with high clouds. The entire evening was characterized by high thin clouds. Stars were visible, and there was a moisture layer up to the top of the mountain which allowed scattered light from very remote cities to be seen. The scattering from upward-directed lights from the villages to the North of the mountain was very conspicuous. The sky was covered the whole night with medium and high clouds and early in the morning low clouds also appeared according to ceilometer measurements.

The manual part of the ornamental lighting was not turned on again, and was therefore not on during the evening. The automatic switch-off of the ornamental lighting in Balaguer took place at 11:30 pm as planned. The lights of Àger were turned off in four steps between 2:06:45 and 2:14:55 (times observed from DigiLum). The switch on of Àger was at 2:59 am. From about 2:00-2:40 am a brightly lit tractor was working in the field near PAM.

Description of activities:

Ribas, Zamorano, Bará, Aube, Schmidt and Hänel travelled in two cars to examine the spectra of lamps that had been replaced in the last two years using two Blue Wave Stellarnet spectrometers. Spectra were obtained in the villages of: Tremp (Sodium and Amber LED), Guardia (filtered white LEDs and amber LEDs), Avellanes (PC Amber LED), and Àger (private old Mercury lamps). Hänel and Schmidt then took photos of the different lamps and spectra through a diffraction grating and with an infrared filter. Following that part of the team moved to Àger to prepare for the switch off. During the trip, Hänel took roadrunner SQM data, and afterwards took handheld SQM measurements at PAM in order to compare to his measurements at other European locations, but the sky was almost overcast at all locations.



Figure 5: Part of the team measuring spectra in Tremp



Figure 6: Street scenes in Tremp. Top: visual light, left: sodium high pressure, illumination levels 50-60 lx, right: pc amber LED, illumination level 35 lx. Bottom: near infrared light, filtered with a 730 nm filter: sodium has bright emission lines at 818/819 nm.

Jechow, Bouroussis, and Spoelstra travelled to Balaguer to observe the switch-off for a third time. This night only the automatic lamps were turned off. The DigiLum was operated by Spoelstra (mounted on a car pointing and pointed at the zenith (see figure 7).



Figure 7: DigiLum installed on the back of Spoelstra car.

A Canon 6D was operated by Jechow, and both a Canon 40D and the Minolta LS-100 luminance meter were operated by Bouroussis. The luminance meter was operated both at zenith and scanning several points slightly above the horizon, towards the skyglow from the spotlight above Balaguer. Jechow also made SQM-V measurements from this site. The group then reproduced the transect from the night of May 3-4 towards Àger under cloudy conditions, using all of the instruments looking both horizontally and vertically, with the DigiLum looking at zenith, and the Minolta looking at both zenith and the brightest area in the sky above Balaguer (scanning by hand).

The group then went to the final location at Port d'Àger, overlooking the valley of Àger. They monitored the switch off of Àger using the DigiLum, and the cameras pointing towards Àger. After the switch off they split up, and Spoelstra and Jechow went into Àger to observe the switch on using all sky images and the DigiLum, reproducing one point from the entrance of the village which had previously been observed on the night of May 3-4.

Kollath ran a Canon 6D and 60D at PAM, and also the Sony with a 90 mm lens to look at the switch off of Àger. The illuminated tractor interfered with the observation of the switch-off.

Wuchterl and Mohar made measurements in Coll d'Ares. Horizontal illuminance was measured with the lightmeters, and in parallel with the prototype nanolux meter, and 3 fisheye cameras were also used for comparison. Both instruments agreed that the horizontal illuminance decreased from 1.4 mlx to 1.2 mlx from 0:30 to 3:30. It looked like there was a layer of humidity as well as a very thin cloud layer. 5th to 6th magnitude stars could be observed through the cloud layer.

The spectrometers of Aubé were run in the same configuration as the night of May 4-5 (2 hour integration time, starting at astronomical twilight, with one spectrum obtained about 5 minutes after sunset. The two ASTMONS were run from 11:30 pm until 2:00 am (when one failed), and 3:30 am.

Instruments operated:

SQMs: all automatically running SQMs were left running on PAM roof.

DigiLum (pointing at zenith): installed on the back part of Spoelstra car doing measurements between Balaguer and Àger.

ASTMON: Both were installed on PAM roof.

Lightmeters: Some lightmeters running in Coll d'Ares and others in PAM-COU

Cameras:

DSLRs: Kolláth, Jechow x1, Bará, Ribas, Zamorano, Kyba, Bouroussis

Apps: None

Spectrometer: Both spectrometers run from the roof

Lamps spectrometer: Two (Aubé & Bará) in Tremp, Avellanes, Guardia and Àger

Day of May 6

The non-weatherproofed ASTMON was removed from the roof around 10 am, and some computers were also removed from the roof because of light rain. Participants had free time and some went on an excursion during the morning and early afternoon. We met again at 5:30 pm to record notes, have discussions, prepare for the final night, and prepare the logistics for removing the instruments. A decision was made to leave many of the SQMs at PAM, and have them mailed back to the participants in several weeks.

Night of May 6-7

Weather and environment:

The weather during the day was overcast with periods of light rain. The forecast for the final evening predicted overcast skies and rain in the early morning.

Description of activities:

Most of the instruments were taken down from the roof of PAM in advance of the predicted rain. A decision was made to leave many of the SQMs, especially the SQM-LU-DLs at PAM to run for a longer period, and then to move them to Lleida in order to have a comparison point with a much larger radiance. They were shipped back to the participants after a few months.

After Campaign in PAM

Some SQM were left on the roof of PAM to extend the baseline of data for possible future cross-calibration. The devices running in PAM from 7th to 18th of May were:

LE: 0849, 1687, 1786, 2437, 2444, 3180, 3181, 3186

LU: 0857, 1055, 1118

LU-DL (working as LU): 2548, 2549, 2552

LU-DL: 1998 (ex-556), 2124, 2129, 2555, 2634, 2749, 2762, 2766

LU-DL-V (working as LU): 2998 (until its failure and sending to Unihedron)

After Campaign in Lleida

As a final step of the campaign we moved some devices (LU-DL) to Lleida city to work in brighter conditions.. The devices running in Lleida from 22th of May up to 14th of June were:

LU-DL: 1998 (ex2556), 2124, 2129 (up to 6th June), 2548, 2555, 2634, 2749, 2762 (up to 6th June), 2766 (up to 6th June)

LU-DL-V (working as LU): 2998 (until its failure and sending to Unihedron), 3003 (starting 27th of May up to 6th of June)

3) Meeting with local authorities

During the morning of 4th of May a meeting of IC participants with representatives of the area took place in Parc Astronòmic Montsec - COU. The authorities and institutions that attended to the meeting were:

- Mr. Lluís Ardiaca, Major of the municipality of Àger (where PAM is placed)
- Ms. Concepció Canadell, President of Consell Comarcal de la Noguera (county council), the institution that officially manages PAM-COU
- Dr. Carlos Garcia, Deputy President of Consell Comarcal de la Noguera and Vice-Major of the municipality of Balaguer
- Mr. Josep Baldillou, General Manager of Consell Comarcal de la Noguera
- Mr. Josep Vilajoliu, Economy & Promotion Head of Consell Comarcal de la Noguera

Ribas introduced each participant to the authorities and also the authorities give the welcome to Montsec to the participants. After introductions there was an open colloquium where authorities could ask participants about the campaign and the measurements done in the area.

Kyba, as MC LoNNe member, explained some general ideas around the project and what this campaign is focused on. Many other participants had the chance to show or explain some preliminary results or data obtained in the first days of the campaign.



Figure 8: Meeting of participants and authorities in PAM-COU

The participants remarked on the good quality of the sky of Montsec and also thanked the authorities for help with the scheduled switch offs of Balaguer ornamental lightning and Àger public lighting systems. The authorities also asked the participants about any idea or suggestion for improving lighting systems in the future in order to keep or improve the night sky quality.

After the colloquium the authorities were invited to visit some of the instruments installed at PAM, especially the ones that are easily accessible such as Digilum and SQM from Spoelstra installed in the parking area of PAM.



Figure 9: Spoelstra explaining how Digilum and SQM measure the NSB

It was a nice meeting with the opportunity to communicate the campaign work and the general ideas of our project to the local authorities. This could also be important for the

Montsec area because these authorities can work towards - or pressure for - night sky protection.



Figure 10: Group picture of participants and authorities in the Telescopes Park of PAM

4) Results and continuing analyses

Study of the data is ongoing, and includes the following projects:

1) Extinction measurements during the campaign

On three days a campaign of extinction measurements was conducted by Wim Schmid, of Sotto le Stelle, the Netherlands. The methodology is simple and makes use of much-used amateur DSLR cameras (see for example Falchi 2011).

Instruments: Tripod with an Astrotec, a portable tracking head. On it a DSLR canon 20D camera with 200 mm lens F 2.8 with a Johnson V filter on it.

Procedure: after polar aligning with a polarscope, raw pictures were made with full aperture, 120 and 180 seconds shutter time, of different parts of the night sky with a remote control. The sky area pictured is around 4.5 by 2.5 degrees.

An extinction measurement series consisted of minimum of 5 different pictures at different elevations, with a minimal elevation of around 15 degrees. Dark images were also acquired. The full series usually required 30-60 minutes to obtain. Afterwards flatfields were made with the same instruments, using a flatfield panel.

Area of the sky: Well known bright stars were chosen as the main targets, in order to make the identification easier. Most of the pictures were taken towards the western sky, because it was

free of both the Milky Way and any visible sky glow. The quality in that direction seemed best.

The majority of the images were taken from the following constellations: Auriga, Gemini, Leo, Ursa Major, Ursa Minor and Boötes. On the final night a region in the north towards the Cassiopeia constellation was chosen, because at that time that was the only direction without cloud forming.

Locations: On the first two nights extinction measurements were conducted at the Parking place of PAM-COU and the Observatory OAdM. On the last night, due to deteriorating sky quality, measurements were only undertaken at the Observatory OAdM

Table 1: Summary of extinction measurements during the campaign.

Location	Day	Begin time	Endtime	Mean time	Extinction	R ²
Observatory	3 May 2016	0:45	0:58	0:51	0.17	0.95
Observatory	3 May 2016	1:21	1:48	1:38	0.15	0.98
PAM-COU	3 May 2016	2:34	2:55	2:43.2	0.37	0.91
PAM-COU	3 May 2016	23:05	23:20	23:12	0.21	0.92
PAM-COU	4 May 2016	0:10	0:24	0:16	0.19	0.88
Observatory	4 May 2016	1:05	1:21	1:12	0.16	0.6
Observatory	4 May 2016	2:15	2:31	2:22	0.17	0.97
PAM-COU	4 May 2016	3:30	3:53	3:41	0.19	0.77
PAM-COU	4 May 2016	4:18	4:38	4:29	0.33	0.93
Observatory	4 May 2016	23:40	23:59	23:49	0.17	0.94
Observatory	5 May 2016	0:41	1:44	1:14	0.15	0.71

Discussion

Most of the time the conditions were fairly stable with a low extinction (less than 0.20) and a high confidence of above 0.90. At the end of the first two nights the conditions deteriorated. The third night the conditions were strange: and at the beginning of the night a horizontal pattern was visible in the sky, but this is not reflected in the numbers. The first series of around 11:45 pm still gave fairly good results, while for the second one around 1:44, the confidence was low although the extinction was still fairly high at 0.17.

2) DSLR cameras in the field: Comparison of switch-off in Balaguer and transect from Balaguer to Àger, switch on and off in Àger

a) Switch-off in Balaguer

During the night from May 3 to May 4 the organized switch-off in Balaguer was tracked with fisheye lens imagery at measurement location LONNE 3 (Outskirts of Balaguer: 41.791100N, 0.797494E, 273m elevation). The sky was clear during this measurement. One of the Canon 6D cameras from IGB was used to take a time series of images starting before the switch off of lights at 11:30 pm. Figure 11 shows false color brightness maps of the night sky luminance

a) before (11:28 pm) and b) after (11:50 pm) the switch-off. The switch-off resulted in a clearly observable change in overall sky brightness detectable by all-sky imagery. Panel c) in Fig. 11 shows the difference in sky luminance obtained by subtracting b) from a). As expected, the biggest change occurred near the horizon in the direction of the city. However, even at the zenith a change of 10% was observed. This measurement was repeated on the evening of May 5th under partly cloudy conditions but, for brevity, those results are not shown here.

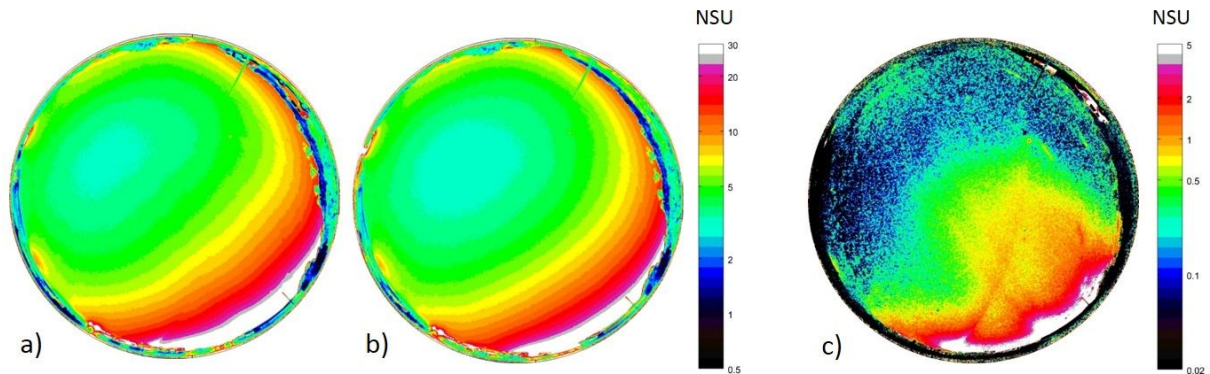


Figure 11: False color images calculated from all-sky pictures taken a) before and b) after the switch-off in Balaguer for clear conditions during the night from 3rd to 4th May. c) shows the difference calculated by subtracting the two original images. (1 NSU = 0.2894 mcd/m² see below).

b) Transect from Balaguer to Àger

After the organized switch-off in Balaguer, a transect from position LONNE 3 (Outskirts of Balaguer: 41.791100N, 0.797494E, 273m elevation) to position LONNE4 (Port d'Àger) was performed. At several stops all-sky images were taken. This was also repeated on the partly cloudy night two days later. The results from two locations are shown in Figure 12. The upper row shows location LONNE 3 about 1.4 km from the centre of Balaguer and the lower row shows a location about 5 km from the centre of Balaguer (41°49'12.00"N; 0°46'21.00"E). For clear sky conditions (left column), the zenith brightness falls off relatively quickly when moving from the first to the second location. However, for the partly cloudy conditions (right column) the zenith sky brightness remains in the same regime. It is also evident, that the amplification of sky brightness by clouds is more dramatic outside of the town than close to the town. Furthermore, light emitted from distant towns seem to have a bigger role for the second location.

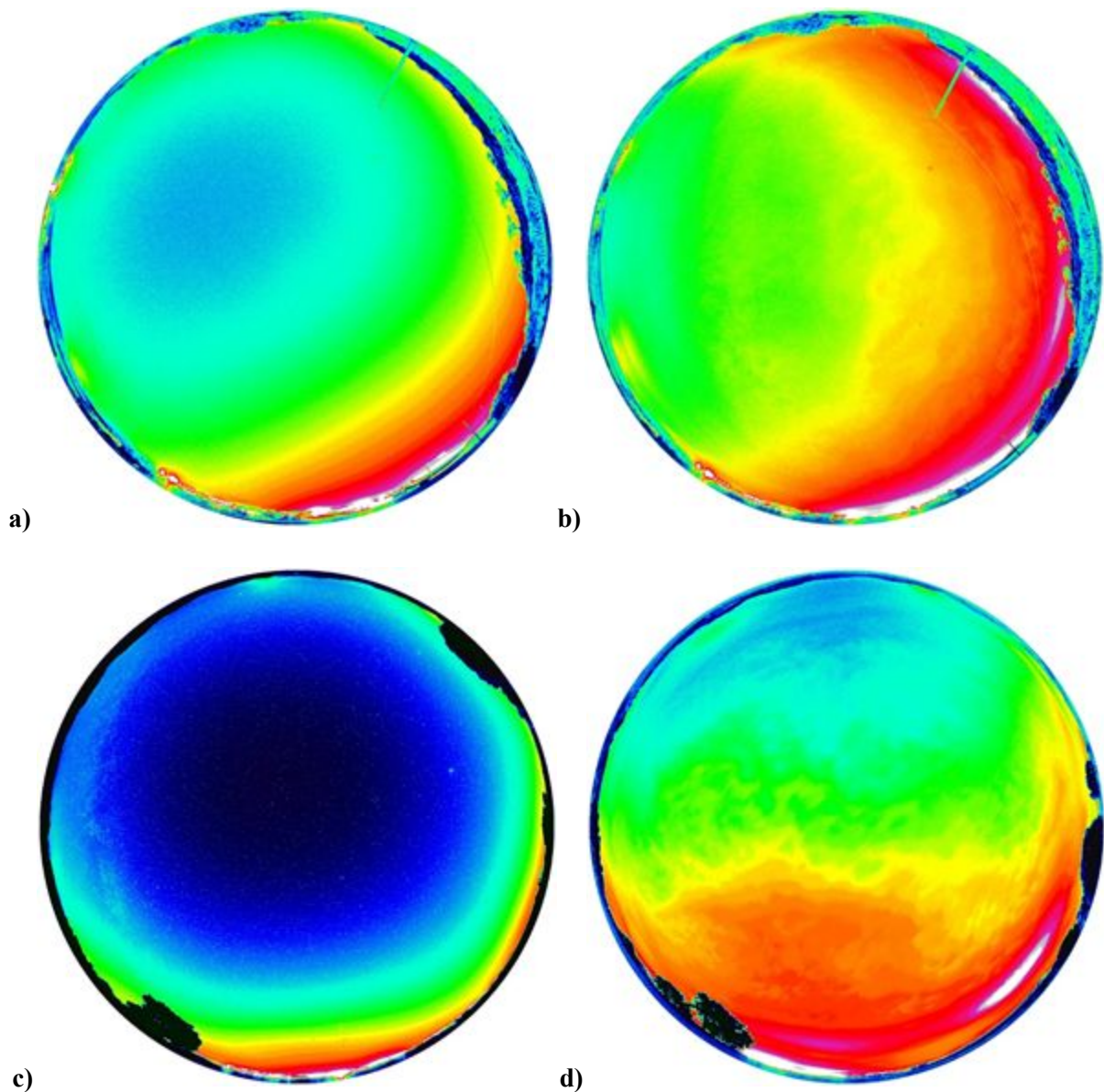


Figure 12: False color luminance plots from all-sky pictures taken at two stops of the transect from Balaguer to Port d'Àger: a) Location LONNE3 clear conditions b) Location LONNE3 partly cloudy conditions; c) d)

c) Switch-on in Àger

During the switch-on of the lights in Àger on the clear night of May 4th 2016 between 4:22 AM and 4:33 AM, one of the Canon EOS 6Ds was positioned on the street at the corner “Carrer de la Font” and “Carrer de la Fontetes” in front of the bakery (42°00'08.9"N 0°45'38.6"E). A series of all-sky pictures was taken from that position. Four of the pictures are shown in Figure 13 with a) before and d) after the switch-on. The images were approximately adjusted to the brightest pixel value to roughly mimic human eye adjustment. When the lights were switched off, the Milky Way was clearly visible and the town had a ghost town like atmosphere (Fig. 13 for RGB and Fig. 14 for false color image). When the lights were switched on, the sudden brightness from the street lights was overwhelming for

the human observers and the Milky Way and stars disappeared also in the all-sky images. The camera suffered from light scattered from dust particles on the lens (Fig. 13c).

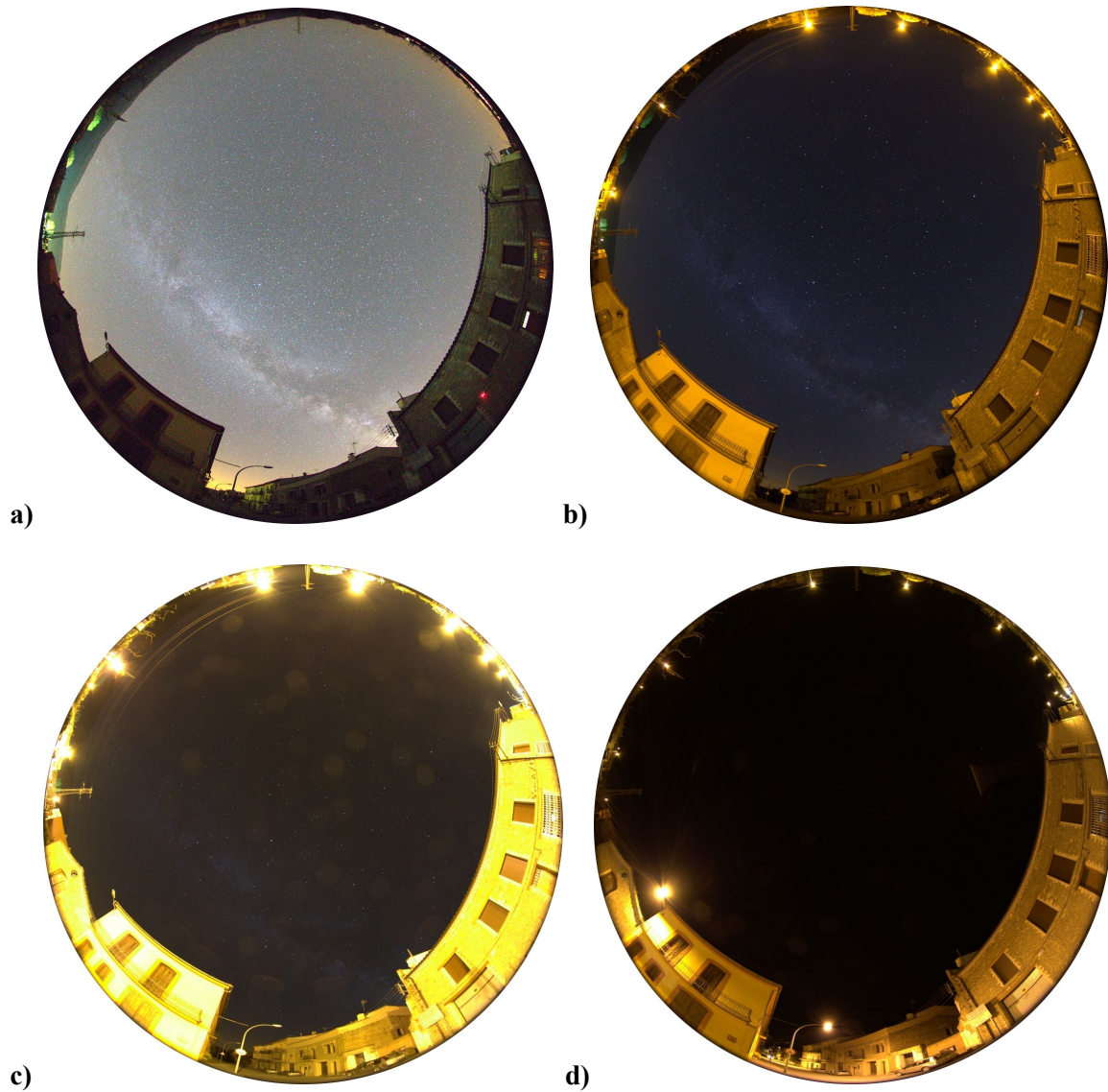


Figure 13: All-sky pictures taken in Åger during the switch-on of the lights on May 4th 2016 a) 4:21 am; b) 4:23 am; c) 4:27 am; d) 4:35 am.

This measurement was repeated during the partly cloudy night from May 5th to May 6th, but from a different observation point that had no or very little direct light shining into the camera. The results are shown in Figure 14 c) before and d) after the light has been switched on. For comparison the false color plots showing luminance values from the bakery location are also included for a) the clear night and b) the partly cloudy night.

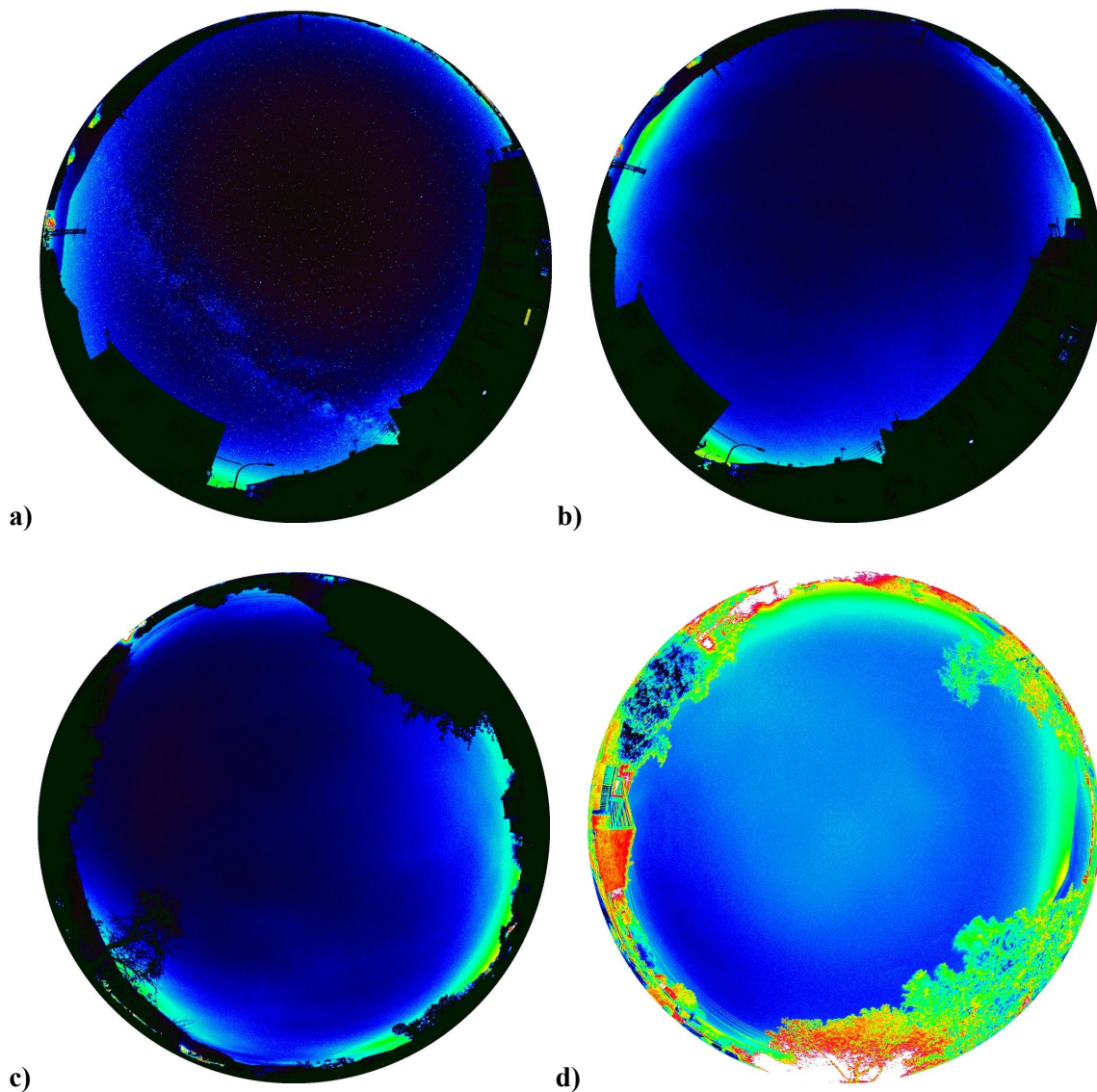


Figure 14: False color luminance plots from all-sky pictures taken in the centre of Ager a) with lights switched off on a clear night, b) with the lights switched off on a partly cloudy night. c) was taken just before (2:46 am) and d) just after (3:15 am) the switch-on of the lights on May 6th 2016.

d) Switch-off in Åger observed from Port d'Åger

The controlled switch-off of the lights in Åger on the clear night of May 4th 2016 between 2:40 am and 2:52 am was observed with one of the Canon EOS 6Ds from the lookout point in Port d'Åger. The camera was aligned horizontally to track changes in sky brightness and direct light from the town simultaneously. For the clear conditions, the changes from Figure 15 a) lights on at 2:34 am to b) lights off at 2:52 am were detectable but marginal.

Especially near the zenith the change was hardly perceptible. On the following night, the measurement was repeated for partly cloudy conditions. Figure 15 c) shows Åger before the switch off at 1:59 am and d) after the switch-off at 2:19 am on May 5th 2016. For the partly cloudy conditions, the change in brightness was also perceptible near the zenith (see upper half of the false color plots).

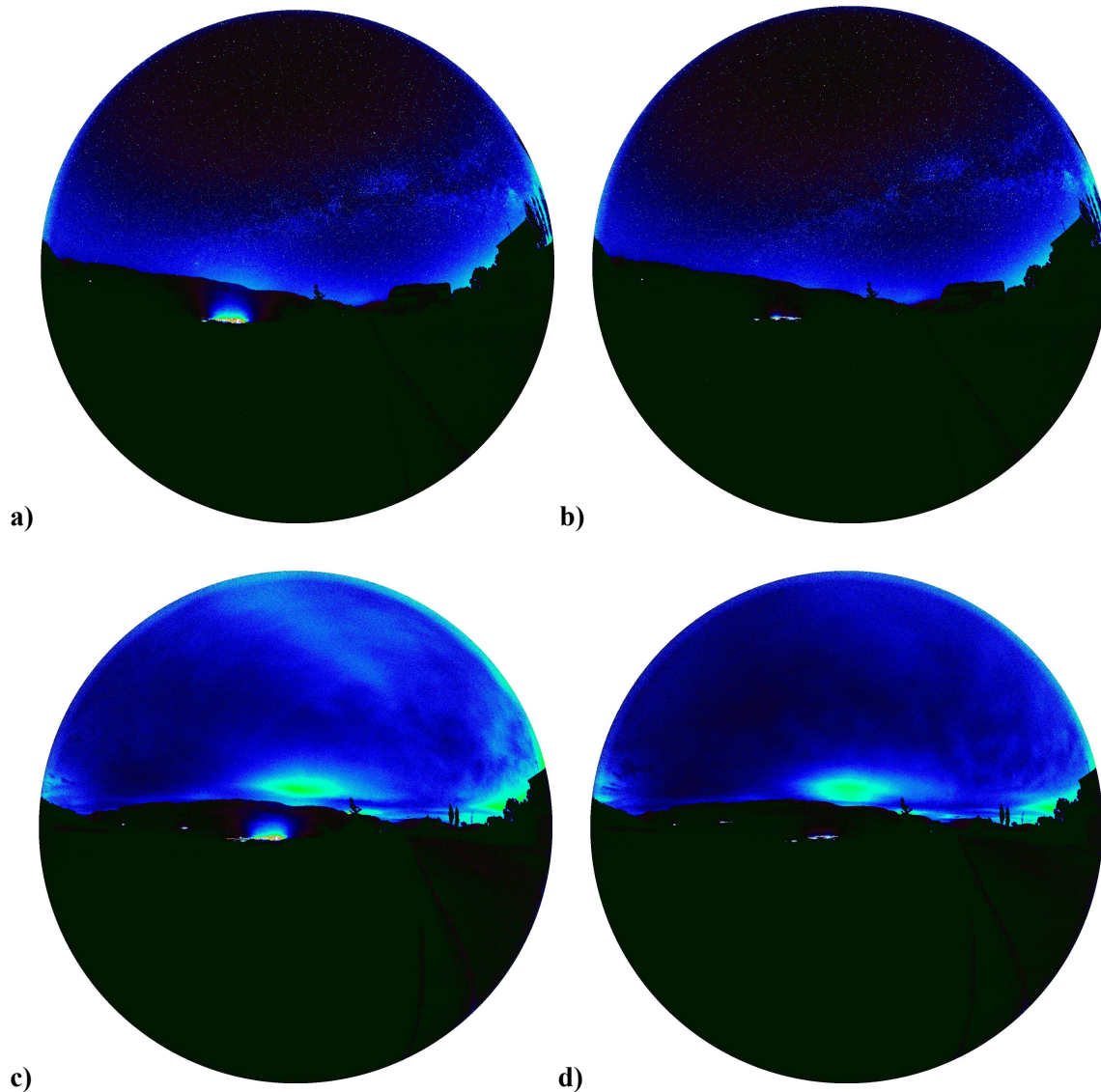


Figure 15: Horizontal fish-eye lens pictures taken in Port d'Àger before (a,c) and after (b,d) the switch-off of the lights on May 4th (a, b) under clear conditions and May 6th 2016 (c, d) under partly cloudy conditions.

e) SQM measurements during switch off

The night of May 5 the public lighting of Àger was switched off to perform a test on how the illumination of this near but small village affects the sky brightness measured nearby. Most of the contribution to the brightening of the sky at PAM-COU is expected to come from Balaguer, Lleida and even Barcelona. That night the sky was cloudy.

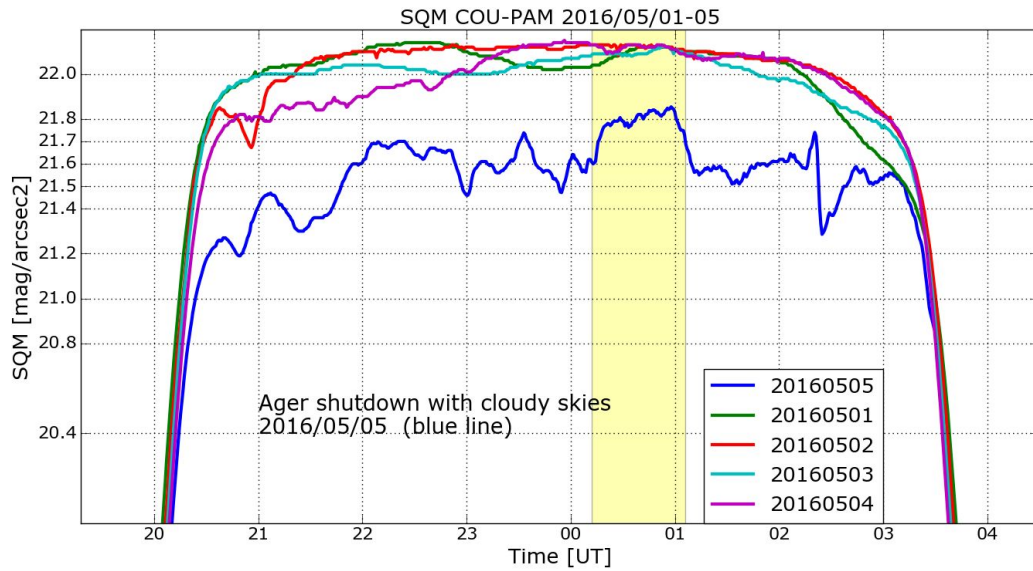


Figure 16: Night sky brightness measured with SQM from PAM-COU for the different nights of the campaign. The darkening during the the test (yellow shadow, blue line) is apparent.

As the sky was cloudy the effects was apparent as it is shown on the plots. The darkening during the the test (yellow shadow, blue line) is around 0.2 magnitudes at PAM-COU (3.3 km from Åger). The same effect was recorded from Cal Maciarol (2.3 km).

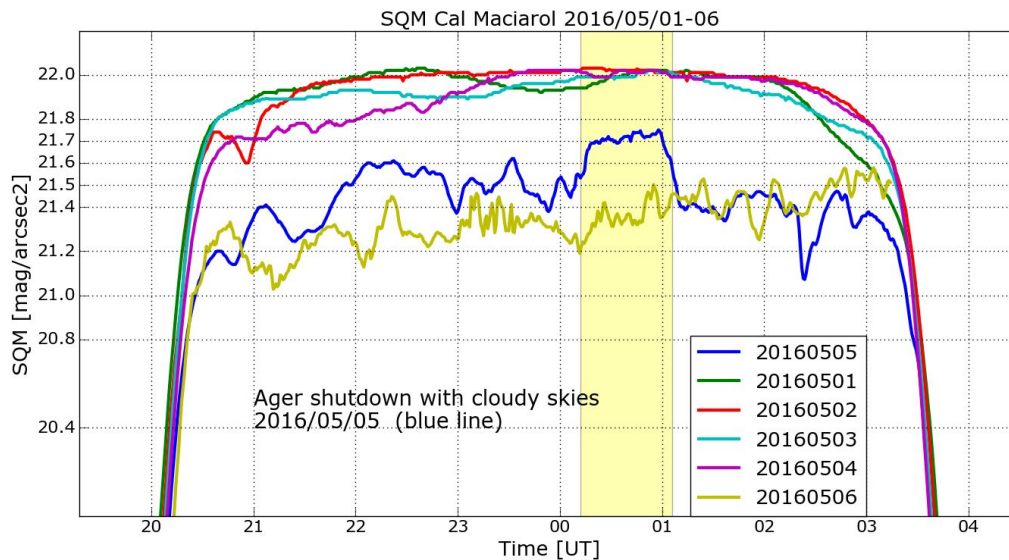


Figure 17. Night sky brightness measured with SQM from Cal Maciarol for the different nights of the campaign. The darkening during the the test (yellow shadow, blue line) is apparent.

3) Comparison of all sky cameras running in parallel

We ran several digital cameras (Canon EOS 6D, 60D, 5DMII, 40D) parallel to perform an intercalibration of the devices. A fit to the mean sky radiance as a function of zenith angle was used to get a well-defined zenith radiance. This value was used for all the comparisons.

For the camera data the radiance is given in Natural Sky Units (NSU, see Jechow et al. 2016), where 1 NSU is equivalent to $21.6 \text{ mag/arcsec}^2$. The Digilum data for the second night was used to calibrate all the cameras. For this procedure the following conversion was used: $1 \text{ NSU} = 0.2894 \text{ mcd/m}^2$ – which is consistent with the SQM definition of NSU.

The cameras performed consistently as the following figures demonstrate:

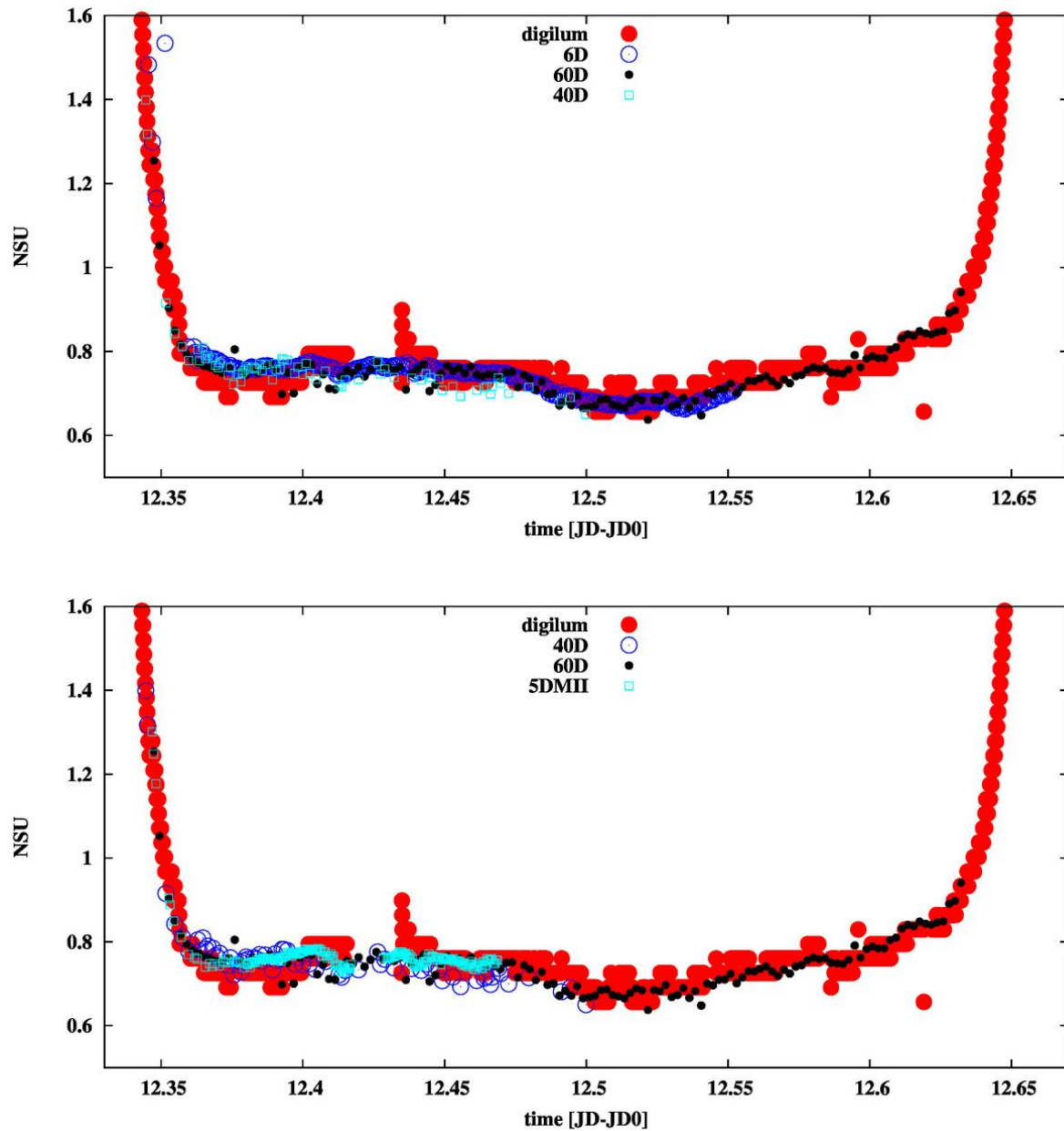


Figure 18: Digital camera measurement of the variation of the zenith sky radiance during the second night (3rd-4th of May) compared to Digilum data.

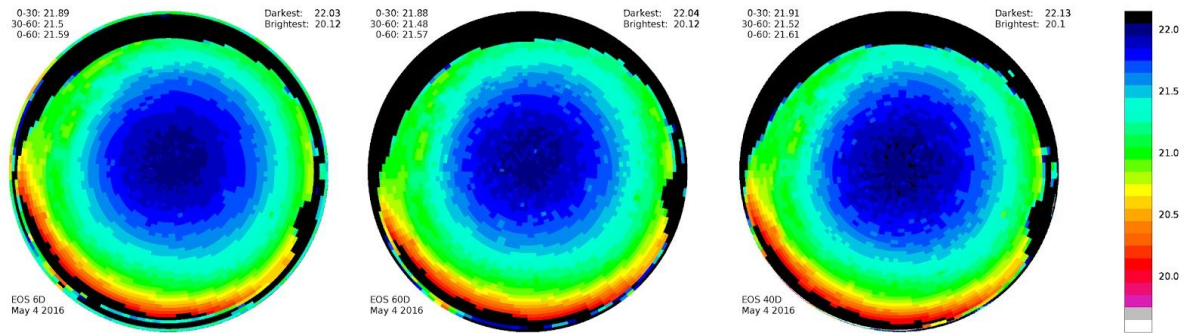


Figure 19: Comparison of the whole sky photometry with 3 different cameras

4) Comparison of measurements taken by CCD cameras and portable Luminance meter

Bouroussis installed a set of CCD cameras made by AVT and calibrated for luminance measurements. A portable luminance meter (Minolta LS-100) was also installed close to the CCD cameras. CCD cameras were equipped with all-sky lenses (Sigma and Fujinon-Panomorph). The instruments are shown in Figure 20.



Figure 20: AVT CCD cameras and Minolta LS-100 luminance meter.

Measurements launched around 19:00 each day from 3th to 5th of May. The Minolta meter was not used during 5th of May because it was used for the Balaguer project. The Minolta meter has a field of view of 1 degree and was pointed to the zenith and the same patch of sky was extracted from the all-sky measurements for comparison. The results of the two types of instruments are shown in Figures 21-23.

The Minolta LS-100 can measure down to 0.001 cd/m^2 , while the uncertainty of measurements is visible below 0.003 cd/m^2 . This can be clearly shown in the corresponding Figures. Data-taking with the LS-100 was stopped after it reached this limit. The CCD cameras continued to measure lower luminances down to 0.0004 cd/m^2 using pixel binning up

to around 02:00 am. We note that both these instruments were calibrated using the same type of luminance source (Illuminant A).

The following graphs show that the two type of instruments have almost identical measurement results for the two nights when data from both were available. The time points where pixel binning occurred are shown as spikes in the graphs, and the capture of dark images is shown as step-down gaps in the graphs.

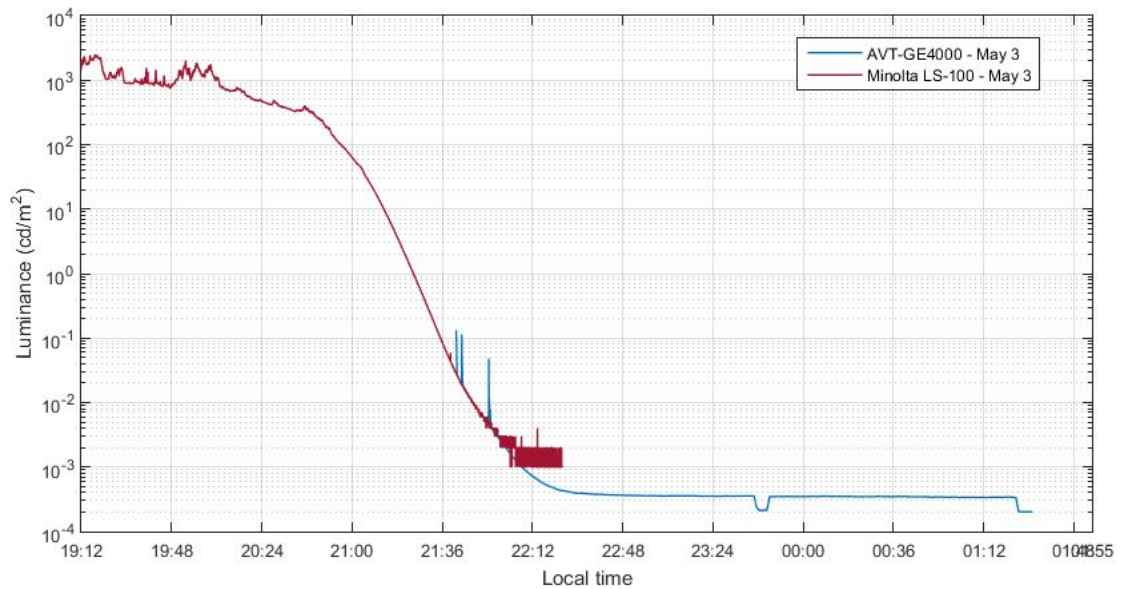


Figure 21: Measurements during May 3.

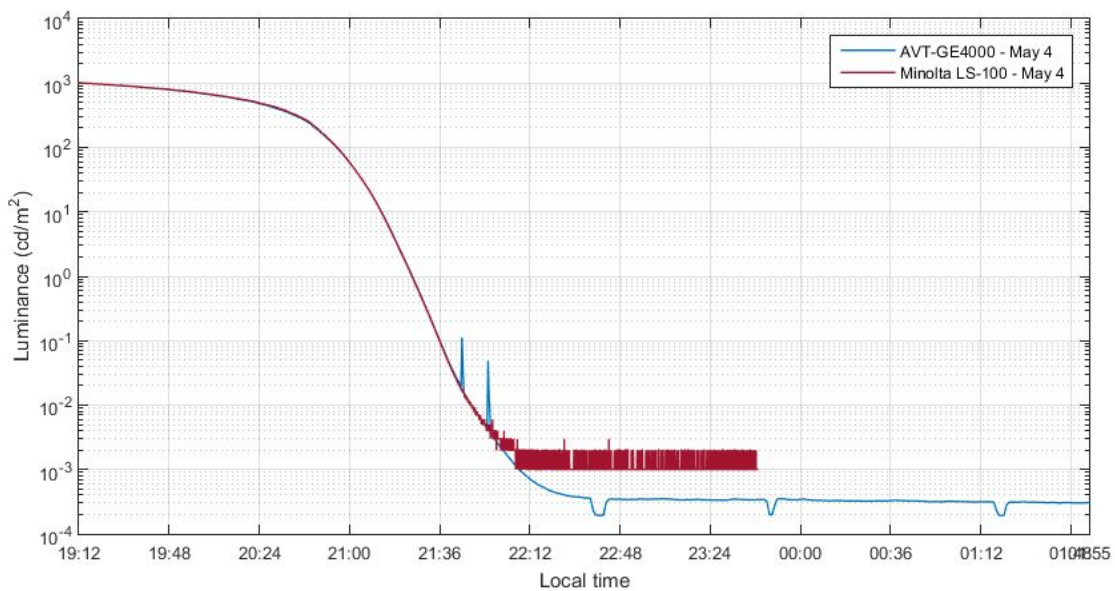


Figure 22: Measurements during May 4.

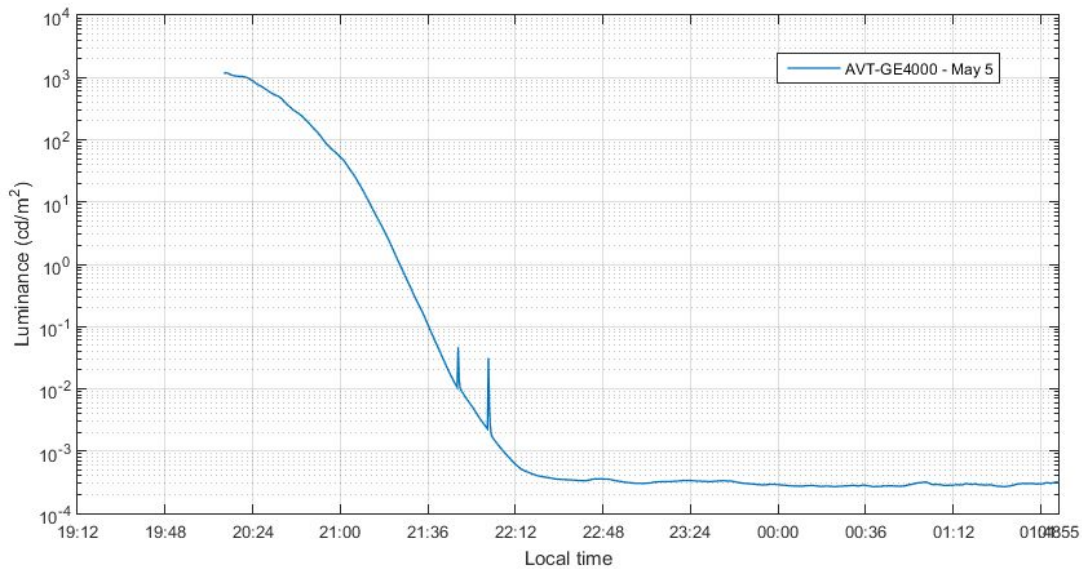


Figure 23. Measurements during May 5. (Minolta LS-100 was used in Balaguer)

5) Lightmeter and Luminance meter

The Lightmeter is an all-weather instrument based on an outdoor photovoltaic cell that is “in-situ” calibrated to luminance or irradiance using natural light sources, notably the Sun and the Moon. The recommended measurement quantity for long term-monitoring with the lightmeter is sky-irradiance (often total radiation or global radiation in atmospheric studies), an energy flux-density expressed in W/m^2 , or the horizontal illuminance expressed in Lux. While the Lightmeter can be calibrated to illuminance, it does not use a CIE-conforming filter. Thus its accuracy depends on the proximity of the main moments of the frequency-distribution of the sky-radiation to the one of solar, lunar and twilight total radiation that is used for calibration.

The Mark 2.31 Lightmeter with the serial number V06.10 S/N 918020.000 (or LP020, for short), was set up on the north rim of the roof of the PAM-COU main building, about 2m to the E of the SQMs, and about 50 cm above the roof-level, but later moved to a location 4m behind the rim and lifted to the same level as the SQMs entry window (about 1m above the roof). Following the measurement concept of the Lightmeter, the instrument was calibrated to the Sun and the twilight with data obtained in-situ at the campaign. This approach is to ensure long-term stability of the Lightmeter's measurement system in the possible presence of unknown ageing effects. The automatic fitting procedure gave a best fit on the morning-to-noon data-stretch of May 4th with a modelled range from 0.00051 to 110,000 lx, with a leading linear coefficient $c = 7.786\text{e-}07 \pm 4.673\text{e-}10$ Lux/count and a conversion factor, f of 110 ± 3 Lux/[Watt/ m^2]. The latter is as usually obtained by a simple atmospheric model to calculate solar total radiation and based on a surface value of 108,000 lx for the Sun. The full set of coefficients a , b , c , x_0 , d , f is $1.95\text{e+}05$, $5.14\text{e-}03$, $8.08\text{e-}07$, $-6.03\text{e-}04$, $6.62\text{e-}03$, 110.8, resp. and a reduced relative reduced chi of 0.043 (i.e., about 4% relative precision when compared to the model). Note that the derived zero-point offset, x_0 , of $-6.03\text{e-}04$ lx, that is determined in the fit routinely to account for a constant background, usually extra air-glow or light pollution, is only about 10% of the natural sky and thus consistent with the Montsec clear-sky-conditions being below the IAU-limit for light pollution in the context of observatory site protection.

For details see e.g. the calibration section of the Lightmeter-Wiki <http://lightmeter.astronomy2009.at>. An overview over the LP020 measurements are shown in Figure 24. Figure 25 shows a zoom into the mlx-domain with a linear ordinate.

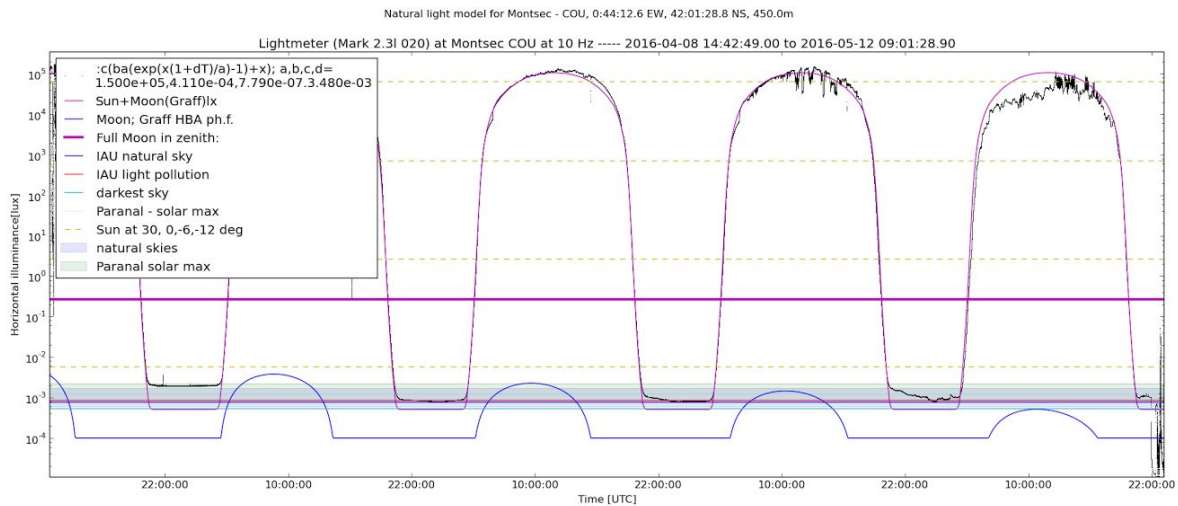


Figure 24: Horizontal illuminance measured by the Lightmeter LP020 with a sampling rate of 10 Hz at the PAM-COU-roof at Montsec – overview. Black: individual measurements; Magenta: Natural light model for Montsec for an assumed extinction coefficient of 0.23 magnitudes per airmass. The model includes the Sun, the Moon, the twilight and constant air-glow. The blue line is the contribution of the Moon alone. The thick horizontal magenta line is the full moon in zenith value, shaded areas denote ranges of natural sky values measured at Cerro Paranal during the solar maximum and minimum (converted from Fernando Patat's, ESO Messenger). Clearly we find natural light levels at Montsec, falling under the IAU-limit for light pollution (horizontal blue line) for significant fractions of the night-time. Very low values (around 10 μ lx) at the lower right corner

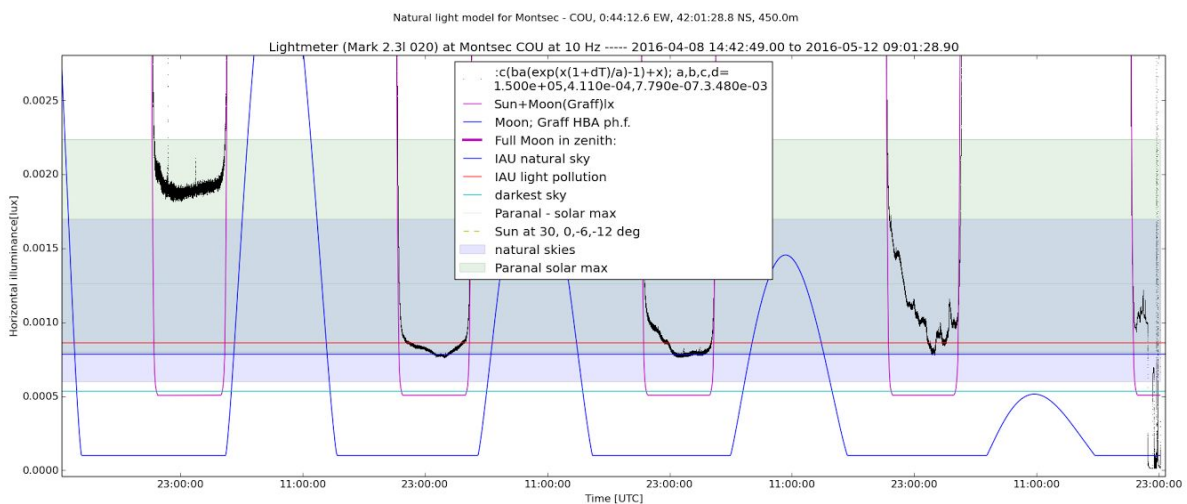


Figure 25: Same as Fig.24 but now with linear ordinate and the mlx region typical for a moonless natural night. Shaded areas denote ranges of natural sky values measured at Paranal during the solar maximum (green) and minimum (blue). In the overlap region, shared by solar minimum and maximum conditions, the two colours of the shading mix to a darker grey. Note the scatter – visible as width of the lines formed by the individual measured points – that is present except on the last evening.

There is an apparent difference in the spread of measurements (apparent thickness of the point cloud of individual measurements that typically combine into a line) between the nights. At first glance this looks like scatter that seems weaker in the second to third night and absent in the final night. But a closer inspection shows that the high sampling rate of the Lightmeter can resolve a regular signal in time, see Fig. 26. An oscillatory signal with an amplitude of $15 \mu\text{lx}$ is detected with a signal-to-noise ratio of close to 100. We note that it looks similar to a partially-resolved beating phenomenon or stroboscopic effect in the illuminance time-series. It is only visible when the time-axis is sufficiently zoomed to see the full 10 Hz resolution. The signal was strongest in the first night and completely absent in the final one. On the first day the amplitude was 5% with 10 maxima in 39s. The “scatter” reduces to less than 1% when a 3.9s median-filter is used. The signal is undetectable on the evening of May 6th.

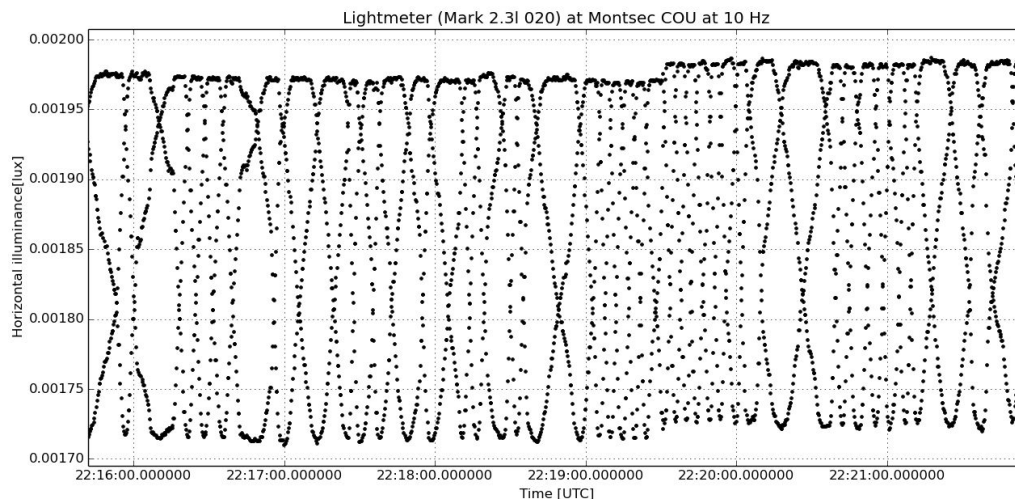


Figure 26: Zoom into the LP020 lightmeter data taken with a 10 Hz sampling. The sample is from just after local midnight (22:00 UTC on May 4th). A pattern reminding of a phase drift of two nearby frequencies, possible the 10 Hz sampling and the 50 Hz of the power network - is visible at this high time resolution. Note the flat tops that need an explanation.

a) Illuminance-distributions of the 10Hz data for the LP020 on the COU roof

Distributions of the light-meter-measurements are shown in Figs. 27-29. Histograms for various sub-samples are drawn in different colours and a narrower sample is always plotted on top of the wider sample. This allows an easy detection of differences because if the number of measurements in two samples is identical the narrower one fully covers the wider one.

A weather indicator to identify clear skies from the time-series is used. It is based on the standard deviation in a sliding window and has been calibrated to Lightmeter-data taken at the VLT site at Cerro Paranal and during the Cerro Armazones ELT site-testing campaign. The indicator has similar properties as the ESO LOSSAM (the ASM Line-of-Sight Sky Absorption Monitor) but has been shown to be much more sensitive for remote clouds because of the lightmeter's all-sky directional characteristic. The “clear” subsample is defined with this indicator. Furthermore the data are sub-sampled using solar and lunar ephemerides for the Montsec site. Subclasses are: (1) All (day and night-time, no selection), (2) Night (only data from refraction corrected Sunset (upper rim) to Sunrise), (3) Dark (with the Moon four degrees below horizon to avoid the Moon and any noticeable effects of the lunar twilight), (4) Clear Dark (Dark nights with the weather indicator signalling no overcast), (5)

Clear Dark no ice (Clear Dark nights with no ice. This is to select data with sensor temperatures above the freezing point to make sure no snow or ice cover is present). The plots show thus a magenta histogram (“no ice”) on top of a cyan coloured histogram of “clear and dark” moments, which in turn is on top of a red histogram for “dark” conditions that include the cloudy ones. The two lowest levels - partially or completely covered by the bins of all other samples if they are not empty - are the green “night” and blue “all” conditions (more than 5 million) that also contain the twilight and daytime measurements, respectively.

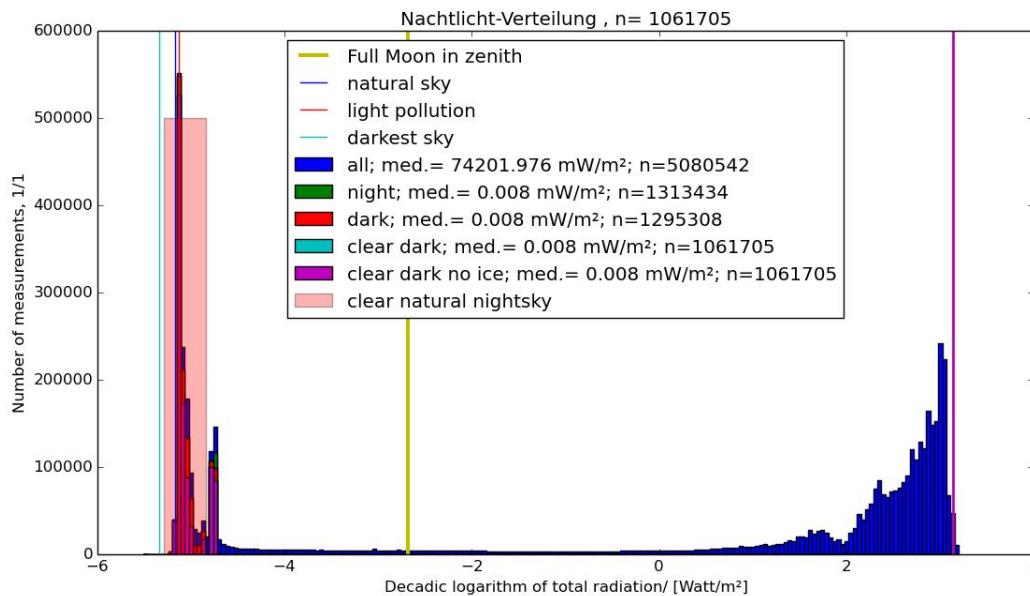


Figure 27: Distribution of horizontal irradiance values measured by the LP020 Lightmeter at the COU roof with reference-values marked by vertical lines and shaded areas. The lightmeter in that case is calibrated to W/m² with a solar total radiation model giving a value of 110.8 Lux/Watt for the conversion to the clear-sky total solar radiation predicted by the model for Montsec. The “Sun in zenith” value is marked by a vertical magenta line

Figure 27 shows the entire range of sky irradiance measured during the campaign. It extends downward from about 1 kW/m² on the right (near the “3” of the decadic logarithm, that is marked on the abscissa). The distribution is dominated by the blue histogram that is due to total solar radiation and the twilight. Note the second maximum, a small bump in the left wing of the daylight distribution near $\log_{10}=2$. These data are from conditions with sufficient overcast to significantly reduce the total solar radiation – usually weak or patchy cloud cover increases the total radiation by increased scattering of sunlight in the atmosphere. The other major structure is the narrow red (the colour for the “dark” sub-sample) peak near 10^{-5} W/m². This peak is entirely inside the pink shaded area of values typical for the clear natural night-sky. The narrow shape of the peak shows the excellent stability of the conditions at Montsec. Note the sub-peak in the right wing, that comes from somewhat brighter situations that are visible for the first night in Fig. 27. This secondary night-peak is about 1/4th in height of the main peak and illustrates the use of the histogram as 1 of 3.5 nights was brighter. My guess is that it is due to extra stray-light from COU during the very long set-up-phase and all night activity with participants being welcomed and setting up instruments almost throughout the night.

During the daytime these total-radiation calibrated distributions of Lightmeter measurements can be directly compared to pyranometer measurements and climate-research time-series

routinely taken for atmospheric physics research. Some of these data are available - e.g. at the OadM - and a comparative investigation should be a priority.

b) Nighttime distributions of horizontal illuminance

For better intercomparison the following light-distributions are shown using the calibration of the Lightmeter to horizontal illuminance expressed in Lux. Because no CIE-filter is used in case of the Lightmeter this calibration has to be viewed as giving a proxy for Lux.

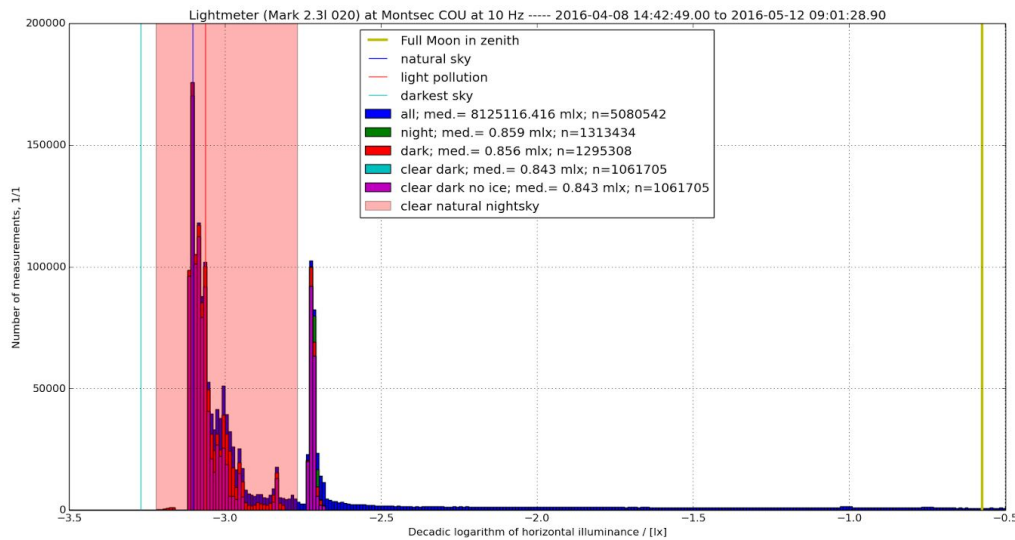


Figure 28 : Distribution of horizontal luminance values measured by the LP020 Lightmeter at the COU roof reference-values. This shows sublunar illuminance values for the same data as in Fig. 27. A conventional illuminance value for the case of the full moon in zenith, 0.26 lx is shown as a vertical yellow bar near the right border of the figure.

Figure 28 shows the distribution of the decadic logarithm of horizontal illuminance measured in Lux for the COU roof and the full campaign duration (cf. illuminance vs. time in Figs 24 and 25). This night-light-level range is dominated by the more than 1.3 millions of measurements obtained during the astronomical nights (Sun deeper than 18° below the horizon, no scattered sunlight in the atmosphere). As is typical for near-natural sites the twilight and moonlight periods that cover a range from a few 100 lx to a mlx contain only a small fraction of the measurements. A part of the thin “twilight bridge” is nevertheless visible in Fig. 28 from the “Moon-value” with about $1/3$ lx to $\log_{10} = -2.5$ (about 3 mlx) as a narrow, essentially flat, blue part of the histogram. The full “twilight bridge” from the daytime maxima around a few 100 Watt/m² to the night-peaks near 10 μ W/m² is visible in Fig. 27. The right peak near \log_{10} of approx. -2.7 in Fig. 28 is dominated by values recorded during the brighter first night, as mentioned above. It most likely reflects the brighter illumination of the roof during that night due to a combination of lights used to assist installation in this set-up night, and also the scattering of office lights via trees and partly by the slopes and nearby mountain-range to the North of the COU, as well as possible residual illumination scattered on the planetarium dome. We also note that during the first night, the Lightmeter was essentially sitting about less than half a meter above the roof below all other instruments and the white SQM housings at 2m distance were visibly illuminated.

c) Natural sky-radiation and distribution of Lightmeter dark-measurements

Finally we focus on the low end of the light-distribution, from a few mlx to $1\ \mu\text{lx}$. Towards the right of Figure 29, the two peaks are visible that correspond to the measuring nights (large peak) and setup night (smaller, peak near the right border of the figure). To the left we see the efforts to determine a dark measurement for the lightmeter – usually a complicated and unnecessary effort due to the high sensitivity of the instrument. To perform this dark measurement the lightmeter sensors, including that of LP20, were covered with two layers of black cloth, though the strong wind made the set-up somewhat unstable by repeatedly (partially) uncovering the sensors. Nevertheless a clear peak of the “dark measurements” is seen at $\log_{10} = -4.9$, i.e. about $1.3\ \mu\text{lx}$. The apparent quantisation of values in this range comes from the design of the Lightmeter that required the lower range of the A/D-converter to be set in a way that maximised the working-range to provide maximum dynamic range. Thus the detector and amplifier noise usually remains invisible.

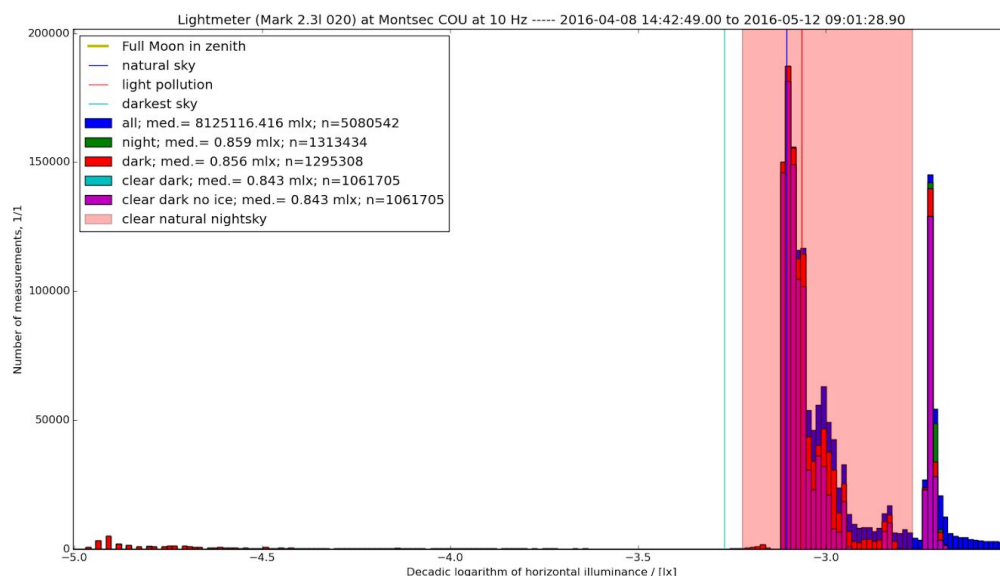


Figure 29: Distribution of horizontal illuminance values measured by the lightmeter at the COU roof with references - mLux range (peaks in and near the shaded area of natural moonless night-sky conditions) and dark-measurements (small bump near the left border at $\log_{10} = -4.9$) with the Lightmeter sensor covered.

d) Comparison to CIE-conforming luminance meters

Measurements with a AVT-GE4000 CCD calibrated to luminance and a Minolta LS-100 luminance meter were done by Costas Bouroussis (see also the respective section for details). These narrow angle (1°) zenith measurements can be compared to the (all-sky) horizontal illuminance measurements of the lightmeter. When the sky luminance is isotropic (and under many other conditions conserving the angle integral) they should be equivalent. Integration and projection results in a conversion factor of π to convert isotropic luminance to horizontal

illuminance. The converted luminance measurements are compared to the Lightmeter in Figs. 30 and 31. Measurements that are most closely consistent with the isotropy assumption suggest that the agreement between luminance measurements should be best with the least cloudy sky (as diagnosed by the afternoon variability), though the all-sky images taken during the night should be used for a detailed analysis. Note how the Lightmeter picks up scattered light well into the astronomical night during the third night shown in Figs. 30 and 31 (evening of May 5th). The CCD measurements (blue) connect very well to the Minolta LS-100 (red), so the former can be viewed as a continuation of the Minolta towards the mlx where its sensitivity and resolution are insufficient. The significant departure of the CCD and the Minolta from the Lightmeter (in black) and the total radiation model (magenta line) before sunset must come from the fact that the zenith luminance connects to the diffuse radiation (measured in a shadow) and not the total radiation that is responsible for horizontal illuminance. With regards to this, note the much better agreement on the third evening of luminance measurements, when cloud scattering produces more isotropic light. Thus the key differences between Lightmeter and luminance meters visible in the figures should come from the different sky coverage – i.e. 1° vs. 2π . Possible effects of cloud and/or sky-colour that may be inherent to twilight comparisons and, in addition, the contributions of scattered artificial light being present could be checked by a future moonlight comparison.

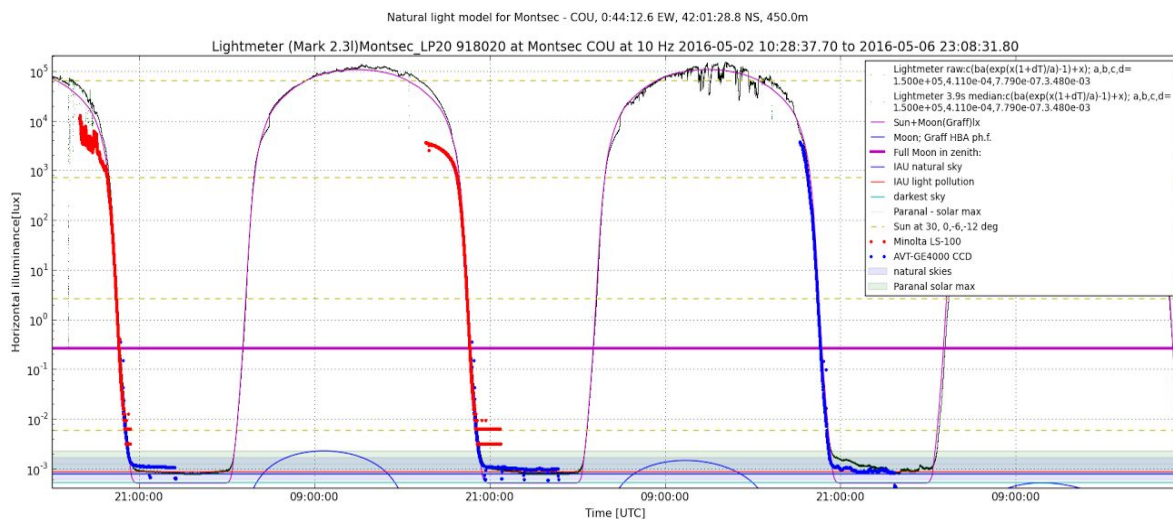


Figure 30: Measurements with an AVT-GE4000 CCD (blue), calibrated to luminance, and a Minolta LS-100 luminance-meter (red). These luminance-meter measurements are converted to horizontal illuminance and compared to the Lightmeter (black). The magenta line is a natural light model – see Fig Wuc02 for a description of the other references. The downward excursions in the blue - i.e. AVT curves - are efforts to measure the dark-current of the CCD. Luminance measurements by Costas Bouroussis

A detail of the luminance meter–Lightmeter comparison is shown on a linear scale in the mlx domain in Fig. 31. In this finer view of the low-light domain, a green “halo” can be seen around the black Lightmeter data-points. This is from points of the original data that contain the “beating” periodic signal described above. The black points are a 10-period (3.9s) running median filter applied to the Lightmeter raw-data. Note how the luminance-meter and illuminance signals follow each other in shape but differ in amplitude, most likely controlled by the angular distribution of light. At the end they completely overlap for about one hour.

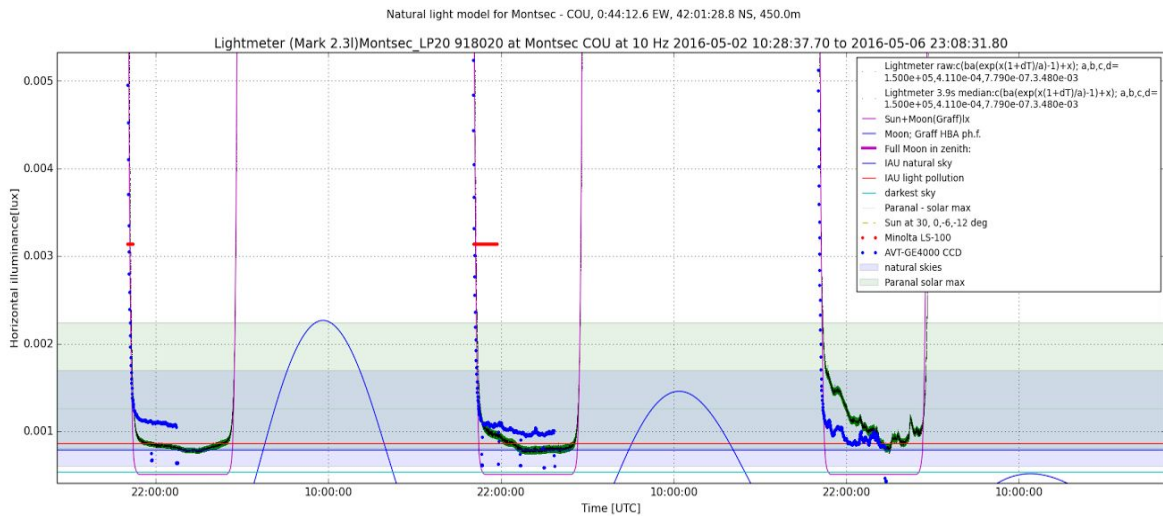


Figure 31: Horizontal illuminance measured by the Lightmeter (black) and 1° aperture zenithal luminance by the AVT-CCD (blue) and the Minolta LS-100 (red) converted to illuminance assuming isotropy of the sky hemisphere. mLux-region with linear ordinate. The dashed horizontal line marks the light levels of a clear sky at the end of nautical twilight, shades are Paranal natural skies. Luminance measurements by Costas Bouroussis

e) Automatic atmospheric extinction from Lightmeter time-series

The Lightmeter time-series can be used to determine the atmospheric extinction when one narrow-angle light-source dominates the horizontal illuminance. In that case, assuming the source is constant, the variation of the length of the optical path in the atmosphere induced by changes in the apparent height of the source can be fitted to determine the extinction coefficient. In astronomy that is done assuming an airmass-apparent magnitude relationship, where airmass is simply given by the secant of the zenith distance, for angles < 80 degrees. By definition, unit airmass is towards the zenith, and typical air-masses towards the horizon are about 30. For consistency, in practice air-masses from 2 to 1 are most often used to cover an airmass range appropriate to most measurements. As comparative measurements are made of an object as the source rises or sets, and conditions can change with time, the atmosphere ideally needs to be in a nearly constant state over the required measurement interval.

In case of the lightmeter the high-cadence, high signal-to-noise illuminance measurements are de-projected with the calculated Sun-altitude, and the resulting inferred brightness measurement of the Sun (actually Sun+sky) is fit against airmass for running time-intervals. If the Sunlight (or at night the Moonlight) dominates, the extinction coefficient can be well fit. In Figure 32 we show the values obtained for the atmospheric extinction at COU in magnitudes per unit airmass as a function of time. Fits are accepted when the correlation coefficient is larger than 0.9 and the residual rms is less than 10%. Statistical error bars are plotted but invisible at the scale of the plot.

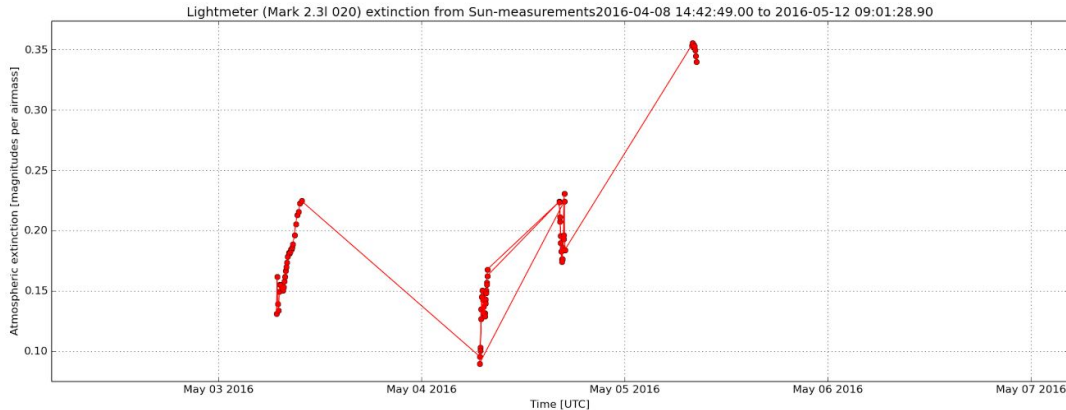


Figure 32 : Atmospheric extinction from Lightmeter time-series data with 10 Hz cadence. The atmospheric extinction is given in magnitudes per unit airmass. Note that this contains only results for daylight-extinction because of insufficient moonlight to apply this method at night.

Values are in the expected range and overlap with those of other instruments at night (c.f. the table of extinction measurements). What is of interest here is the variation in extinction that is implied by the lightmeter time-series. First the day-to-day variation, which was obvious by looking at the sky, but should be noted here that the lightmeter extinction coefficients are robust in the sense that they use an all-sky method where the scattered light is not (easily) lost because of the large angular response. Thus the Lightmeter can determine average extinction values even with significant overcast because with constant cloud conditions the optical path variation can still be detected. However, when there is patchy cloud the variation due to shading may override the optical path variation. This is the reason why the Lightmeter extinction coefficients are mostly for the time before local noon. In Montsec that is the time before the sun-induced thermals create the world-famous paragliding-conditions – but also scattered afternoon clouds as a side effect.

To determine the extinction at night the Lightmeter needs some moonlight. Thus a recommendation would be to include moonlit nights into future campaigns. They would not only allow a simultaneous high-cadence extinction time-series but also the use of the Moon as a well characterised – and, in recent years a very time-independent calibration standard for Earth climate observatories – and sufficiently constant, highly predictable reference source with an intensity in the range typical of light pollution levels measured in areas with high population density. Thus intercomparison techniques should be at a remote site that is well shielded from urban glow so that signal-to-noise is high for the comparison measurements, but nevertheless the Moon as a bright, high signal-to-noise but constant and predictable source can be used for precision comparisons.

6) Evaluation of differences between SQMs

a) Systematic differences between permanently mounted SQMs

During this intercomparison campaign we had the chance to obtain measurements of many SQM devices at the same time in the permanent measurement site of Parc Astronòmic Montsec - Centre d'Observació de l'Univers. As described in Section 2, around 20 poles were prepared to install SQM with housings, and all the data were stored in the same server in PAM. For those meters connected to the system this prevents any possible offset for time settings, and collects the data in the same place for easier comparison.

One of the first tests with this data was a rough evaluation of the offsets between different devices. This kind of evaluation is very common for the intercalibration of devices of a network as in the studies of the Netherlands (den Outer et al 2011) or Catalonia (Ribas 2016). We have followed the same strategy to use a set of SQMs to define a ‘virtual reference’ detector. With this reference detector we can compare and determine the offsets of each of the instruments used in the intercalibration and also propagate this calibration to other devices not used in this first step. A description of the strategy can be found in Ribas (2016).

For these preliminary results we have studied two samples selected from a range of measurements and devices. We have selected the devices controlled by server and not the ones with Datalogger to be sure of the time keeping. Because we have data for many days, this work will be extended in detail in future publications, and here only we report only on data from the campaign days that have been analyzed so far.

Sample 1

The first sample includes all the devices (LE & LU) with complete available data during four nights from 2nd to 5th of May. Thirteen devices have been used for this comparison. All the data have been resampled to measurements at a minute timescale and we have defined the ‘virtual reference’ instrument as the mean value, in each timespace, of all the devices of the sample. With this ‘virtual reference’ we have determined the offset of all the instruments of the sample in two situations: measurements that were taken only in astronomical night, and those covering the whole set of data.

Table 2: Offsets obtained with Sample 1.

Instrument #	Whole set of data		Only Astronomical Night data	
	Offset (mag)	Sigma (mag)	Offset (mag)	Sigma (mag)
LE 0729	-0.31	0.71	-0.16	0.01
LE 0849	0.12	0.24	0.10	0.01
LE 1759	-0.27	0.71	-0.12	0.02
LE 1786	-0.03	0.38	0.02	0.02
LE 2437	-0.02	0.25	-0.06	0.03
LE 2444	0.00	0.22	0.00	0.01
LE 3180	0.05	0.26	0.02	0.02
LE 3181	0.10	0.20	0.10	0.02
LE 3186	-0.03	0.33	-0.15	0.03
LU 0857	0.10	0.26	0.11	0.02
LU 1055	0.05	0.24	0.03	0.02
LU 1118	0.12	0.46	0.03	0.03
LU 2117	0.13	0.44	0.08	0.02

Clearly the offsets obtained with the whole set of data show a big scatter. On the other hand, the set of data which contain only astronomical night data provides less scattered offsets. The offset values obtained are compatible in both sets of data, except for the devices with higher scatter in their measurements.

Sample 2

The second sample includes all the devices of the first sample plus the devices without data during the first night (2nd of May). So with this sample we have more devices (18 SQM) but just three nights (from 3rd to 5th of May). As in sample 1 all the data has been resampled to minatural measurements and we have defined the same ‘virtual reference’ strategy and the same two sets of data: those taken only in astronomical night, and those covering the whole dataset.

Table 3: Offsets obtained with Sample 2. In *italic* the devices added to this sample.

Instrument #	Whole set of data		Only Astronomical Night data	
	Offset (mag)	Sigma (mag)	Offset (mag)	Sigma (mag)
LE 0729	-0.35	0.75	-0.19	0.01
LE 0849	0.08	0.22	0.07	0.01
LE 1759	-0.30	0.74	-0.14	0.03
LE 1786	-0.07	0.43	0.00	0.02
LE 2437	-0.07	0.25	-0.09	0.03
LE 2444	-0.04	0.26	-0.02	0.01
LE 3180	0.00	0.25	-0.01	0.02
LE 3181	0.05	0.23	0.06	0.01
LE 3186	-0.07	0.27	-0.17	0.03
LU 0857	0.05	0.31	0.08	0.02
LU 1055	0.01	0.28	0.01	0.02
LU 1118	0.07	0.36	0.01	0.03
LU 2117	0.09	0.37	0.05	0.02
<i>LE 2606</i>	0.07	0.23	0.11	0.02
<i>LU 2113</i>	0.10	0.29	0.08	0.02
<i>LU 2548</i>	0.12	0.41	0.07	0.03
<i>LU 2549</i>	0.11	0.40	0.06	0.01
<i>LU 2552</i>	0.15	0.55	0.05	0.02

As in sample 1 the offsets obtained with the whole set of data are showing a big scatter. On the other hand, the set of data containing only astronomical night data provides less of a scatter in the determined offsets. The offset values themselves are also compatible in both sets of data except for those devices with higher scatter.

We can also compare the offsets determined for the first thirteen devices in both samples and the offset difference in the case of astronomical night data and we find less than 0.03 magnitudes per square arcsecond (mpsa) between the two samples. These differences are clearly compatible with the scatter.

Table 4: Comparison of offsets determined with two sample of data in Astronomical Night.

Instrument #	Sample 1 - Astron. Night Offsets	Sample 2 - Astron. Night Offsets
LE 0729	-0.16	-0.19
LE 0849	0.10	0.07
LE 1759	-0.12	-0.14
LE 1786	0.02	0.00
LE 2437	-0.06	-0.09
LE 2444	0.00	-0.02
LE 3180	0.02	-0.01
LE 3181	0.10	0.06
LE 3186	-0.15	-0.17
LU 0857	0.11	0.08
LU 1055	0.03	0.01
LU 1118	0.03	0.01
LU 2117	0.08	0.05

b) Systematic differences between handheld SQMs

Handheld SQM observations were acquired at a near-pristine location on the night of May 2-3 (Observatory), and at a polluted location on the night of May 3-4 (outskirts of Balaguer). The procedure was as recommended in Bará et al. (2015): Kyba first aligned his body facing North, took a measurement at zenith, and then rotated 90° to face East. Four measurements were taken facing in the four compass directions and Kyba called out the measurement for Spoelstra to record. After each set of four measurements, a new SQM was selected. Each SQM was sampled 3 times by four directions, for a total of 156 measurements on May 2-3 and 180 measurements on May 3-4. The temperatures reported by the SQMs were also recorded during the final series on May 2-3.

Preliminary analysis of the data reveals that the variance in SQM field observations due to orientation is of a similar size to the unit-to-unit differences in offsets. Averaging the effect therefore considerably improves the accuracy of handheld SQM observations. Assuming that the difference is due to the SQM not pointing directly upward, it suggests that the size of this effect would be larger in cases where there is a strong gradient in either skyglow or natural light.

c) Comparison of Roadrunner measurements

During the night or the 3rd of May there were two teams of measurements equipped with SQM devices used in RoadRunner setups. Team 1 were using two SQMs in RoadRunner setup (PAM 1040 & UB 1871). Team 2 were using one SQM with the Road Runner (UCM 1738). Both teams did measurements in a transect between Balaguer and Àger with a time difference between their passage so that the stability of the measurements could be evaluated, and also if there were notable differences between one device and the others.

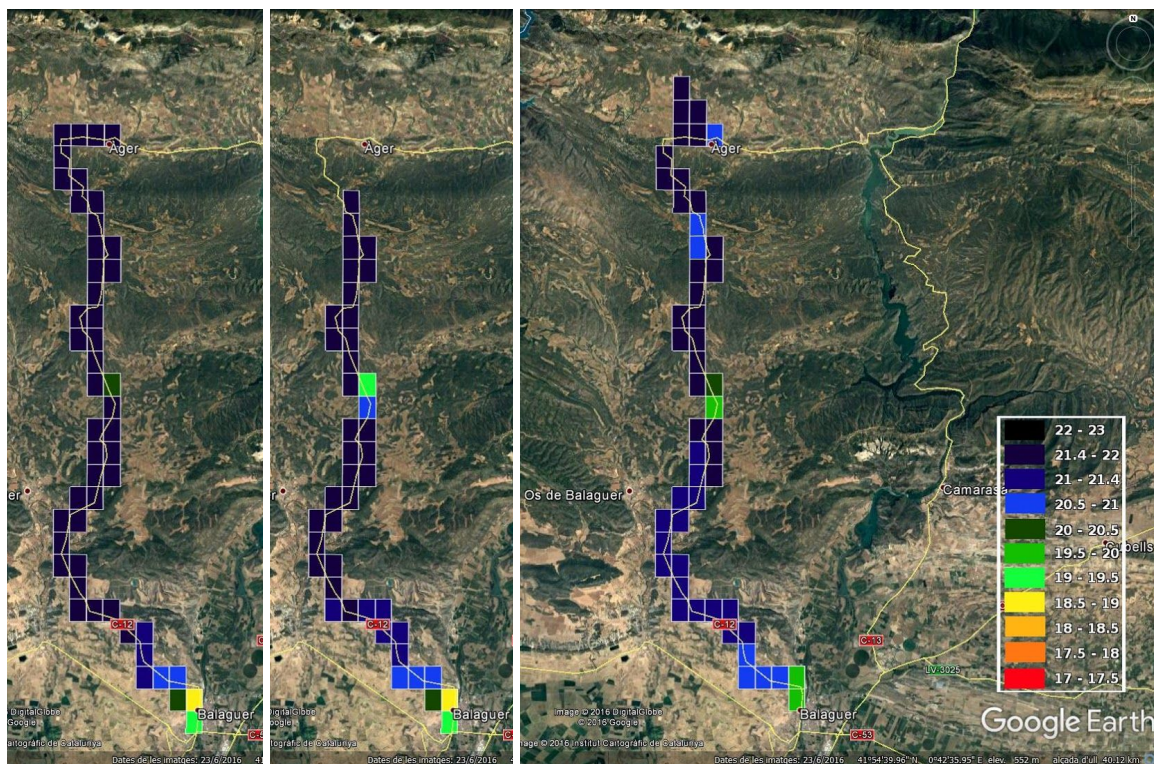


Figure 33: Comparison of measurements with three SQM Roadrunner devices. Left panel is PAM #1040, central panel is UB #1871 and right panel is UCM #1738. PAM and UB devices were mounted in the same car with only a small offset in measurement time so the results are almost the same. UCM device travelled in a different time and shows few differences.

The comparison of the three measurements showed not many differences. Specifically, the devices mounted in the same car (UB and PAM), so they are measuring almost at the same time (some instrumental offset could be present), show complete agreement. The UCM device mounted in a different car shows some differences, with the main one being in the area close to Balaguer (southern part), which is a bit brighter, though even this is around 0.1 mpsas. In Figure 33, some clear blue parts (equivalent to 20.5 - 21.0 mpsas) in the northern part are not well understood but may be an effect of passing through a small village.

As we can show in the figures, all the measurements during the transect can be plotted on a map. We had the option to test two methods of creating these kind of maps: the method developed by the team of Universidad Complutense de Madrid (Zamorano et al 2016), and that developed by the team of Parc Astronòmic Montsec (Ribas 2016). Both methods generate a map based in sectors or ‘boxes’, where inside of each sector the mean value is computed and assigned to the complete sector. The method of UCM involves a human controlled filtering to remove scattered values and to also the values due to the villages. In PAM

method, an automatic filtering system is used to remove scattered values and filter the data automatically and the village data are not removed by hand.

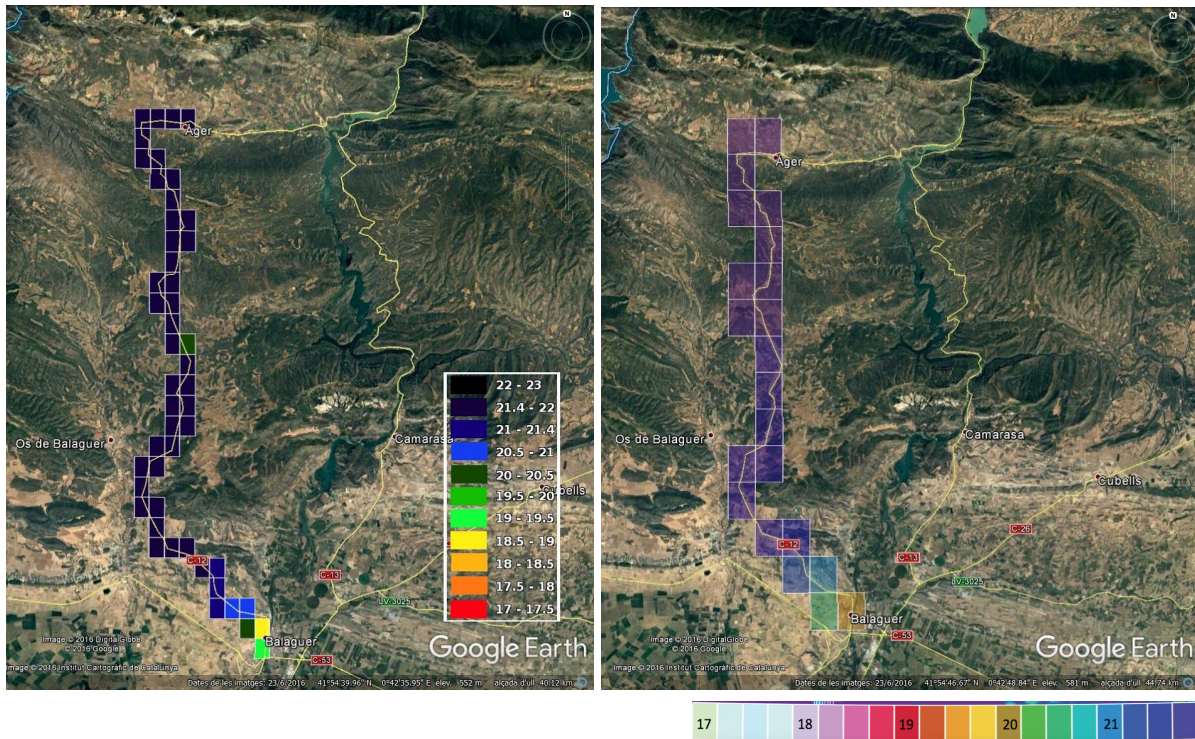


Figure 34: Comparison of measurements with PAM #1040 using both mapping methods. Left panel is shown the map plotted with PAM method and the right one using UCM method. Except for colour scale applied and size of boxes no relevant differences are present.

The comparison of both methods shows no relevant differences. These methods use different sizes of boxes and different colour scales but clearly both methods are generating comparable maps so there is not a ‘mapping method’ effect. Only in the surroundings of villages, or in the passages through them, do some differences appear, as in the figure the sector in green (20 mag) with PAM method due to the crossing of Avellanes municipality, that is removed with the human filtering of the UCM method.

d) SQM linearity tests

Espey carried out a number of linearity checks on SQM devices, as well as tests of the Unihedron SQM-DL-V unit which can provide maps of nightsky brightness. All data were obtained from the roof of the PAM Planetarium building.

Unfiltered data

On the night of 2-3 May, Espey performed tests of the response of two SQM units during twilight. SQM-DL #2634 is an older unit, while #3281 is an SQM-DL-V (vector) unit, fitted with a new ball lens which improves on the original. For this test, both units were mounted in Unihedron housings, and an offset of -0.11 mpsas has been applied to both sets of readings to account for losses in the glass window.

The parameters of the formal best-fit linear model are shown on the graph in Figure 35. Although the formal fit differs from perfect agreement, a fit with the slope constrained to pass through the origin yields a best-fit slope of 0.9956, with a R^2 value of 0.9994. When calibrating SQM meters, comparison of the meters over smaller intervals could conceivably lead to differing conclusions with regards to the offsets that need to be applied to meters, so care needs to be exercised when making judgements regarding meter calibration offsets. It is possible that there may be small-scale differences in behaviour of meters at different light levels (see Figure 36) and the weighting of the fit in terms of the number of points and their brightness distribution needs to be considered when making detailed comparisons and considered in relation to the typical brightness level of the site being monitored. In particular, at the faintest levels, appropriate to natural sky backgrounds, meters may differ somewhat in accuracy and this would affect, for instance, classification of night sky quality based on rigid numerical criteria that reference SQM data alone.

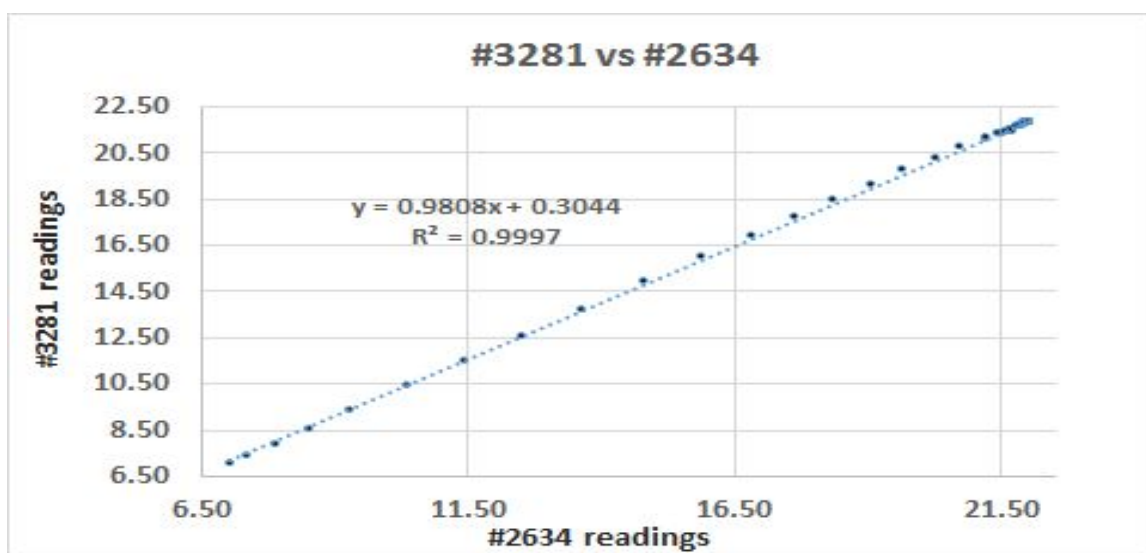


Figure 35: Direct comparison of the evening twilight readings for evening twilight on 2 May from SQM-DL-V unit #3281 with those of SQM-DL unit #2634. Note that the best-fit slope of the fitted curve to these data is less than unity and there is a significant offset, although a fit forced to pass through the origin yields a slope of unity, and an almost identical R^2 (see text).

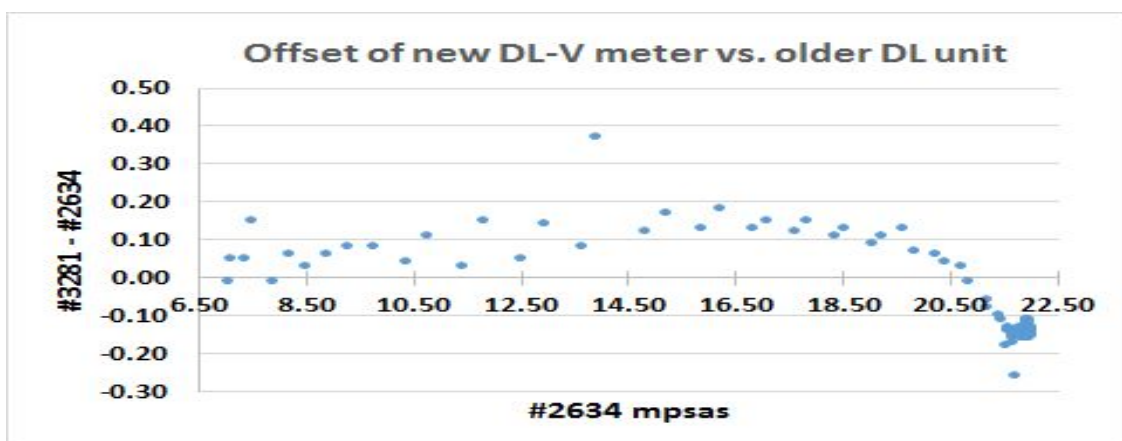


Figure 36: A pot of the differences of the new vector SQM unit relative to the older data-logging unit taken in evening twilight on 2 May. Note that the agreement is generally good, with deviations becoming apparent for magnitudes fainter than 19.5 - compare this plot with Figure 40 below.

Filtered data

On the nights of 3-4 May and 4-5 May, Espey performed SQM linearity tests to check the response of the SQM meters at low light levels by making observations of the zenith. The meters used were SQM-DL #2634 in a Unihedron housing, a SQM-LR unit with a ND 2 (nominal 1% transmission) neutral density filter attached to a laptop via a USB adapter, and a number of measurements with a SQM-DL-V unit. Unihedron's recommended correction of -0.11 mpsas has been applied to the #2634 readings to correct for the window of the instrument housing: the other meters were run without housings so no correction was necessary.

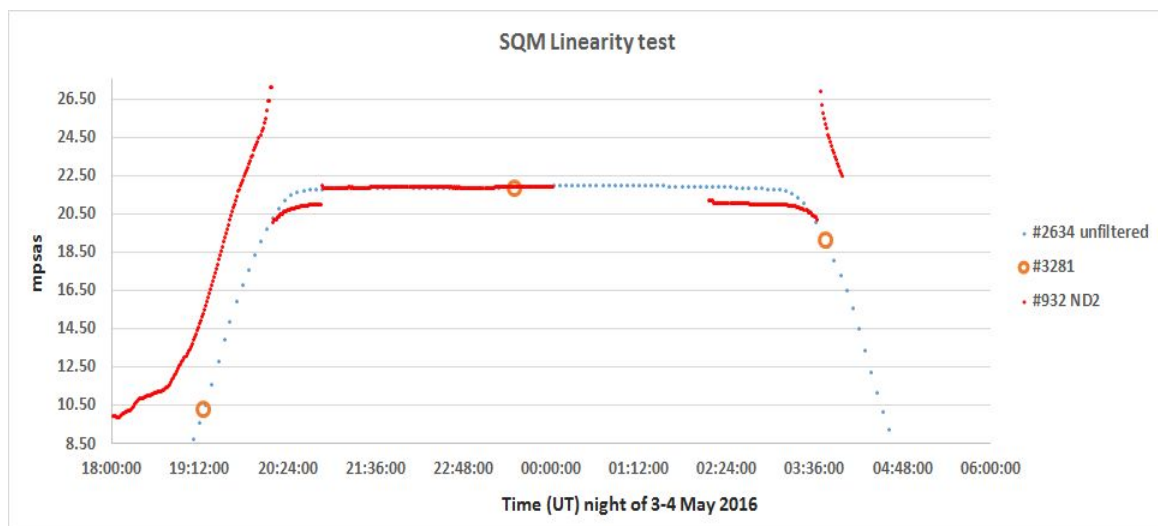


Figure 37: Measurements from three SQM units plotted against UT time for the night of the 3-4th May. Note the discontinuities in the filtered readings when compared with the smooth behaviour of the unfiltered readings.

Readings from #2634 were taken every 5 minutes, whilst those from the filtered unit were taken every minute. Aside from the variations in intensity around sunset, there are slight distortions in the filtered results when compared with the unfiltered readings, and to make these more apparent Figure 38 shows a different representation of the same data. It is apparent from this plot that there are variations in the response between the two meters and a drift with fainter magnitudes, although it is not possible to isolate the contribution of the unfiltered meter to small-scale differences (see the comparison plots from the 2-3 May). For filtered measurements of 20.5 - 25.0, the deviation from the offset at brighter (smaller mpsas) readings is an additional 0.4 mpsas, increasing significantly beyond that point. Of significance is the behaviour for fainter observations, which leads to a sharp discontinuity and apparent brighter values, subsequently settling back to values similar to the unfiltered meter. Similar behaviour in the opposite sense occurred in the morning twilight.

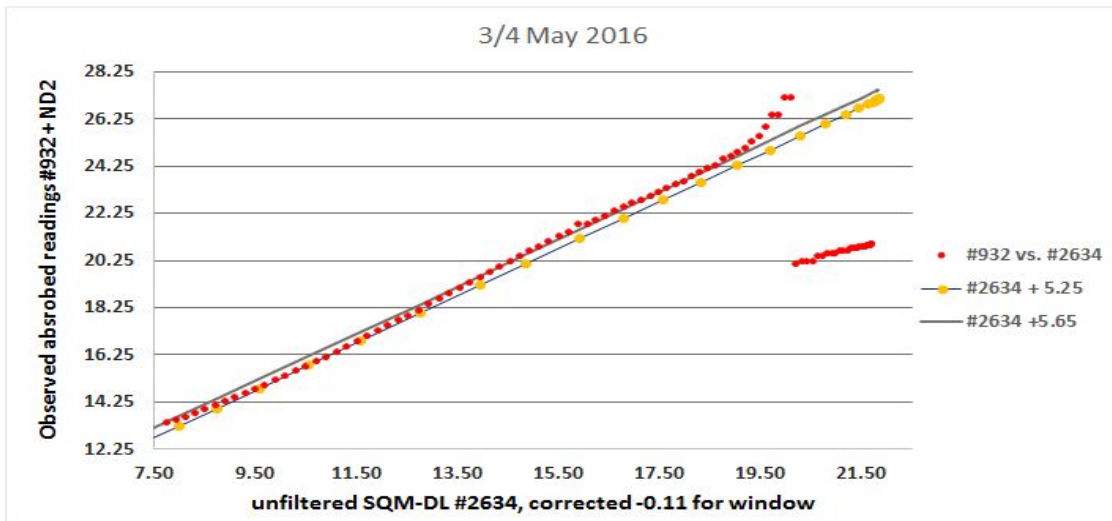


Figure 38: Another plot displaying the filtered data against the equivalent unfiltered measurements, interpolated to 1 min intervals. The diagonal lines represent offsets of the unfiltered data offset by +5.25 and +5.65 mpsas to emphasise the offsets and non-uniformity of the filtered data.

For the night of the 4-5 May, a further test of filtered behaviour under low light conditions was performed, and the data for evening twilight are shown in Figure 39 below. A confirmation of the similar behaviour of the two meters under filtered/unfiltered conditions was performed at the start and end of evening twilight, and no large discrepancy was seen. The offset of the filtered observations is most clearly shown in Figure 40 in which the difference between the filtered and unfiltered data are displayed against the filtered brightness.

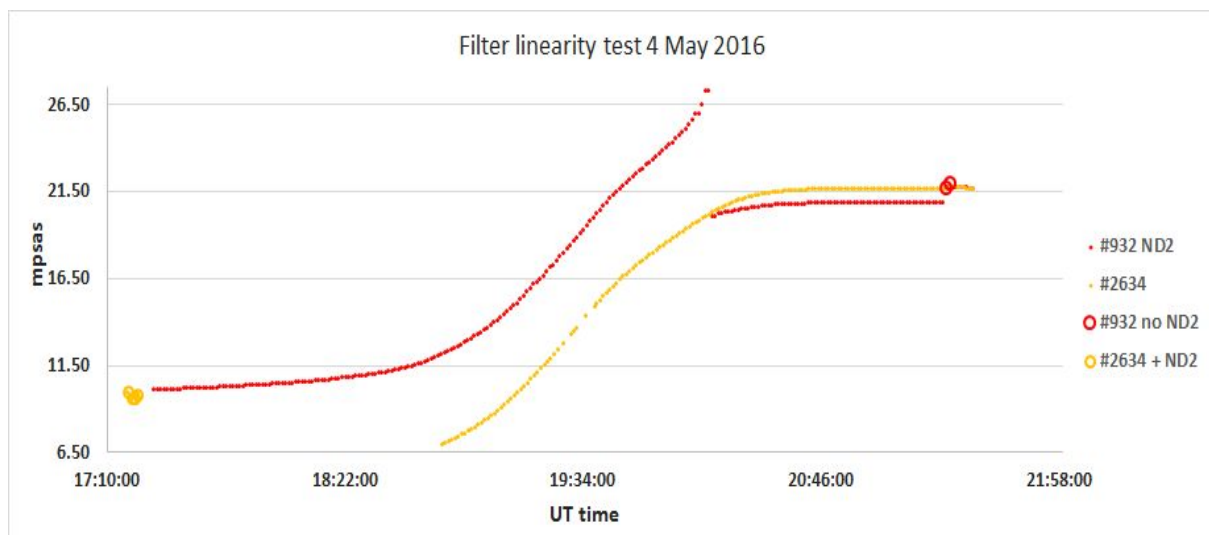


Figure 39: Evening twilight observations for 4 May which tested SQM linearity a faint light levels. The night started with observations with SQM-DL #2634 with the ND2 filter (extreme left, open gold points), then filtered observations with SQM-LR #932 and unfiltered data with #2634, then finishing with a check with unfiltered observations with #932 (open red points). Note that there is good consistency with the behaviour of the meters (unfiltered with unfiltered, filtered with filtered), and the behaviour of the filtered observations at low light levels is consistent with those taken on 3-4 May.

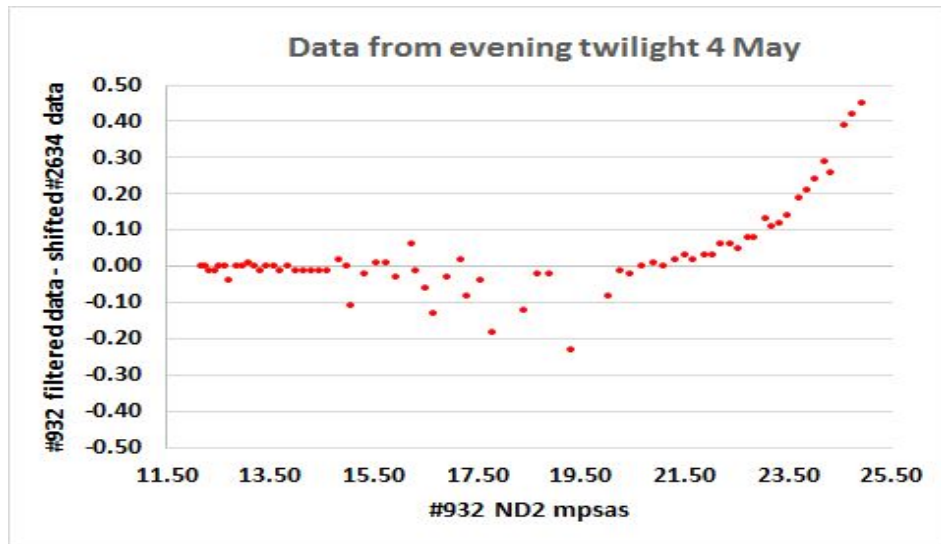


Figure 40: The filtered and reference unfiltered meter data covering 18:51-21:32 was differenced to accentuate the difference between the filtered and unfiltered results. An offset of +5.22 has been applied to the reference data before differencing. There are some missing data points in the reference data and thus possible evidence for issues with data-taking, however it appears that the meters are linear down to 23.5 mpsas.

The main difference with the data from the previous night is that the observing cadence of both instruments was set to 1 minute intervals with readings taken at the same clock time so differences could be formed which refer to similar lighting conditions. Although there were some missing data points from the reference meter #2634, the meters seem to be well-behaved, and the SQM produces increasingly fainter observations beyond 21.5 mpsas.

The conclusion from these two nights of linearity tests is that care needs to be taken when using filters in dark sites, or for nights when overcast conditions lead to fainter than natural skies, as SQM meters will systematically underestimate the sky brightness. Further work is necessary to see if the smooth change in offset is repeatable and potentially correctable in software. However, from our observations there is a fundamental limit of ≈ 27 mpsas to the construction of the SQM, and presumably this applies to all models.

e) SQM-DL-V sky mapping observations

The SQM-DL-V is a handheld SQM unit that records the sky brightness reading together with the azimuth and altitude of the instrument, permitting a crude map of the sky to be reconstructed via the Unihedron software (<http://www.unihedron.com/projects/sqm-lu-dl-v/>). Espey made a number of observations with SQM-DL-V unit #3281 on the nights of 4-5 May and 5-6 May and two surveys are shown in the Figures below.

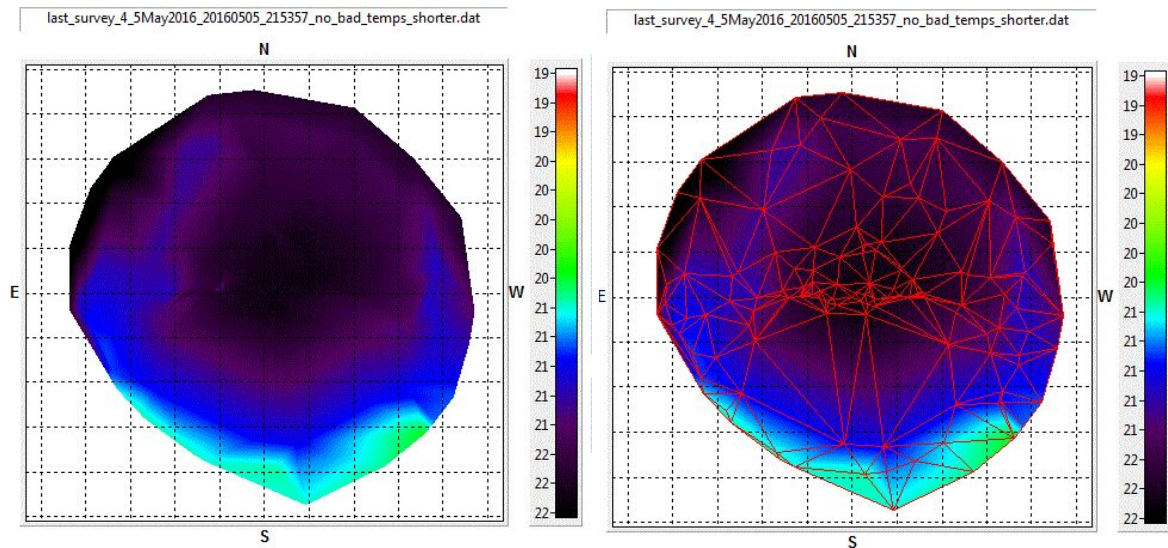


Figure 41: A total of 151 measurements taken with the SQM-DL-V unit were plotted using the Unihedron Device Manager software to produce the plots shown here. The data on the right show the same dataset, but with the interpolation mesh points (i.e., the points at which data were taken) indicated by the crossing points of the triangles. Data were taken around 01:16 on 5 May 2016 and the magnitude at the zenith is recorded as 21.9 mpsas, similar to that recorded by other SQM units at that time. Compare these measurements with those for the evening of the 5 May shown in Figure 42 below.

Although there is a difference in the measurements from the sky images and the vector SQM unit due to the smoothing (FWHM of the SQM = 40°) there is a reasonable agreement in the grosser features, with the light from the town to the S, and the shadow of the mountains to the N, although artefacts due to the interpolation process can be seen. In terms of brightness, the following estimates of SQM (and camera) data were obtained: zenith: ~ 21.3 mpsas; close towards the mountains on the horizon to the N: 21.5; towards the town: ~ 19.5 . The SQM data is consistent with other data with SQMs, so the ~ 1 magnitude fainter offset from the all-sky images needs to be examined as the offset for natural sky observations is expected to be only 10% of this based on tests by Cinzano (2005).

As an aside to the above measurements, it was noted that the SQM-DL-V unit achieved readings under dark conditions in less time than the standard SQM-L unit, even achieving readings at 22.3 mpsas (when pointed towards the dark background of the mountains) in 1 seconds or so.

The conclusion from this work is that the SQM-DL-V is a handy unit to provide a quick-look view of sky conditions, although care must be exercised in obtaining sufficient numbers of data points to accurately reflect the variation across the sky, particularly in regions where the sky brightness changes dramatically. It must also be remembered that the FWHM of the instrument precludes study of fine detail, and the effect of the ground or surroundings will have an effect on the final sky map, just as they affect regular SQM-L measurements. There seem to be no major differences from the standard SQM-L unit, aside from the ability to acquire data more quickly in dark-sky conditions.

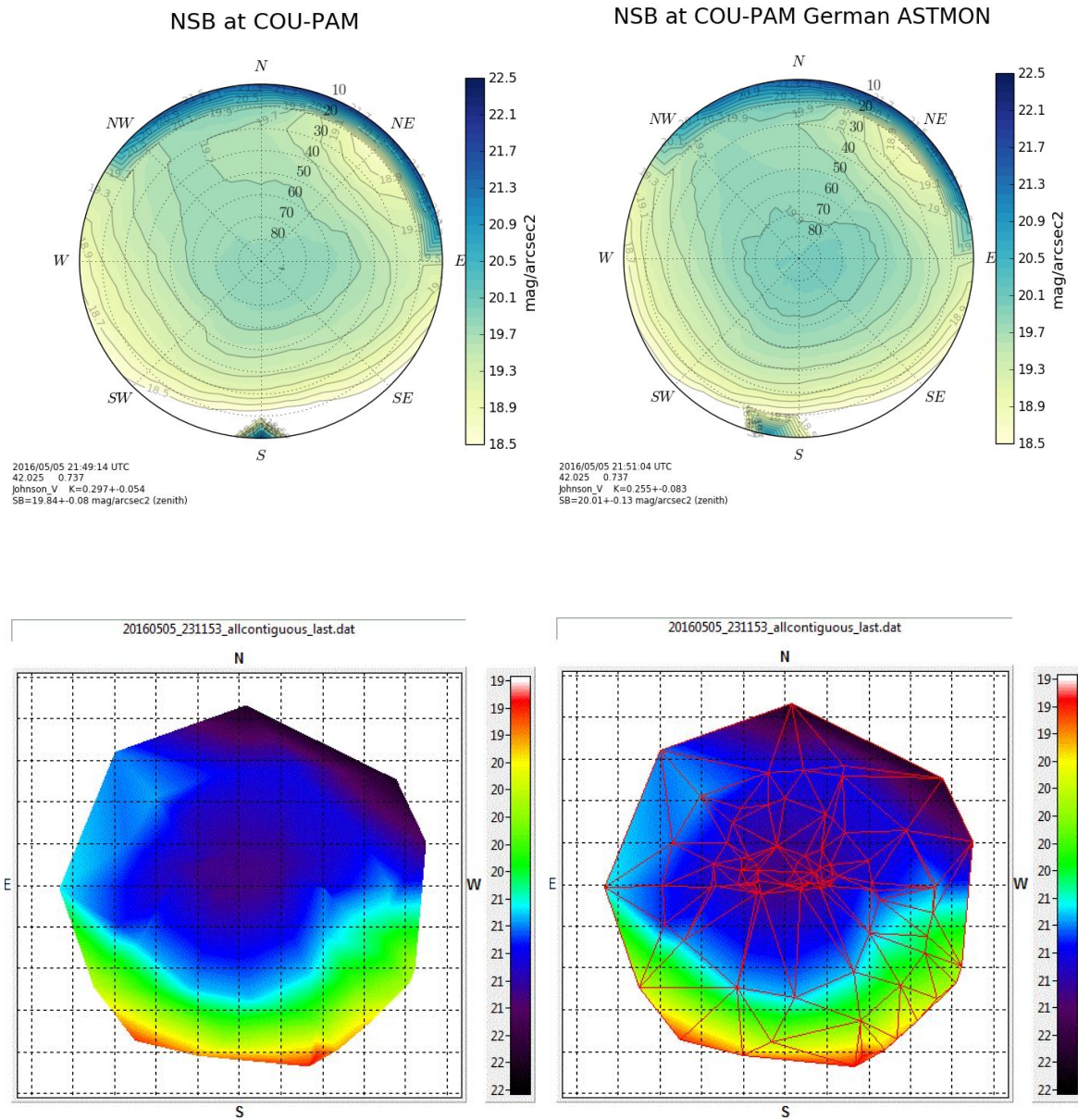


Figure 42 Top images show data taken with two of the all-sky cameras and the bottom images show measurements with the SQM-DL-V meter, constructed into an all-sky image by the Unihedron Device Manager plotting tool. A total of 98 data points were used to construct this image, with data taken around 21:50 UT on 5 May. In the SQM plots, the image on the left shows a plot of the data themselves, whereas on the right the image is overlaid with the locations of the observed positions and the triangular interpolation mesh used by the software. The location of the villages to the S of the observing location is readily seen, as is the darker area to the N of the image where the mountains block the sky. The display scale is the same as for Figure 41 above and indicates that the sky conditions were worse than the previous night, with a zenithal magnitude of 21.3, similar to that recorded by the fixed SQM units.

f) Observations with an astronomical V filter

A series of measurements were taken using a Custom Scientific astronomical V broadband filter which mimics the Bessell prescription of the Johnson standard (Bessell 1990). From previous studies in suburban skies, we find that the V-band results are similar to those obtained using broadband Custom Scientific G filter. Based on comparison, unfiltered, data taken with the same meter immediately prior to the filtered observations, the offset between the two is +1.8 mpsas.

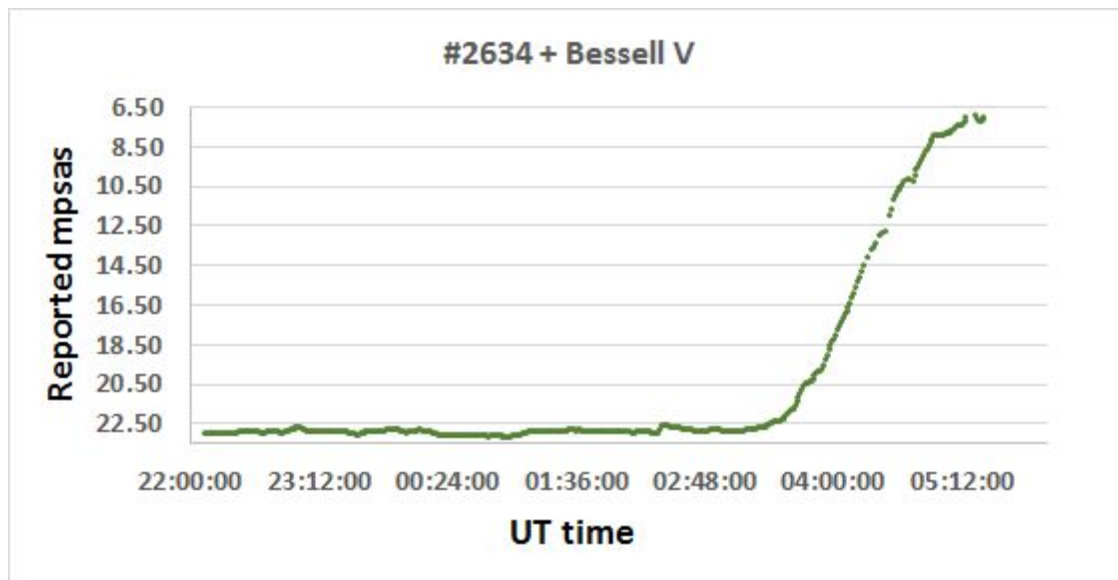


Figure 43: Zenithal observations with #2634 with a Bessell V filter placed over the lens. The unit also contained the standard Hoya filter. Note that a correction of -0.11 mpsas has been applied to correct for the absorption in the window of the Unihedron housing.

7) Naked eye observations during twilight

Naked eye observations were taken on the evening of May 3 from 21:21 until 22:17, and during the morning of May 4 from 5:11 until 6:34. Kyba used the Loss of the Night app in both sessions, and in the evening session Wuchterl also made simultaneous observations of the appearance of the stars of the Little Dipper. The sky was extremely clear, with extinction measurements around -0.2 (see Table 1). Data for the evening twilight is shown in Figure 44. Stars deemed visible with direct vision are shown as black stars, stars visible only with averted vision are shown as black '+' symbol, stars that were not visible are shown as red circles, and the prediction of Schaefer (1998) is shown as a dotted blue line. Wuchterl's observations of the appearance of the Little Dipper stars are shown as purple squares.

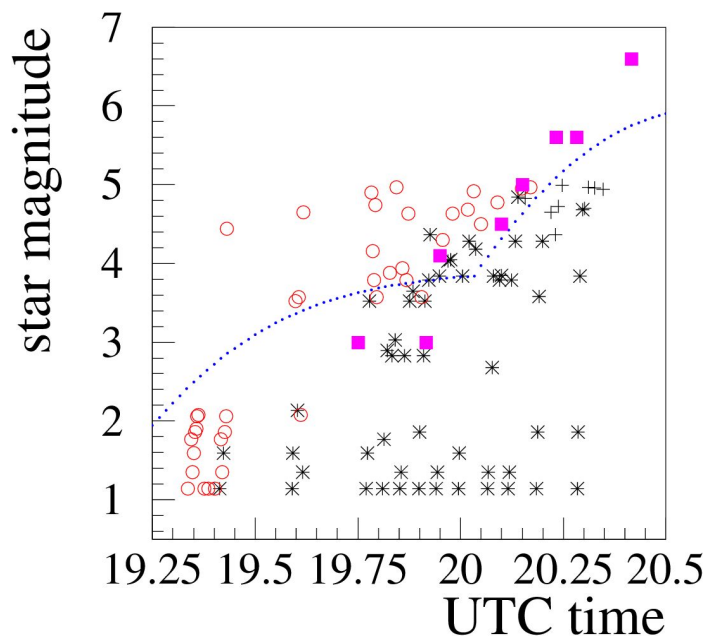


Figure 44: Naked eye observations during evening twilight.

There is a clear separation between visible and not visible stars. This boundary is the limiting magnitude, which is increasing over time as the twilight fades. There is reasonable agreement with the model of Schaefer, especially for limiting magnitudes above four. For limiting magnitudes below 2, it appears that the model overestimates the limiting magnitude. The morning twilight data show a similar trend, with no gaps in the time series. The complete dataset will be presented in a future publication.

8) Preliminary evaluation of TESS

Two of the first units of the photometer that is being developed for the STARS4ALL project were placed at the rooftop of COU in order to perform an intercomparison with the SQMs. The reference SQM used for intercalibration was that located near Cal Maciarol which is operated by Josep Lluís Salto for the Spanish Light Pollution Research Network (REECL).

The first device TESS-stars2 connects directly to the router to send the data to a broker using messages with the MQTT protocol. Unfortunately the MQTT broker was off line and no data was archived. The TESS-stars3 could be connected via USB to record data locally to a computer and to send data to a repository. We use the local mode to record data from two nights.

The analysis of the data indicates that the TESS-stars3 has a calibration constant or zero point $ZP = 19.74$ while $ZP (SQM) = 19.86$, i.e. TESS-stars3 is 0.12 mag less sensitive. This result complements the tests that we are performing at the laboratory and in other fixed sites: Coslada, near Madrid, and Villaverde del Ducado (Guadalajara) which is a rural area.

TESS-stars3 has a near-infrared rejection filter similar to that of the SQM photometer (Hoya CM500 or Schott BG39) while the TESS-stars2 has been fitted with a dichroic filter with higher transmission. The results with this dichroic filter are promising since the gain is around a factor of 1.7 (0.6 magnitudes) with respect to the SQM photometer.

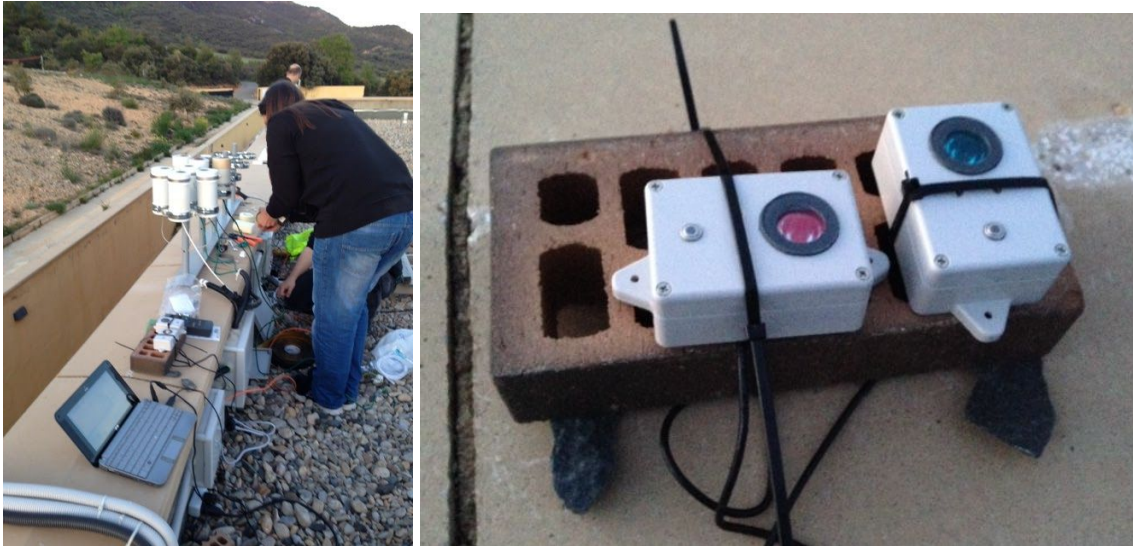


Figure 45: Setup for the two STARS4ALL TESS photometers tested at PAM-COU.

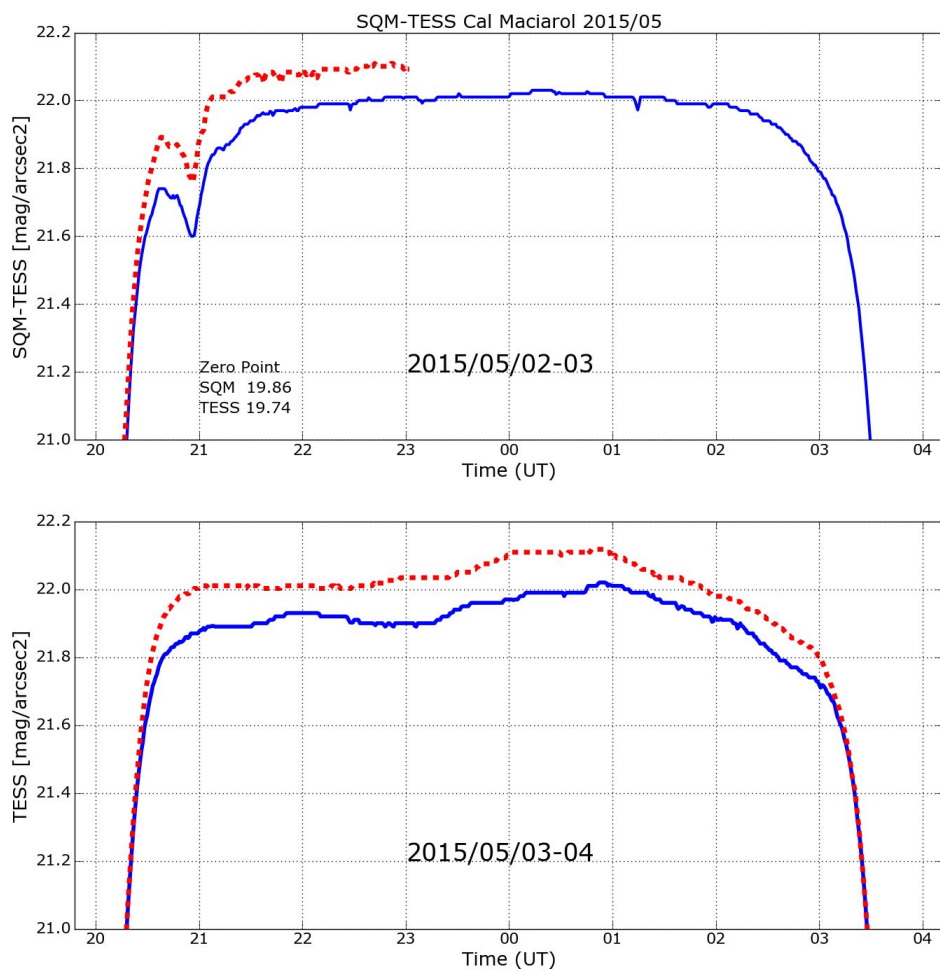


Figure 46: Comparison of the Night sky brightness plots for the night of 2015/05/02-03 and 03-04. The dotted red line corresponds to TESS-stars2.

9) Twilight luminance measurements with commercial handheld luminance meters

During twilight of May 4, Haenel and Bouroussis installed side-by-side two commercially available handheld luminance meters, the Gossen Mavo-Spot 2 and the Minolta LS-100. Both instruments are used in variety of luminance measurements (indoor and outdoor), with the maximum permitted measurement up to thousands of cd/m^2 down to mcd/m^2 . Minolta has its lower limit to $0.001 \text{ cd}/\text{m}^2$ while Gossen down to $0.01 \text{ cd}/\text{m}^2$. Both instruments were aimed to zenith and the measurements started around 20:30, with the instruments set to log data every few seconds. The results of the measurements are shown in Figure 47. The two instruments were measured zenith luminance until the lower limit of each one was reached. Gossen Mavo-Spot 2 reached the limit of $0.04 \text{ cd}/\text{m}^2$ (higher than the manufacturer's claim) while Minolta LS-100 reached the limit of $0.001 \text{ cd}/\text{m}^2$ as expected.

The difference between the two instruments was systematic (around 3%) until the Mavo-Spot approached the lower limit, where the uncertainty of measurements increased and the difference became chaotic. After this time, the difference increased as the Mavo-Spot constantly measured the same value (lower limit). The systematic difference could be due to one or more of the following reasons:

1. Calibration accuracy of each instrument.
2. Quality of photometric filters - $V(\lambda)$
3. Slightly different aiming point at zenith

A conclusion of this experiment is that using these types of instrument one can easily track the twilight, but not in pristine dark skies. It is clear that the same experiment must also be undertaken in a highly polluted area, either pointing at zenith or towards a lower point on sky containing some skyglow.

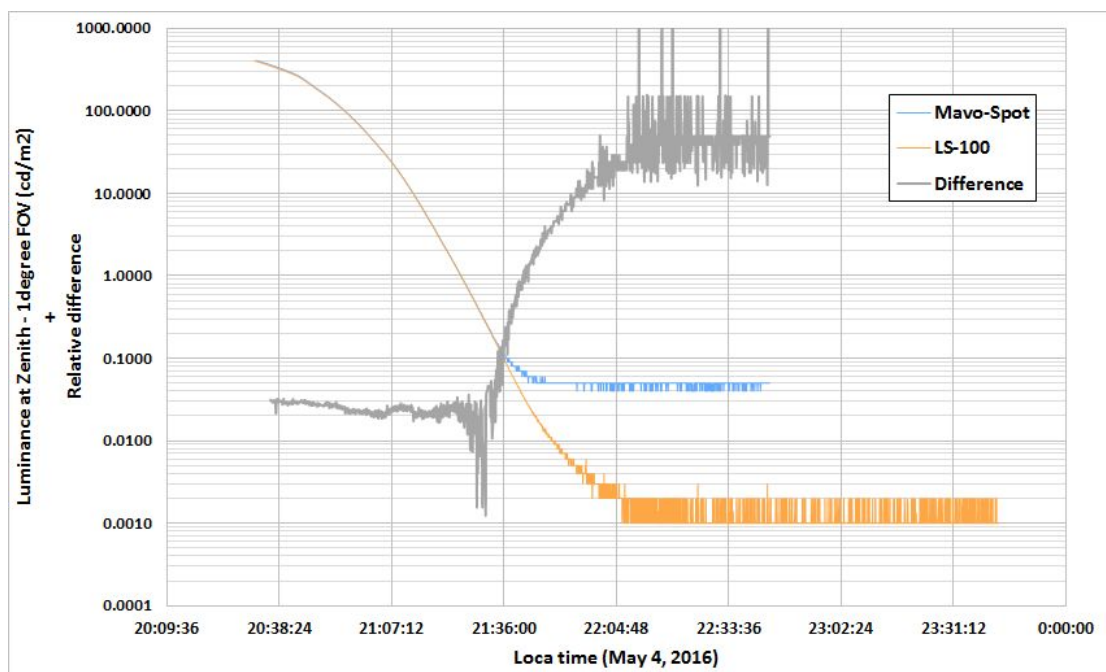


Figure 47. Comparison of luminance measurements between Gossen Mavo-Spot 2 and Minolta LS-100 with 1 degree FOV, pointing at Zenith.

10) Low temporal resolution characterization of the zenith sky spectrum at PAM

We sampled the sky spectrum with two SAND units simultaneously using the SAND-4B and the SAND-4C units. Unfortunately the sensitivity of the SAND-4C appeared to be too low to obtain relevant measurements. For that reason, this later instrument will be installed permanently in an urban site (namely Barcelona Universitat physics faculty building). In the present report we will then only show the data acquired by the SAND-4B system.

Below are some spectra acquired respectively on May 3, 4, and 5. For the 2 first nights the sky was almost clear while there were more clouds on May 5. It is evident on the spectrum of May 5 that the artificial contribution to the sky spectrum is at least 3 times larger than for the 2 previous nights.

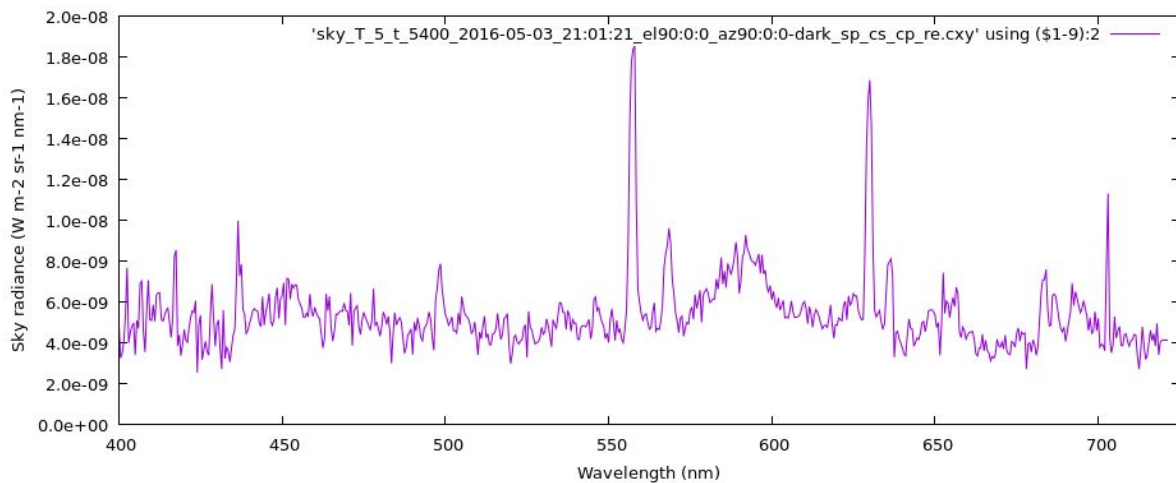


Figure 48: Zenith sky spectrum recorded in PAM-COU on May 3 2016. The acquisition started at 21:01 with an integration time of 5,400s. We found after this night that we must increase the integration time to increase the signal-to-noise ratio for the following nights.

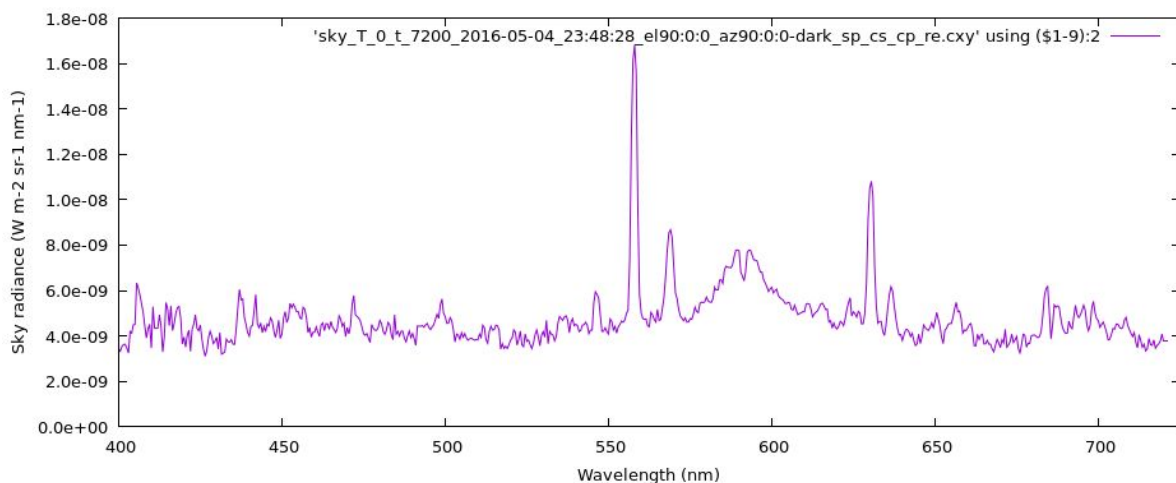


Figure 49: Zenith sky spectrum recorded in PAM-COU on May 4 2016. The acquisition started at 23:48 with an integration time of 7,200s.

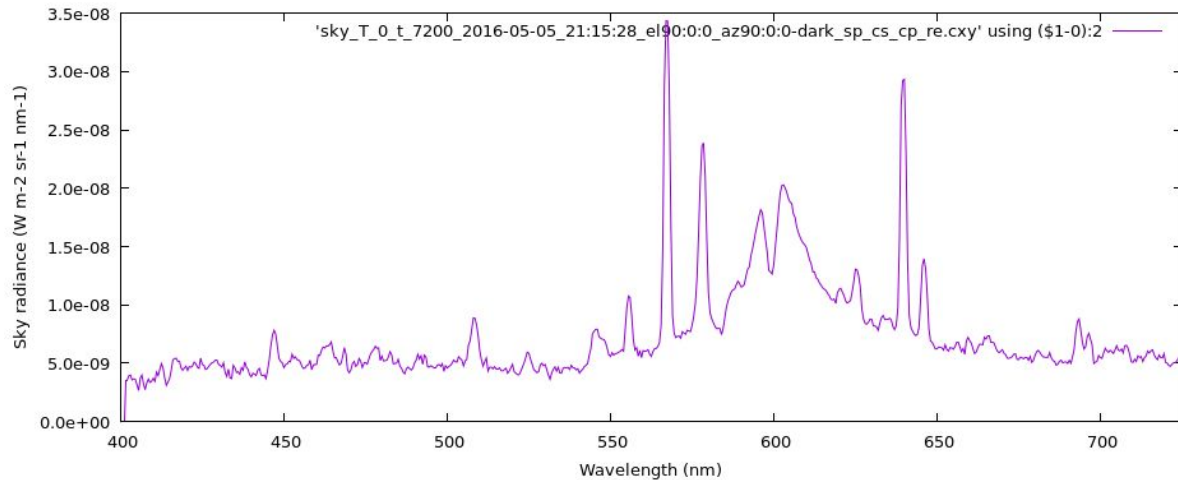


Figure 50. Zenith sky spectrum recorded in COU on May 5 2016. The acquisition started at 21:15 with an integration time of 7,200s.

The mean natural sky spectrum (coming mainly from the star background) is relatively constant from one night to the other. In the 3 plots the highest spectral line around 557 nm is due to the OI auroral lines. The sodium line around 589nm and the mercury line around 546nm are also clearly visible. The large feature just before 600nm is the so called High Pressure Sodium emission.

11) Spectra of lamps in the villages

During the night of 5th to 6th of May 2016 we also performed measurements of spectra of different kinds of lamps available in the area using two calibrated StellarNet BlueWave spectrometers. One of the them works in the range 350-1150 nm, and the other 350-800 nm. We measured in Tremp, Guardia de Noguera, Les Avellanes, and some old lamps from Àger private campsite. We also took some pictures and observed the spectra visually with a small diffraction grating.



Figure 51: Tremp, Rambla Dr. Pearson (PC amber), Guardia de Noguera (amber filtered LED), Guardia de Noguera (green-yellow filtered LED), Les Avellanes (PC amber), Banyoles (PC amber Ignialight).

Tremp on Rambla Dr. Pearson (May 5, 2016, 21:45 UT):

We sampled some PC amber LED street lights and also a high-pressure sodium lamp in a neighbouring street. According to these spectra (see plot below) the LED units seemed to be pure amber ones (no blue peak); however, and somewhat surprisingly, visual inspection using Andreas Hänel's diffraction gratings revealed the presence of a conspicuous blue band (suggesting they would rather be pc-amber LED) that does not appear in these initial spectra.

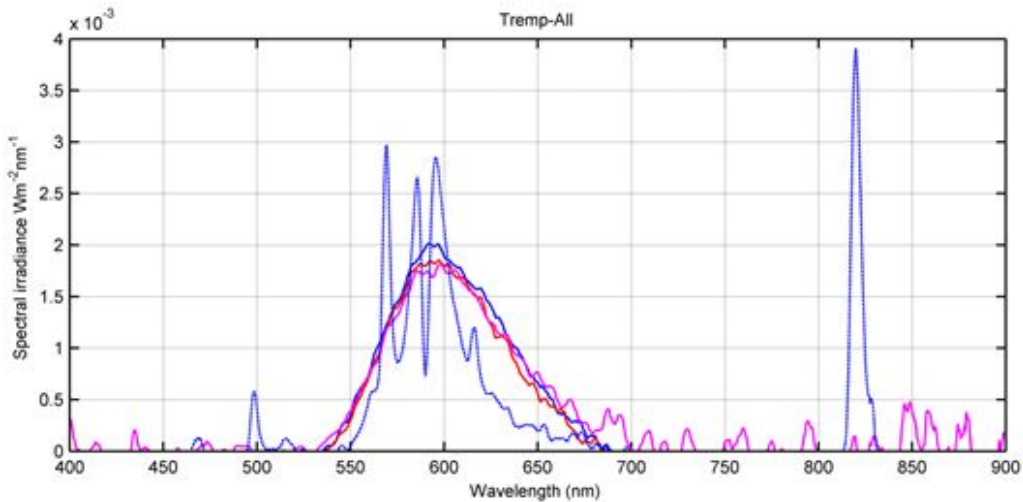


Figure 52: Three LED spectra (full lines) and HPS lamp (dotted line) obtained in Tremp. The blue peak visually detected is not visible here.

After the visual observation of a blue content in the spectrum we decided to increase the integration time to 60 second and then the spectrometer recorded a tiny blue contribution.

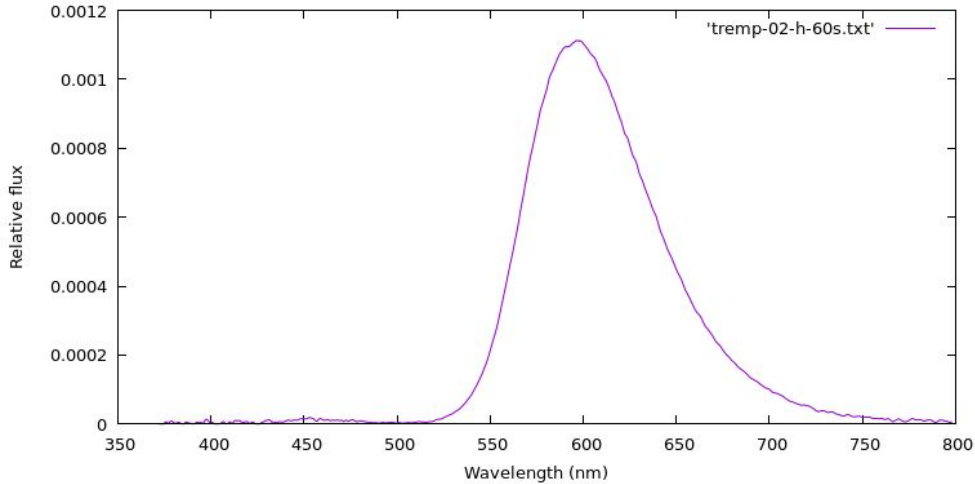


Figure 53: Tremp pc-amber LED spectra. Increasing the exposure time shows some blue features.

Les Avellanes (May 6, 2016, 23:33 UT):

This village has replaced some lamps from HPS to PC amber LED, but still some HPS lamps are working, so we sampled HPS and PC amber LED in this site. We sampled many HPS lamps but we show here only two of them. It is clear that they correspond to the same lamp model because the two spectra are almost identical. The same comment apply to the PC Amber LED. In the PC Amber spectra, the blue content is not perceived because we used a shorter integration time than in Tremp.

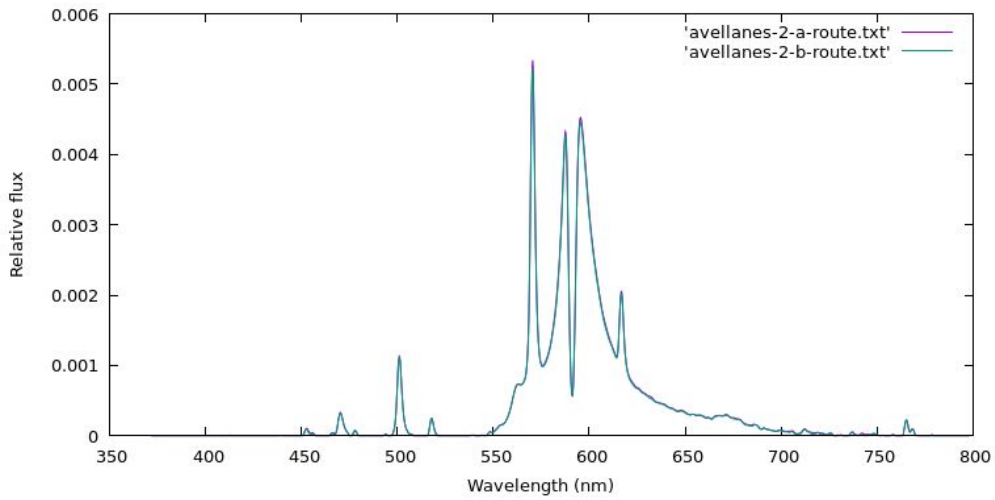


Figure 54: High Pressure Sodium spectra acquired in Avellanes on May 6 2016

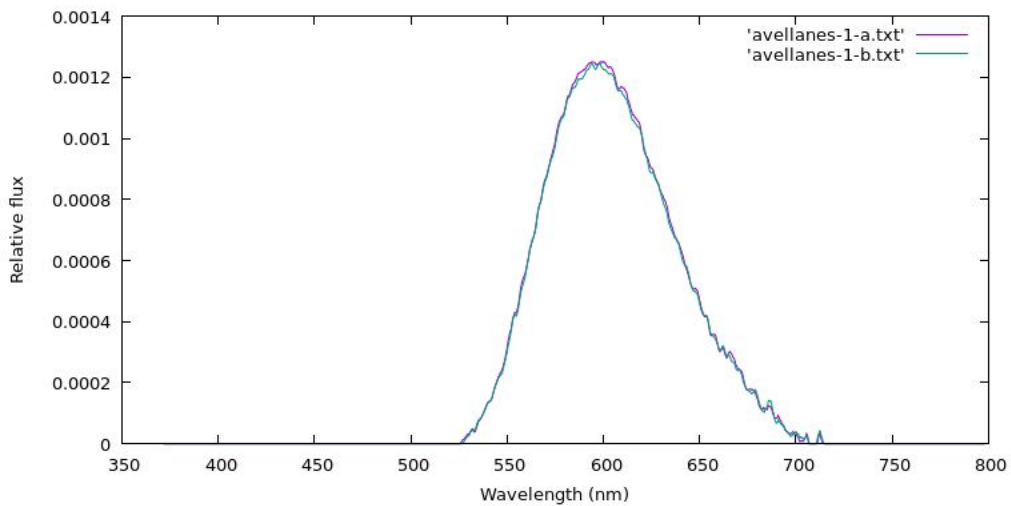


Figure 55: Pc-amber spectra acquired in Avellanes on May 6 2016

Guardia de Noguera (May 6, 2016, 22:45 UT):

Guàrdia de Noguera is a village that installed in 2011 white LED in an area where this kind of lamps are not allowed, so they changed to a strange yellow-green filtering system. Last year they have replaced part of this yellow-green filtered by Amber filtered LED. We have sampled the two different technologies of filtered LED.

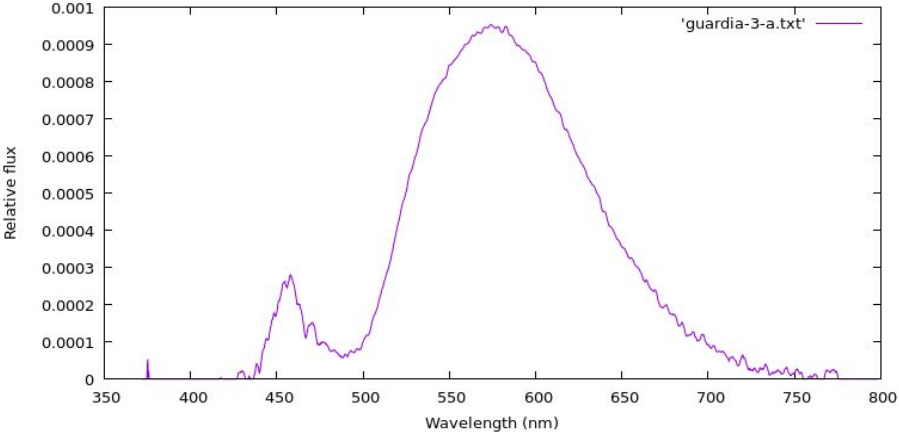


Figure 56: Filtered white LED spectrum acquired in Guardia on May 6 2016

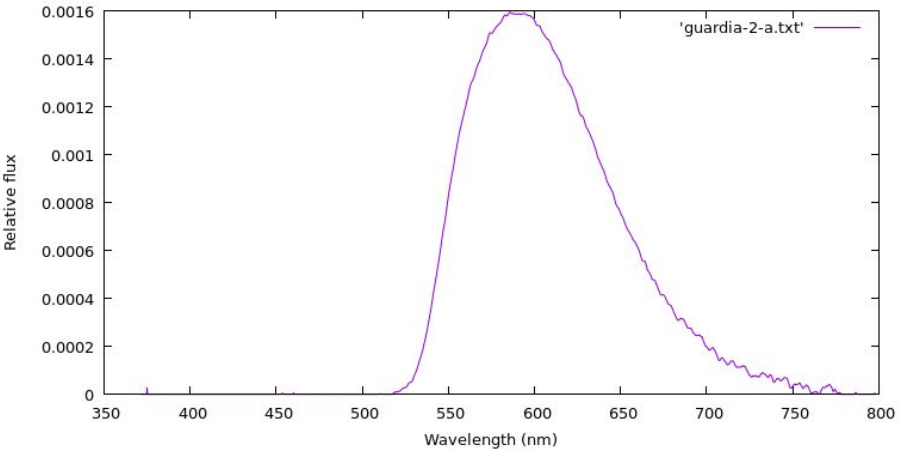


Figure 57: White 4000K LED filtered with Amber filter (Salvi manufacturer) spectrum acquired in Guardia on May 6 2016

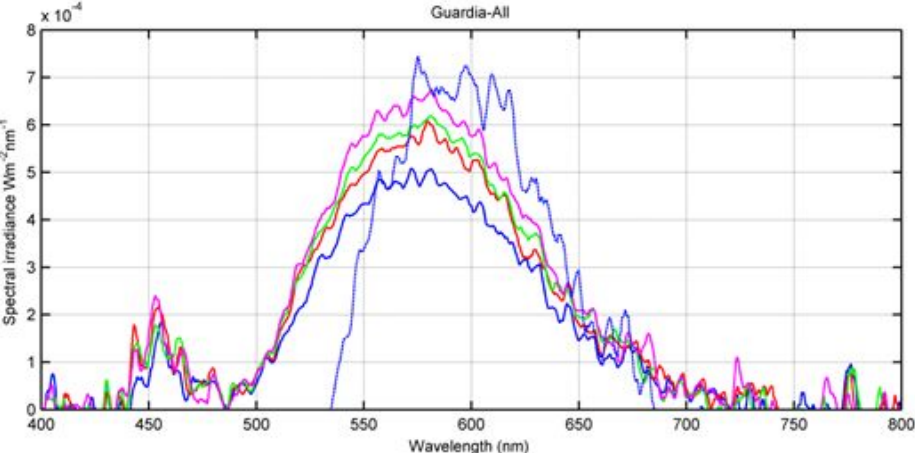


Figure 58: All spectra, a bit noisy, but displayed at the same plot.

Àger's campsite Badia (May 6, 2016, 00:27 UT) :

In the second part of the night there was an scheduled switch off of public lighting in Àger village with the idea to do some measurements of night sky brightness. We have used this switch off to acquire some spectrum of the very bad whitish lighting systems of one of the local campsites (Camping Badia). The campsite has old white fluorescent lamps in the entrance and inside there are around 6-8 poles with old ball lamps (ULOR around 50%) equipped with obsolete mercury systems.

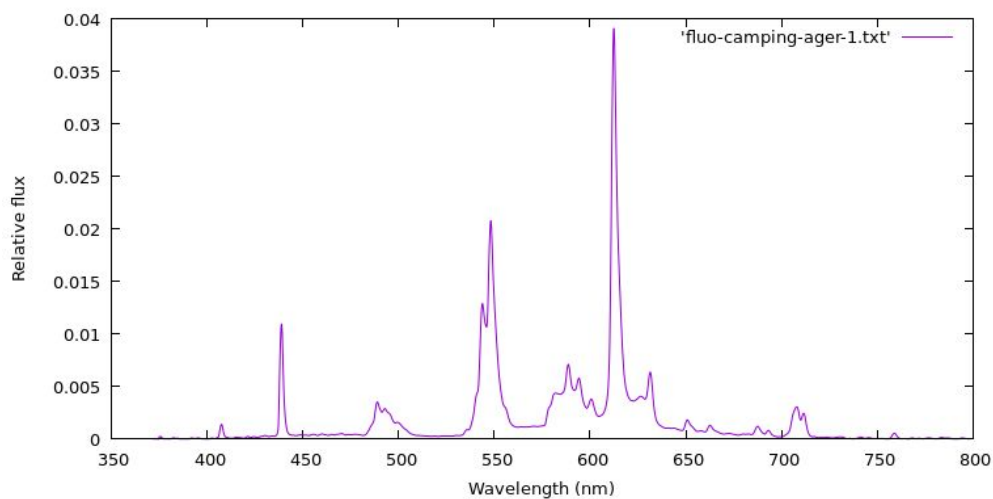


Figure 59: Fluorescent spectrum acquired in Àger's campsite Badia on May 6 2016

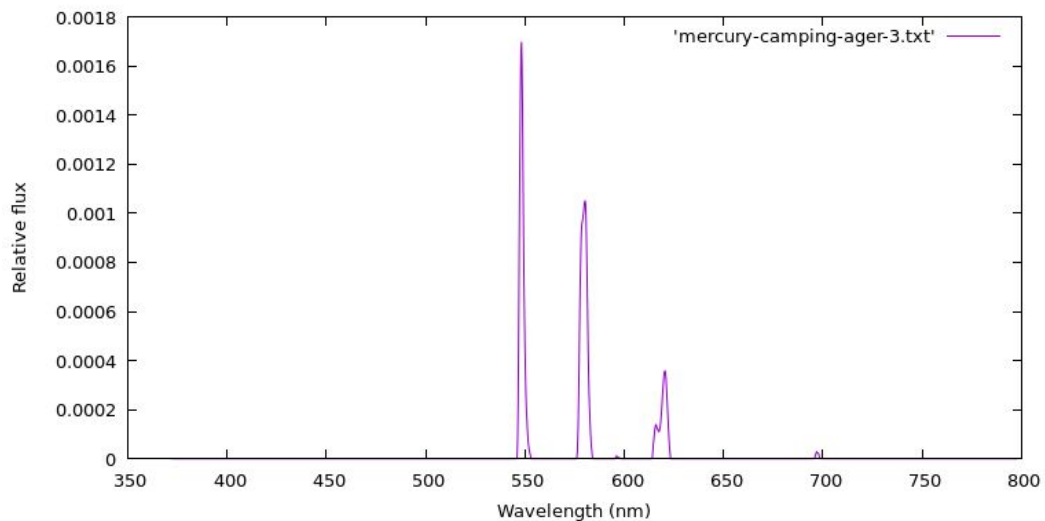


Figure 60: Mercury lamp spectrum acquired in Àger's campsite Badia on May 6 2016

12) Extra corrections on Digilum measurements

Observations:

For the measurements of May 2, 3 and 4 it showed that extra corrections on the measured values for the Digilum were needed. This was due to the unusual setup of the readout unit as will be explained in this section. In normal use no extra corrections are needed.

Explanation:

The sensor of the Digilum exhibits a natural dark current as function of the temperature. This dark current adds to the signal when light is measured. To compensate for this the manufacturer has mounted a temperature sensor at the back of the light sensor and has established a dark current - temperature function (polynomial). This has been done using measurements in which the Digilum was exposed to temperatures between -10°C and 25°C in a climate-controlled chamber. When performing luminance measurements the measured values in the readout unit are automatically corrected for this dark current. The dark current calculated with this polynomial at the measured sensor temperature is then subtracted from the light measurement readings.

During the measurements at the PAM (May 2, 3 and 4) dark current measurements were performed as a quality check by covering the light entrance of the Digilum sensor with a cap. It showed however that the residual dark current measurements (after correction with the internal polynomial) were exceeding the uncertainty specifications ($>0.05 \text{ mcd/m}^2$) and are at a level of 0.1 to 0.2 mcd/m^2 (see Fig. 61). This means that the measured night sky brightness values were also too low.

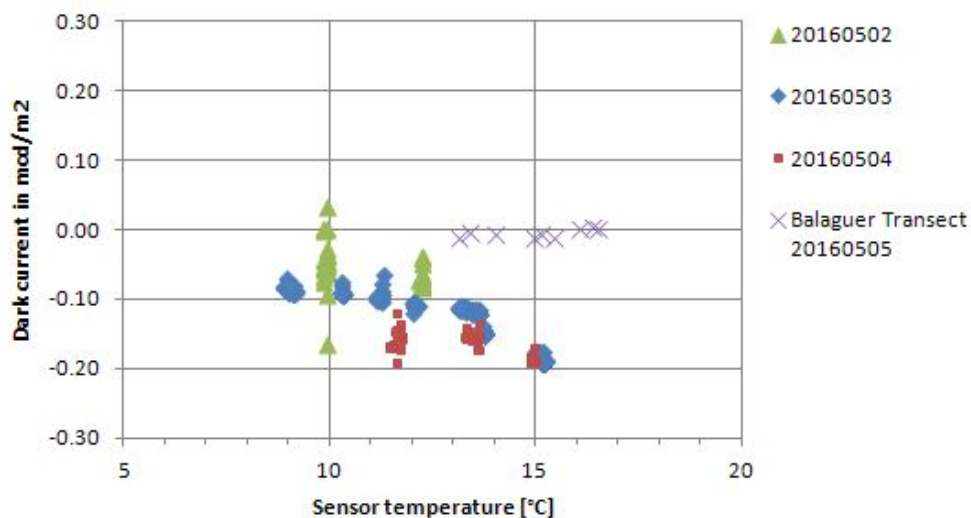


Figure 61: Residual after internal polynomial correction

The remarkable point is that during the Balaguer transect on May 5, the residual dark current is within the specifications of 0.05 mcd/m^2 . This behaviour was never detected during the 6 years of use of the Digilum. When the dark current before polynomial correction is plotted against temperature it shows that the measurements during the Balaguer transect exactly matches the originally established manufacturer's polynomial function (see Fig. 62).

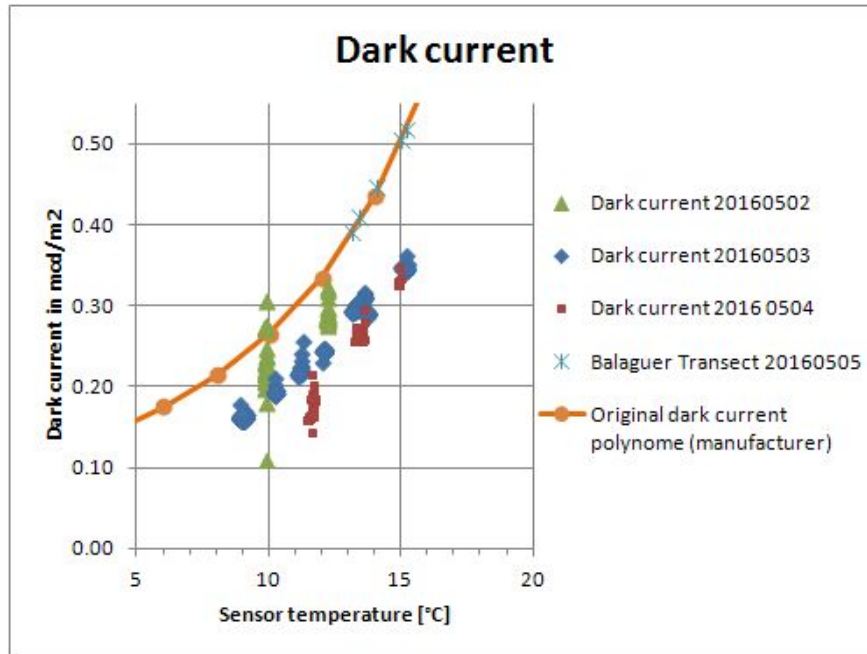


Figure 62: Plot showing dark current versus temperature

At first it was thought that the polynomial might not be applicable anymore, or that the internal parts of Digilum sensor had experienced some damage due to the transport to Montsec. However the residual measurements on the fourth day (May 5th) of the Montsec measuring campaign shows to be within the specifications and the dark current shows excellent agreement with the original polynomial. Transport damage therefore could be excluded.

The only plausible explanation for this behavior is that the Digilum sensor and the read-out unit did not experience the same ambient temperature. The readout unit was placed in a plastic box with other equipment including a laptop which produced quite some heat, hence raising the temperature of the readout unit. As the dark current is measured in pA (pico Ampères) one can imagine that some electronic circuitry is slightly influenced by temperature. During the night of May 4-5 the temperature did not drop below 12°C and thus heat could build up more than during the previous night May 3-4 in which the temperature dropped to about 9°C. This explains why the residual dark current on May 4-5 is lower than on May 3-4. However, it is unclear why the data on May 2-3 scatter strongly. A possible explanation is that the scatter is due to the fact that the box was opened twice to inspect the laptop, which could have cooled down the readout unit.

In the week after the Montsec campaign *additional* dark current measurements were performed during both day-time and night-time in which both the sensor and readout unit were set-up under the same ambient temperature (on May 11 and 12). These tests showed that the dark current matches very well the original polynomial between 10°C and 20°C (see Fig. 63), and that the residual dark current is well within the 0.05 mcd/m² specifications (see Fig 64).

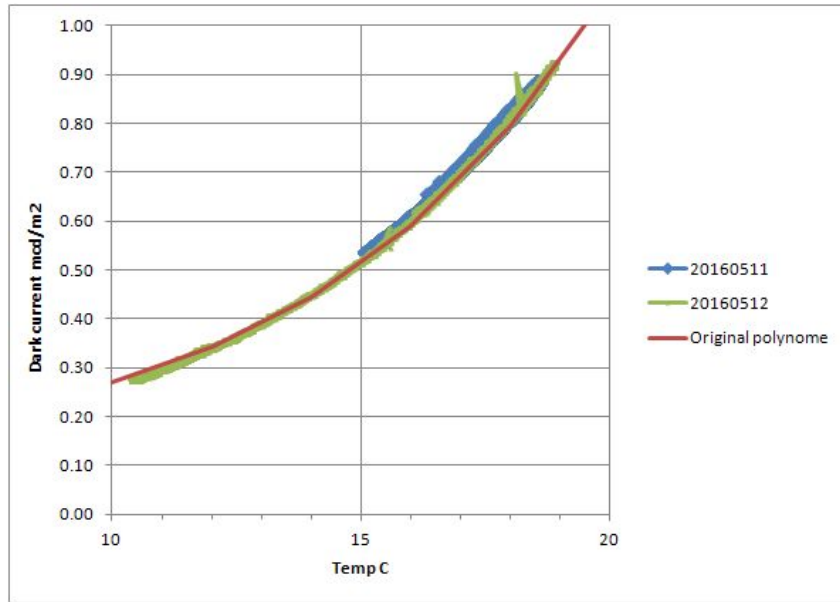


Figure 63: Fitting of dark current versus Temperature.

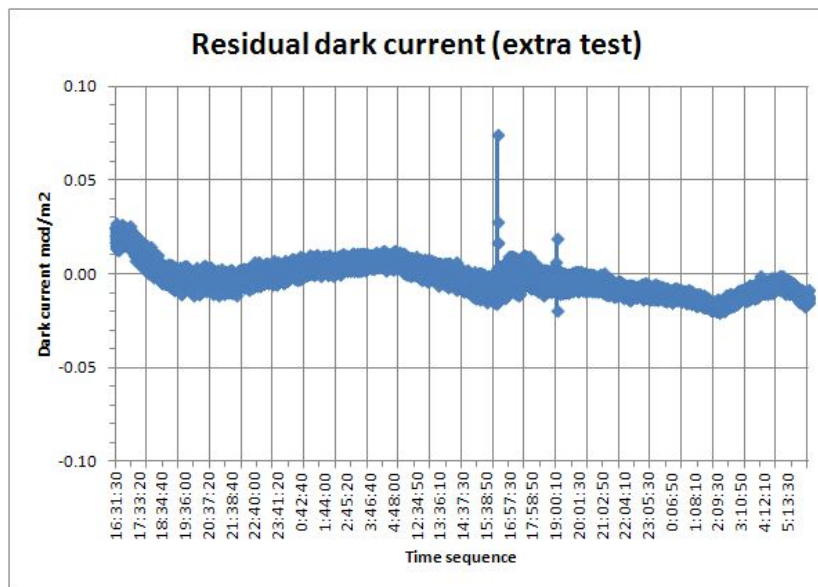


Figure 64: Residual of dark current are below 0.05 mcd/m²

The dark current measurements during the Balaguer transect and the extra tests one week later clearly show that when the read-out unit and the sensor are at the same temperature the Digilum behaves within specifications (as it should).

Applied correction:

As dark current measurements have been performed during May 2, 3 and 4 it is possible to perform a correction to the measured data. This has been performed by fitting the residual dark current as function of temperature and correcting the data with this fit. For May 2 and 4 a linear fit was applied and for May 4 polynomial fit (see Fig. 65).

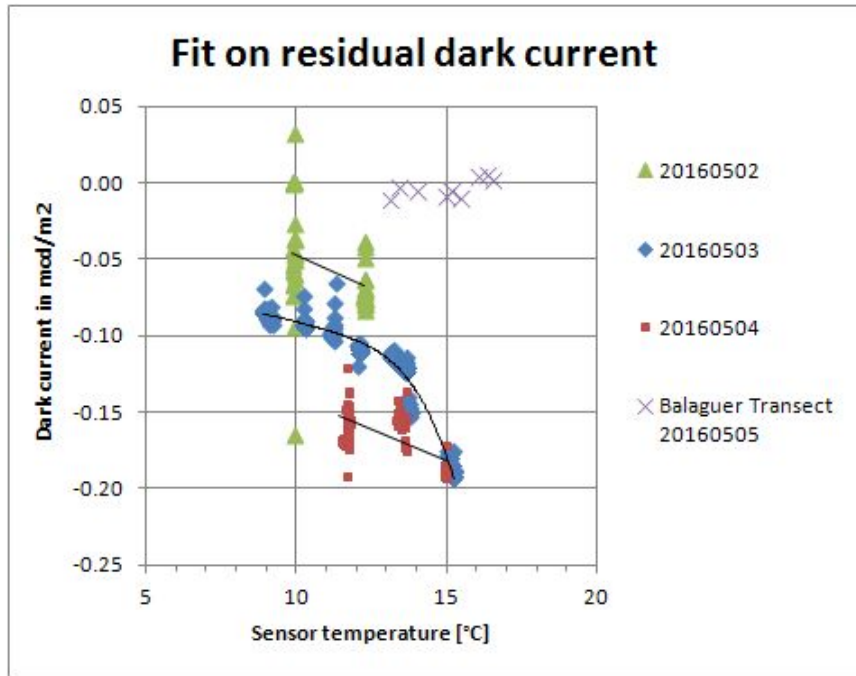


Figure 65: Fitting on residual dark current

The residual dark current *after* this extra correction is on average very close to zero, which is shown in Figure 66.

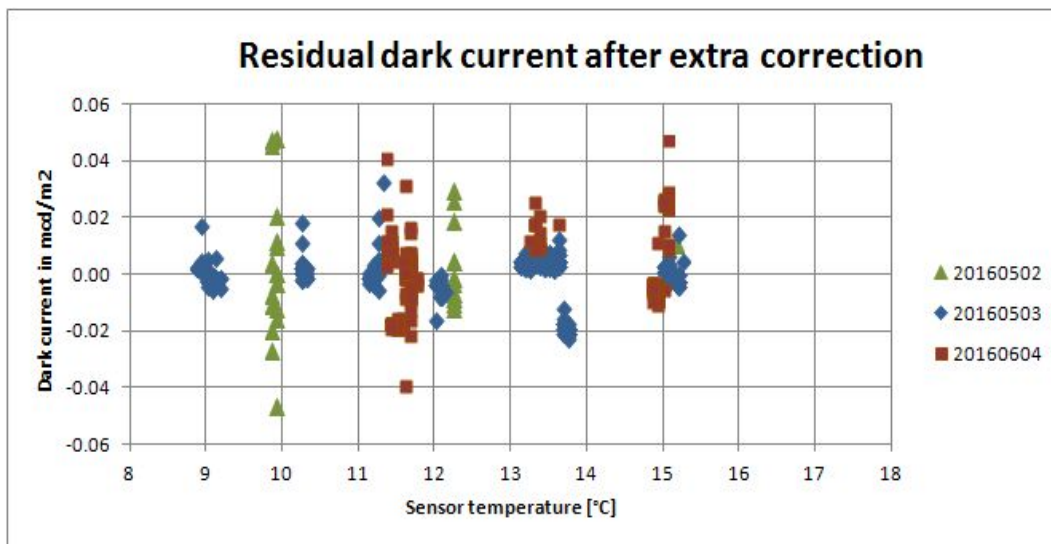


Figure 66: Residual dark current after extra correction

The night sky brightness data for May 2, 3 and 4 have been corrected by applying these fits (the data for the Balaguer transect on May 5 did not need any correction). The resulting tough corrections to the data amount to 0.05 to 0.15 mcd/m² (i.e., 0.6 to 0.8 mags/arcsec²). Due to these extra corrections the uncertainty in the night sky brightness data is slightly increased, and it is estimated that the uncertainty in the reported (and corrected) data are ± 0.05 mcd/m² (± 0.3 mags/arcsec²) or slightly higher.

5) Goals and recommendations for light pollution intercomparison measurements

The Montsec campaign reached a peak in diversity of instrumentation and completeness of the covered light situations, together with the most complete control of environmental light and perturbing light sources of any intercomparison campaign to date. This is an outstanding achievement, but also allows a clear perspective on the next steps. The following remarks are a prioritized list:

- 1. Atmospheric diversity:** Extinction was measured as the first “additional parameter” together with light related quantities during the campaign. This approach to record the atmosphere together with the light it scatters clearly should be continued, e.g. by nearby simultaneously measured aerosol profiles, preferably with size distributions. We recommend to identify, perhaps with an open call, the most important atmospheric quantities to be monitored during future campaigns. At low light-levels, airglow indicators should also be recorded.
- 2. All weather:** Artificial sky brightening is heavily weather-dependent. A synoptic approach containing all weather conditions is essential for providing data for environmental and health studies. We thus recommend that campaigns be designed in such a way that measurements under all weather conditions are supported (i.e., power infrastructure, instrument, and personnel protection); We also recommend to plan for at least one week of measurements. This typical weather time-scale ensures a high probability for stable night hours as well as some diversity in conditions.
- 3. Site-stability:** Campaigns should be preferably held at a dedicated site with full control of all light sources and a protocol for instrument and infrastructure light emission. Practically we see only two options: remote places in protected areas, or astronomical observatories or research stations. Our impression is that most of the “noise” we see during the campaigns actually is a signal of some kind: thus we could strengthen the conclusions by maximising site control and reproducibility of coincidental artificial light.
- 4. Standard Sources:** The usual focus of the campaigns is on the zenith sky brightness – a kind of common ground of all methods – but with diverse angular and spectral response as well as measurement cadence. We recommend agreement on a set of standards and procedures that every instrument should measure and follow. Some options are the Sun, the Moon and the twilight, but artificial standard sources are also worth considering.
- 5. Standard contingency information:** Inter-comparison plots typically involve conversion and conversion assumptions (natural and instrumental constants, assumptions about the atmosphere (extinction, aerosols, scattering, airglow) and their distributions). A recommended set of these constants and assumptions should be

worked out and distributed to the participants, including a protocol for necessary measurements to determine model parameters, the determinations of the extinction coefficient during the Montsec campaign being the most important example so far.

6. **Connecting measurements and methods:** There should be a priority on measurements that may serve to transform between the various measurement concepts and instrumental systems. The US National Park Service all-sky system with its large effort, but very clear concept, is a good example for that. Additional measurements should be done with instruments outside their “comfort-zone” to help to connect to the other approaches. Again the twilight series at Montsec were a first step and moonlight conditions would be the logical next one, although here the discrete source response of individual instruments becomes important, particularly for wide-field integrating instruments designed to measure diffuse sources (e.g., SQM).
7. **Hierarchy of Methods and their overlaps:** Montsec showed very good examples of SQM proxies and zenith luminance derived from other data, e.g. from all-sky DSLR-images. This should be followed further by an explicit concept to provide data-assisted conversion from one system to the other. An example would be the extinction measurement that facilitates the conversion from large angle DSLR measurements to those taken with the narrower angle SQM, and finally to the narrow angle Digilum.
8. **Technical Support:** All campaigns were characterized by organizers that did super-human and in our opinion almost sleepless efforts to help the participants. Any further supporter of campaigns should provide adequate and reliable funding for those people that provide the preconditions for the measurements such as transport, power and network supply. A healthy ratio would be an equal amount of funding for support and scientists. That would help the campaigns as rest-periods are essential for quality (scientific) work.

Additionally, the following recommendations should also be considered for future campaigns, subject to the instrumental abilities and the research goals of the campaign:

9. **Natural light diversity:** Solar, twilight and lunar modulation: The twilight has extensively and successfully been used during the Montsec campaign. We recommend to design the campaigns in such a way that they contain a balanced time-fraction of the Sun, the Moon and twilight. While the moonlight is of the same scale as anthropogenic light pollution, it is much more predictable and also of better consistency. Furthermore, the moonlight enables atmospheric studies to be carried out at higher signal-to-noise than with other natural night-time sources.
10. **Site recommendations:** Montsec with its infrastructure, asymmetric skies and double altitudes was our preferred location of the campaigns so far, followed by Lastovo for its isolation and controllability, although this location was somewhat compromised by also having less science-technical infrastructure. The ideal site for a campaign should have skies within less than a factor of two of the natural night sky, be within 8 km of a site with a complete set of atmospheric monitoring instruments and have a “protection zone” to fully control every light within sight or a distance of <5 km. From what we know, that can only be provided by astronomical observatories or research stations in national parks.

References

- Aceituno, J., Sánchez, S. F., Aceituno, F. J., Galadí-Enríquez, D., Negro, J. J., Soriguer, R. C., & Gomez, G. S. (2011). An all-sky transmission monitor: ASTMON. *Publications of the Astronomical Society of the Pacific*, 123(907), 1076-1086.
- Bará, S., Espey, B., Falchi, F., Kyba, C.C.M., Nievas Rosillo, M. et al. (2015) Report of the 2014 LoNNe intercomparison campaign. URL: <http://eprints.ucm.es/32989/> (Accessed 13 May 2016).
- Bessell, M.S. (1990) UBVRI Passbands *Publications of the Astronomical Society of the Pacific*, 102, 1181-1199.
- Cinzano, P. (2005). Night sky photometry with sky quality meter. ISTIL Int. Rep, 9. URL: <http://www.lightpollution.it/download/sqmreport.pdf> (Accessed: 30 March 2015).
- den Outer, P., Lolkema, D., Haaima, M., Hoff, R. V. D., Spoelstra, H., & Schmidt, W. (2011). Intercomparisons of nine sky brightness detectors. *Sensors*, 11(10), 9603-9612.
- Duriscoe, D. M., Luginbuhl, C. B., & Moore, C. A. (2007). Measuring night-sky brightness with a wide-field CCD camera. *Publications of the Astronomical Society of the Pacific*, 119(852), 192.
- Falchi, F. (2011). Campaign of sky brightness and extinction measurements using a CCD camera. *Monthly Notices of the Royal Astronomical Society*, 412, 1, 33-48.
- Falchi, F., Cinzano, P., Duriscoe, D., Kyba, C.C.M., Elvidge, C.D. et al. (2016). The New World Atlas of Artificial Night Sky Brightness. *Science Advances*, 2(6), e1600377 DOI: 10.1126/sciadv.1600377
- Jechow, A., et al. "Evaluating the summer night sky brightness at a research field site on Lake Stechlin in northeastern Germany." *Journal of Quantitative Spectroscopy and Radiative Transfer* 181 (2016): 24-32.
- Kolláth, Z. (2010, March). Measuring and modelling light pollution at the Zselic Starry Sky Park. In *Journal of Physics: Conference Series* (Vol. 218, No. 1, p. 012001). IOP Publishing.
- Kyba, C.C.M., Bouroussis, C. Canal-Domingo, R. Falchi, F., Giacomelli, A. et al (2015a) Report of the 2015 LoNNe Intercomparison Campaign. URL: <http://gfzpublic.gfz-potsdam.de/pubman/faces/viewItemOverviewPage.jsp?itemId=escidoc:1124000> (Accessed 13 May 2015)
- Kyba, C. C., Tong, K. P., Bennie, J., Birriel, I., Birriel, J. J., Cool, A., et al. (2015b). Worldwide variations in artificial skyglow. *Scientific Reports*, 5.
- Müller, A., Wuchterl, G., & Sarazin, M. (2011). Measuring the night sky brightness with the lightmeter. *Revista Mexicana de Astronomia y Astrofisica*, 41, 46-49.
- Nievas, M. (2012). Fotometría absoluta y brillo de fondo de cielo con AstMon-UCM. *E-prints Univ. Complutense de Madrid*. URL: <http://eprints.ucm.es/16974/>
- Ribas, S.J. (2016). Caracterització de la contaminació lumínica en zones protegides i urbanes. PhD Thesis, Universitat de Barcelona.
- Schaefer, B.E. (1998). To the Visual Limits. *Sky and Telescope*, 95(5), 57.
- Zamorano, J., Sánchez de Miguel, A., Ocaña, F. et al (2016) Testing sky brightness models against radial dependency: A dense two dimensional survey around the city of Madrid, Spain. *Journal of Quantitative Spectroscopy & Radiative Transfer*, 181, 52-66.

Acknowledgements

We would like to thank:

- The Stars4all project, for providing financing the event.
- The municipalities of Àger and Balaguer for permitting and assisting with public light switch offs.
- Parc Astronòmic Montsec for hosting us and significant preparatory work beforehand
- Hotel Cal Maciarol for hosting us and accommodating our unusual work and activity schedule

We acknowledge the financing by the European STARS4ALL Collective Awareness Platform for Sustainable and Social Innovation (CAPPSI). Although the project was conceived and planned as a milestone within the EU COST Action ES1204 (Loss of the Night Network), the EU COST office waived the financing of the final intercomparison campaign, due to administrative problems and changes in the grant periods. This decision was unforeseen and concerned all participants and the organizers.



Figure 67: Campaign participants 2016 with local authorities. Missing from image: Andreas Hänel, Guillem Marti, Pol Massana.

STARS4ALL

A Collective Awareness Platform for Promoting Dark Skies in Europe



European
Commission

Horizon 2020
European Union funding
for Research & Innovation



LONNe

ES1204

Loss of the Night Network